UPTEC W09 033
Examensarbete 30 hp
December 2009

NAPL spill modeling and simulation of pumping remediation

NAPL modellering och simulering av pumpning

Kristina Rasmusson
Maria Rasmusson

ABSTRACT

NAPL spill modeling and simulation of pumping remediation

Kristina Rasmusson & Maria Rasmusson

This Master Thesis presents TMVOC simulations of a NAPL-spill (non-aqueous phase liquid) and following pumping remediation. TMVOC is a simulation program for three-phase non-isothermal multicomponent flow in saturated-unsaturated heterogeneous media. The models presented are based on an actual remediation project. The aim of the thesis was to study if the historical development of the NAPL-spill could be simulated and how long time the pumping remediation would take. A 3D-model and a radially symmetric cylindrical model were created.

A large effort of the work done was in taking the complex TMVOC model in use and modifying it for the problem at hand. Therefore, the numerical results of the simulations should be considered as preliminary and as forming basis for future studies.

The results from the spill simulation and historical pumping simulation indicated that the spill volume could be less than the estimated 1400 m^3, perhaps around 700 m^3, assuming a leakage time of 30 years.

The historical pumping simulation of a 700 m^3 diesel spill showed good agreement with measured values for some wells, but overestimated the recovery in other wells. The overestimation could be due to the fact that the 3D-model did not take seasonal changes in the groundwater level into consideration. Also, the model did not account for any heterogeneity or compartmentalization in soil material properties that could explain the differences between the wells.

Assuming the same spill of 700 m^3, future pumping was simulated. The results from these simulations indicated the remediation time to be long due to fast decreasing mobility of the NAPL phase. The NAPL flow rate to the wells was halved in a couple of years. Much of the NAPL was distributed over a large area at near residual saturation with the highest NAPL saturation found at the opposite side of the pumping wells in the model.

Future simulation studies should address the effect of discretization as well as the effect of uncertainties in material properties e.g. conductivity, residual NAPL saturation and soil heterogeneity.

Keywords: NAPL, TMVOC, multiphase flow, simulation, remediation

Department of Earth Sciences, Air, Water and Landscape Science, Uppsala University, Villavägen 16, SE-752 36 Uppsala Sweden.

ISSN 1401-5765

REFERAT

NAPL modellering och simulering av pumpning

Kristina Rasmusson & Maria Rasmusson

Denna uppsats presenterar TMVOC-simuleringar av ett NAPL-läckage (non-aqueous phase liquid) och efterföljande pumpsanering. TMVOC är ett program för trefas-multikomponent-flöde i icke-isotermiskt mättad/omättad heterogen media. Modellerna baserades på ett verkligt saneringsprojekt. Målet med uppsatsen var att studera om NAPL-läckagets händelseförlopp kunde simuleras och hur lång tid en efterföljande pumpsanering skulle kräva. En 3D-modell och en radialsymmetrisk modell skapades.

Arbetet har fokuserat på att anpassa TMVOC-modellen för det specifika problemet. De erhållna simuleringsresultaten är preliminära och utgör en bas för fortsatta studier.

Resultatet från simuleringen av läckageförloppet och den historiska pumpningen tydde på att volymen NAPL i marken skulle kunna vara mindre än den antagna på 1400 m^3, eventuellt 700 m^3, vid antagandet att utsläppet skedde under en period av 30 år. Simulerad pumpad NAPL-volym efter utsläpp av 700 m^3 diesel överrensstämde bra med de uppmätta utpumpade volymerna för några av brunnarna, men överskattade pumpad NAPL-volym i andra.
En potentiell orsak kan vara avsaknad av fluktuationer i grundvattennivå i 3D-modellen. Modellen tog inte heller hänsyn till heterogenitet i marken vilket skulle kunna förklara skillnaden mellan brunnarna.

Simulering av framtida pumpning av ett 700 m^3 stort NAPL-läckage tydde på att saneringstiden skulle bli lång beroende på snabbt avtagande tillflöden av NAPL i brunnarna. Efter bara några år av pumpning hade flödeshastigheterna till brunnarna halverats. NAPL-linsen hade stor utbredning i marken och mättnad nära residualmättnad. Högst NAPL-mättnad återfanns på motsatt sida av brunnarnas placering i modellen.

Framtida simuleringar skulle kunna utreda diskretiseringens inverkan på resultatet samt effekter vid olika val av materialegenskaper t.ex. konduktivitet, NAPL- residualmättnad och heterogenitet i marken.

Nyckelord: NAPL, TMVOC, flerfas flöde, simulering, sanering

Institutionen för Geovetenskaper, Luft-, Vatten- och Landskapslära, Uppsala Universitet, Villavägen 16, 752 36 Uppsala.

PREFACE

This Master Thesis completes the final course of the Master of Science in Aquatic and Environmental Engineering program at Uppsala University. The work comprises 30 ECTS. Supervisor was Professor Auli Niemi at the Department of Earth Sciences, Air, Water and Landscape Science, Uppsala University, and subject reviewer was Fritjof Fagerlund Assistant Professor at the same department. Our contact at Environmental & Water Resources Engineering Ltd (EWRE) in Israel was Jacob Bensabat. We would like to thank EWRE for making it possible for us to visit the remediation site. We also thank EWRE for letting us reuse pictures from their reports in our thesis. We also would like to thank Auli Niemi, Jacob Bensabat and Fritjof Fagerlund for the help and support we received during the work with the master thesis.

This Master Thesis is the result of collaboration between the authors and below follows a specification of the person with the main responsibility for different sections of the essay:

Kristina Rasmusson: Background, Location, TMVOC, Soil, Single well simulation.

Maria Rasmusson: Abstract, Referat, Preface, Populärvetenskaplig sammanfattning, Pollution, Temperature, Simulation of current pumping regime.

Joint responsibility: Objectives, Remediation, Chemical composition of the pollution, Groundwater table, Remediation system, Grid, Historical simulation, Discussion, Conclusions.

UPTEC W09 033, ISSN 1401-5765
Printed at the Department of Earth Sciences. Geotryckeriet. Uppsala University. Uppsala. 2009.

POPULÄRVETENSKAPLIG SAMMANFATTNING

NAPL modellering och simulering av pumpning

Kristina Rasmusson & Maria Rasmusson

Organiska bränslen används dagligen. När läckage av dessa sker hamnar föroreningen ofta i mark och grundvatten med potential att sprida sig ytterligare. I sakens natur ligger också att läckagen uppstår på platser där människor fortsättningsvis kommer i kontakt med föroreningen, ett ur hälsosynpunkt ogynnsamt läge. Om föroreningen består av organiska kolföreningar med en densitet lägre än vatten benämns denna LNAPL (light non-aqueous phase liquid). Vid ett eventuellt spill kommer spridningen i stora drag för en LNAPL utgöras av perkolation genom markens omättade zon för att därefter bilda en flytande lins ovanpå grundvattenytan. Vidare spridning sker genom diffusion i vattenfasen och gasfasen. Till LNAPLar hör bland annat diesel. Diesel består av en mängd olika kolväten med varierande sammansättning. En möjlig saneringsteknik vid dieselutsläpp är pumpning av grundvatten med syfte att försöka fånga upp LNAPL-linsen och kontaminerat grundvatten.

Ett verktyg vid saneringsprojekt är datormodellering, där specifika platsförhållanden används i modellen. Med hjälp av detta är det möjligt att översiktligt undersöka hur spridningen skulle kunna se ut i marken samt hur en saneringsteknik som till exempel pumpning skulle inverka. Detta är vad denna uppsats kommer handla om. Uppsatsen baseras på ett verkligt saneringsprojekt. Det rör sig om ett utsläpp av diesel uppskattat till 1400 m^3 som antas ha pågått under 30 års tid på en bangård i Haifa, Israel. Målet med saneringsprojektet är att avlägsna så mycket NAPL som möjligt. Under projektet har brunnar borrats och sanering sker med hjälp av pumpning av dieselfasen ur brunnarna med jämna mellanrum. Uppsatsen syftar till att med hjälp av datorbaserad modellering i stora drag försöka återskapa läckagets historiska förlopp och undersöka hur lång tid det skulle kunna ta att sanera området med den metod som används idag.

För att lösa uppgiften användes TMVOC, skriven i FORTRAN. TMVOC är en numerisk simulator för trefas (luft, vatten, NAPL) icke-isotermiskt flöde av flera komponenter (kolväten) i mättad eller omättad heterogen media. TMVOC är en modell som tillhör TOUGH-koderna och har utvecklats vid Berkeley i USA. Dess styrka är möjligheten att kunna simulera spridningen av flera komponenter samtidigt, vilket är speciellt lämpligt och gör TMVOC intressant i fallet med dieselutsläpp.

Parametrar för att beskriva utsläppsplatsen och föroreningen samlades in, så som markegenskaper, klimatförhållanden samt dieselsammansättningen och dess komponenters egenskaper. En multikomponentdiesel samt en enkomponentdiesel skapades. Den verkliga platsen med koordinater för pumpbrunnar och observationsbrunnar överfördes sedan till ett grid-nät med en linjekälla som tillämpades i modelleringen. En 3D-modell med måtten 180 m x 130 m x 6 m skapades. I denna simulerades utsläpp av en komponent (beräknade medelegenskaper för diesel) samt pumpning. Dessutom skapades en radialsymmetrisk modell (25,5 m i radie och 6 m djup) där enkomponentsdiesel injicerades och utsattes för pumpning. Inverkan av förenklingar i modellen undersöktes med hjälp av denna. I den radialsymmetriska modellen simulerades effekten av variation i temperatur och grundvattenytans läge på föroreningens spridning. Grundvattenytans läge visade sig ha stor inverkan på utpumpad volym diesel.

Simuleringar genomfördes för NAPL-läckage och efterföljande pumpning och resultatet jämfördes sedan med uppmätta värden på pumpad NAPL-volym från fält. Resultaten från simuleringar av det historiska läckageförloppet i 3D-modellen tydde på att utsläppet skulle

kunna vara mindre än det estimerade 1400 m^3, eventuellt 700 m^3 över en period på 30 år. Mätvärden på pumpad diesel och simulerad pumpad diesel jämfördes. Överensstämmelsen var god för några brunnar samtidigt som utpumpad dieselvolym överskattades för andra brunnar. Överskattningen skulle kunna bero på att 3D-modellen inte tog hänsyn till en fluktuerande grundvattenyta. Modellen tog inte heller hänsyn till heterogenitet i marken vilket skulle kunna förklara skillnaden mellan brunnarna.

Simuleringsresultat av framtida pumpning av ett 700 m^3 stort NAPL-läckage tydde på att saneringstiden skulle vara lång på grund av snabbt avtagande tillflöden av NAPL i brunnarna. Efter några år av pumpning hade flödeshastigheterna till brunnarna halverats. NAPL-linsens utbredning i marken var stor och mättnaden nära residualmättnad. Högst NAPL-mättnad återfanns på motsatt sida av brunnarnas placering i modellen.

De erhållna simuleringsresultaten är preliminära och utgör en bas för fortsatta studier. Dessa skulle kunna utreda diskretiseringens inverkan på resultatet samt effekter vid olika val av materialegenskaper t.ex. konduktivitet, NAPL- residualmättnad och heterogenitet i marken.

Contents

1. INTRODUCTION

1.1 BACKGROUND

Light non-aqueous phase liquids (LNAPLs) are organic compounds with densities less then water. E.g. diesel, gasoline and jet fuels belong to this category of pollutants. When a fuel spill occurs and a LNAPL is released into the ground it will percolate down through the unsaturated zone, as long as residual saturation is exceeded. When the LNAPL reaches the water table the density differences between the two fluids will result in a floating LNAPL-lens on the groundwater table (Domenico & Schwartz, 1998), fig 1.1.

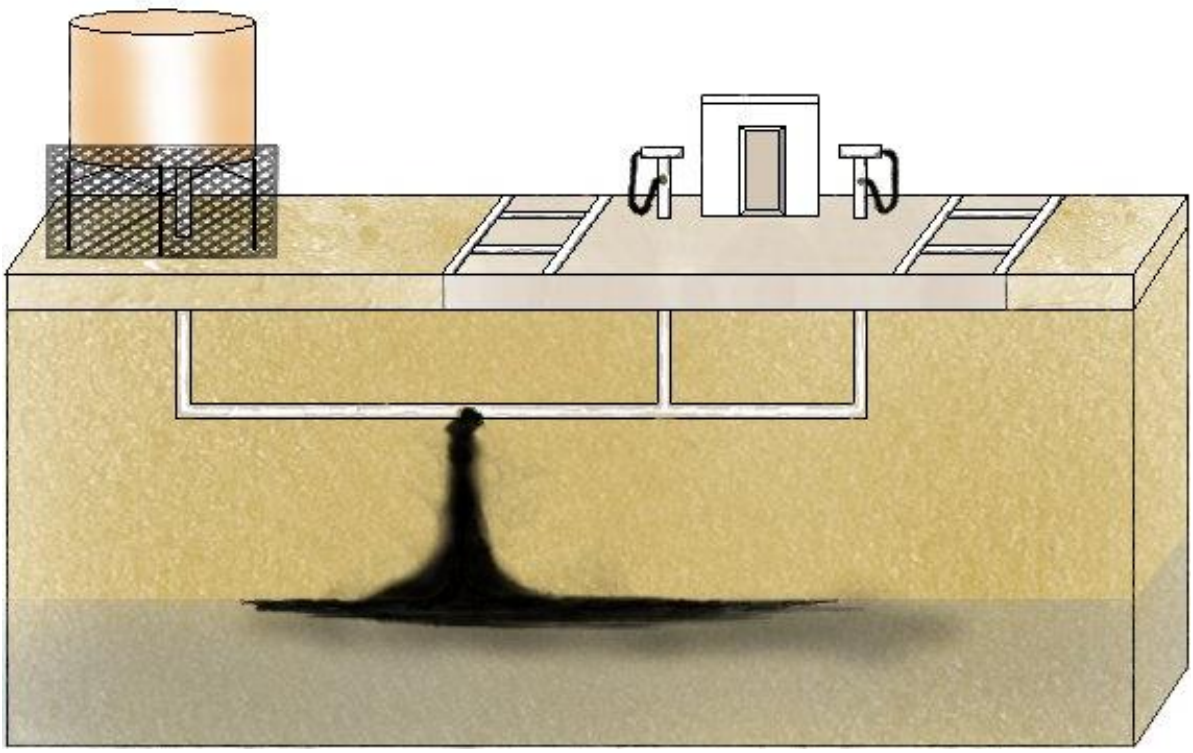

Fig. 1.1. LNAPL movement in the ground.

The NAPL, being immiscible with water, has its own liquid, dissolved and vapor phase which have to be considered when accounting for migration (Fetter, 1999).

The NAPL migration in the ground is effected not only by the NAPL's own chemical and physical properties but also by the soil properties and the climate. A changing groundwater level due to seasonal fluctuations in recharge will impact the distribution of LNAPL in the ground, enhancing the spreading (Domenico & Schwartz, 1998).

Tracking of LNAPL contamination can be done with monitoring wells. The NAPL lens is however thicker in the well than in the surrounding ground. As the groundwater table (and therefore also the NAPL) descend or ascend residual NAPL will remain in part of the pore spaces it initially occupied. This may led to effects like absents of LNAPL in wells despite a polluted ground. Other effects can be NAPL entrapment as the water table ascends resulting in reduced NAPL migration and a decrease in NAPL thickness in wells (Fetter, 1999).

Modeling of NAPL pollutions can be carried out with multiphase simulators e.g. TMVOC (Pruess & Battistelli, 2002) and ARMOS (Kaluarachchi et al., 1990). Earlier TMVOC has been used to model multicomponent organic mixture spill in a coastal site combined with sea water intrusion and containment in the form of an impervious wall (Battistelli, 2006) and to model gasoline pollution as a reference to another model (Fagerlund & Niemi, 2007).

The purpose of this master thesis was to simulate, using the TMVOC model, an existing diesel (LNAPL) spill and ongoing remediation conducted by Environmental & Water Resources Engineering Ltd (EWRE). Simulation results were compared to historical pumped NAPL volumes and the required remediation time using the current pumping regime was estimated. The effect on NAPL distribution was also of interest. It was of importance to collect knowledge about the site.

To achieve this chemical and soil properties resembling the pollution and actual site characteristics were implemented in a 3D-model and a representation of the remediation system was added. The effect of a fluctuating groundwater table and temperature was also studied in a small scale single well radially symmetric model and possible impacts of model simplifications (not taking into account in the 3D model) evaluated.

1.2 OBJECTIVES

The objective of the master thesis was to create a TMVOC model for the site and to use this to answer the following questions:

- Can the history of the pollution be simulated? Are the assumptions made about the origin and amount of the spill in alignment with the measurements retrieved?
- How long time will it take to remediate the ground using the present pumping regime? And what is the effect on the NAPL distribution?

2. MATERIAL AND METHOD

Information about the site, spill and remediation system was collected. Together with knowledge about the TMVOC model this served as a base for model implementations and the following simulations.

2.1 SITE DESCRIPTION

2.1.1 Location

The site of interest is located at the Israeli Railroad Compound (IRC) in the industrial zone of Haifa, Israel. The area has for a long time been used as a refueling and maintenance center for trains (EWRE, 2005), fig. 2.1.

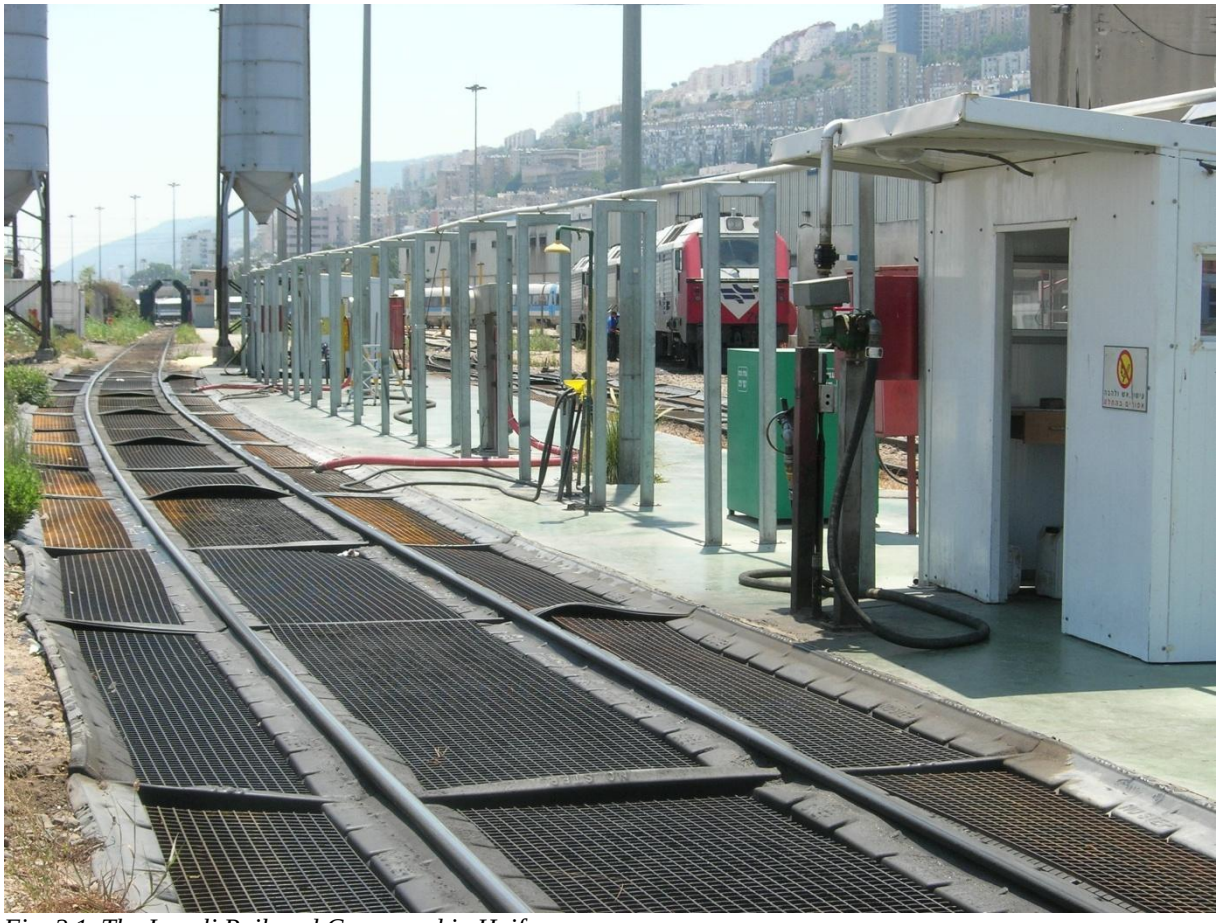

Fig. 2.1. The Israeli Railroad Compound in Haifa.

The local lithology consists of filling, sand and clay layers to a depth of 10 m, see fig. 2.2 and fig. 2.3. The filling material is a construction material and contains conductive boulders but otherwise having the same properties as sand. No field or laboratory tests of conductivity or permeability have been conducted (Bensabat, 2009).

A perched aquifer underlay the site and the groundwater table can be found at a depth of approximately 3 m (EWRE, 2007). The groundwater level has a seasonal variation of 1.5 m, due to recharge from the mountains, reaching the highest elevation in May and the lowest in September. The groundwater table is always found in the sand layer and never in the filling layer (Bensabat, 2009). In fig. 2.4 the groundwater level in the fall of year 2005 can be seen.

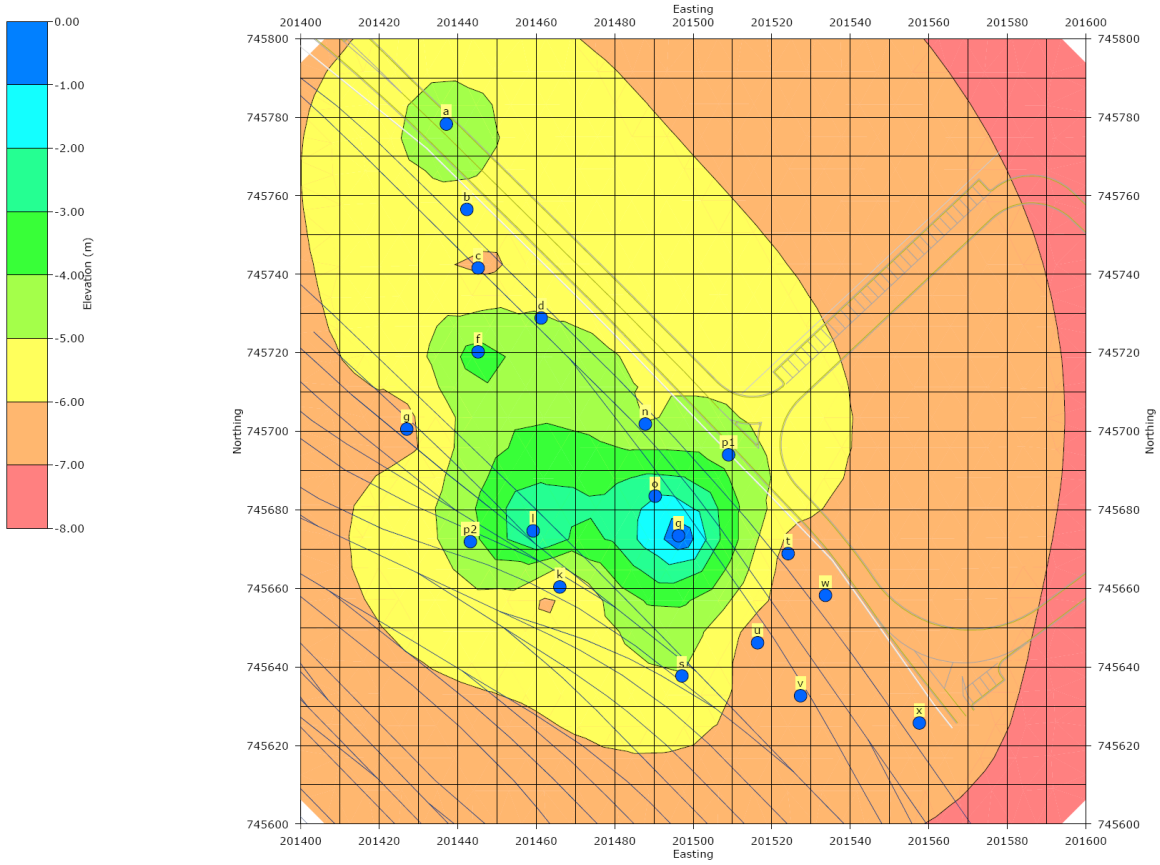

Fig. 2.2. Elevation (m above sea level) of the top clay layer. EWRE (2005), with permission.

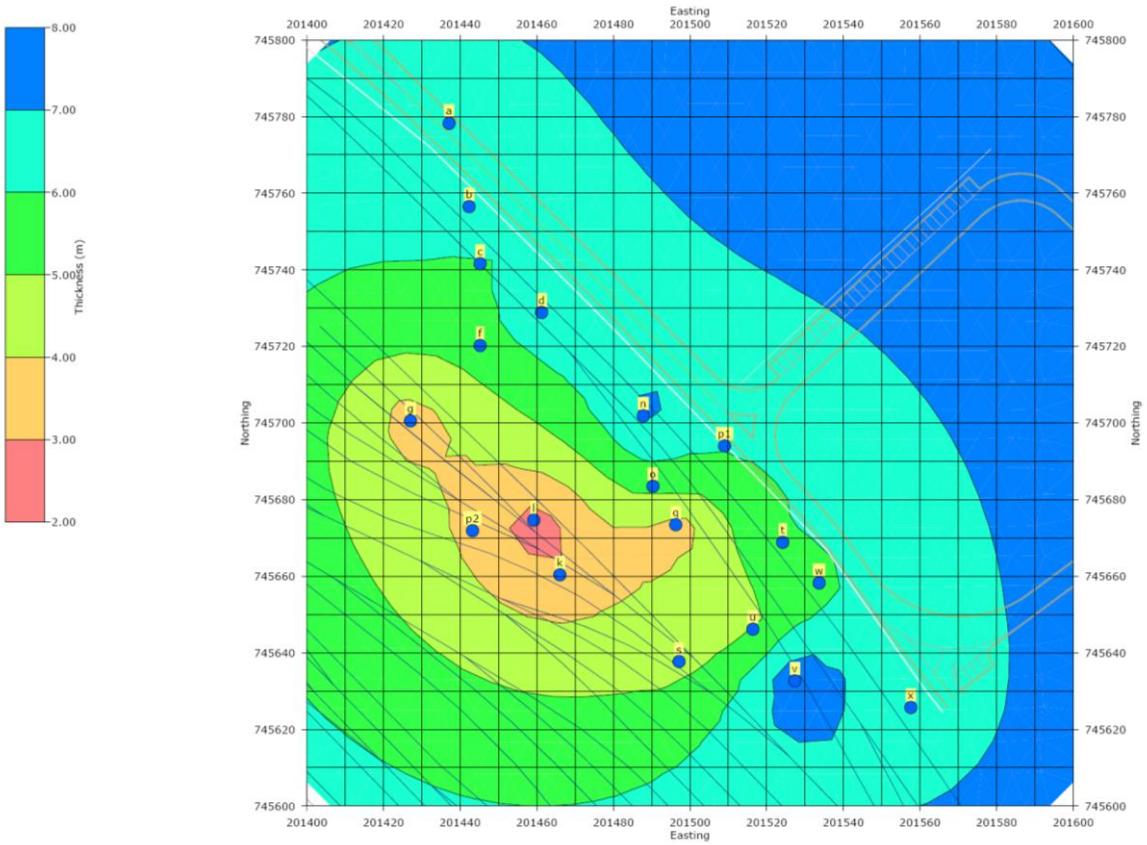

Fig. 2.3. Thickness (m) of the sand and fill layer. EWRE (2005), with permission.

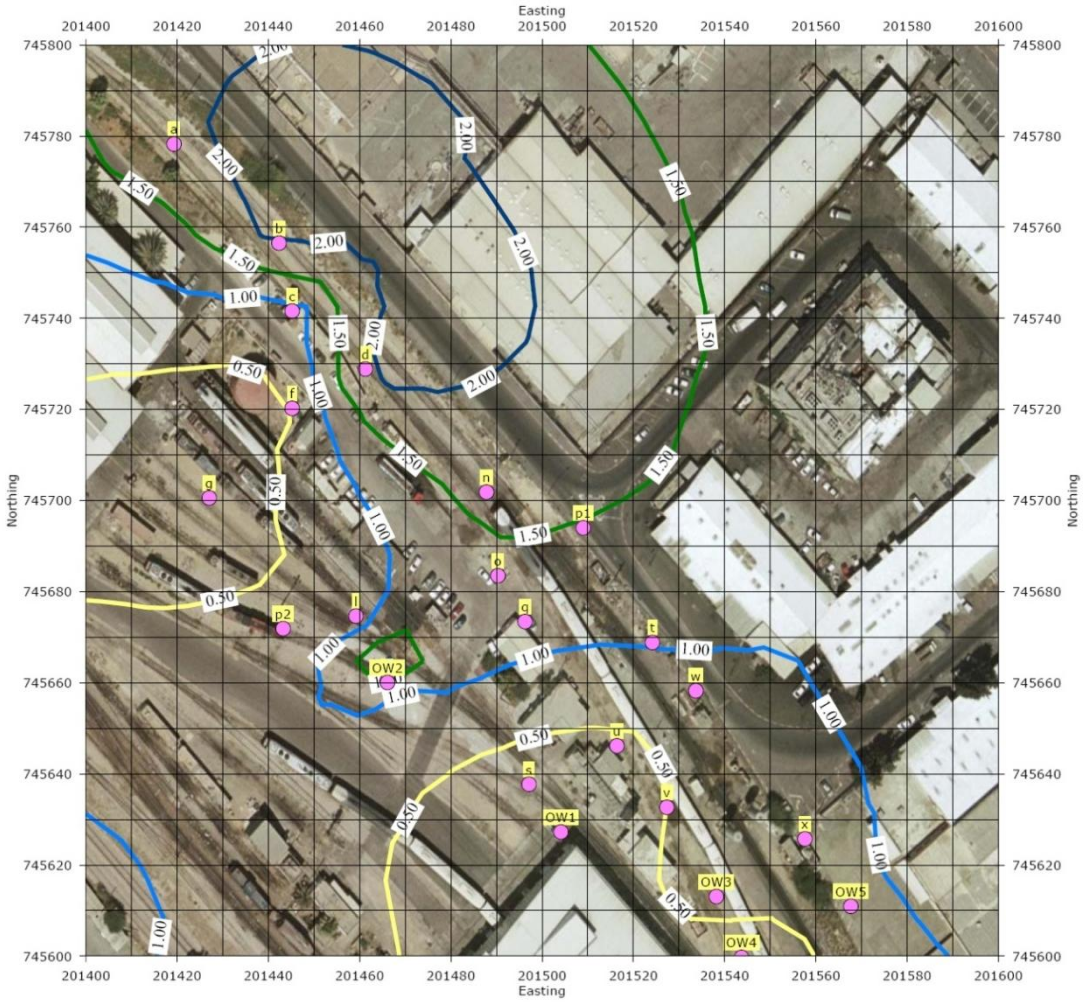

Fig. 2.4. Groundwater level (m above sea level) in the fall of year 2005. EWRE (2005), with permission.

The underground infrastructure is unknown (not mapped) but there are electrical wiring, pipes and structures present. There could also be a water leakage from a sewage pipe effecting the groundwater level (Bensabat, 2009).

Haifa has a Mediterranean climate and the air temperature varies between 8 °C and 40 °C during the year. Average temperature, precipitation and potential evaporation are presented in table 2.1. Due to large evaporation local groundwater recharge (precipitation) is negligible.

Table 2.1. Average values for temperature, precipitation and potential evaporation (IMS, 2007). The temperatures are taken at a soil depth of 10 cm. The potential evaporation values are for the central Coastal aquifer.

	Jan	Feb	Mar	Apr	May	Jun	Jul	Aug	Sep	Oct	Nov	Dec
Average min. T [ºC]	8.9	8.7	10.5	13.6	17.2	20.6	23	23.6	21.7	18.5	14.1	10.9
Average max. T [ºC]	17	17.5	19.6	23.9	26.2	29.3	31.1	31.4	29.9	28	24	19.2
Average monthly percipitation [mm]	124.9	92.2	52.8	23.6	2.7	-	-	-	1.2	28	77.4	135.5
Average no. of rain days, > 1 mm	11.5	9.3	6.7	2.6	0.7	-	-	-	0.2	2.8	6.3	10.1
Average monthly potential evaporation [mm][A]	46.5	58.8	89.9	123	155	165	176.7	164.3	138	102.3	72	52.7

A The average monthly pot. evaporation was calculated from average daily pot. evaporation values for each month multiplied by the number of days in the specific month (31, 28, 31 and so on).

2.1.2 Pollution

Trains in Israel are fueled with gasoil, diesel. Polluting can occur through e.g. leakage from underground pipes (connected to refueling stations) or mismanagement during refueling resulting in the release of diesel to the surrounding environment.

Neither the origin of the investigated spill nor for how long the leakage has occurred is known. But five years ago a discrepancy between the amount of oil bought and the amount sold was discovered. A soil survey was conducted and soil samples (TPH, Total Petroleum Hydrocarbons) showed high concentrations (1000 mg/kg) of oil components in the soil and the occurrence of an oil lens (EWRE, 2005).

A hydrologic survey was conducted and the extent of the oil pollution was estimated by measuring the oil thickness in monitoring wells. The total oil lens volume was assessed to equal 1250 m^3 and to cover an area of 13000 m^2 (calculations were based on a porosity of 25 percent and included area outside the railroad zone). The amount possible to extract through pumping was estimated to be 1000 m^3. The remaining 20 percent of the oil was considered trapped due to soil properties (EWRE, 2005).

In December of year 2006 the oil volume was estimated to 1400 m^3 with the main area of the oil lens being inside the railroad zone (EWRE, 2007).

The oil lens is not at steady state. As the groundwater level and flow direction change with time so do the extent, thickness and flow direction of the oil lens. From measurements in year 2005 a spatial variation of the oil lens thickness (from 1 cm to 1 m) could be seen (EWRE, 2005). Fig. 2.5 shows the oil thickness in the fall of year 2005.

The compound is located in the industrial zone of Haifa and the groundwater has no practical use. But the environmental department wants a solution to the oil lens problem and the area is being remediated. The purpose of the remediation is to remove as much NAPL as possible (Bensabat, 2009).

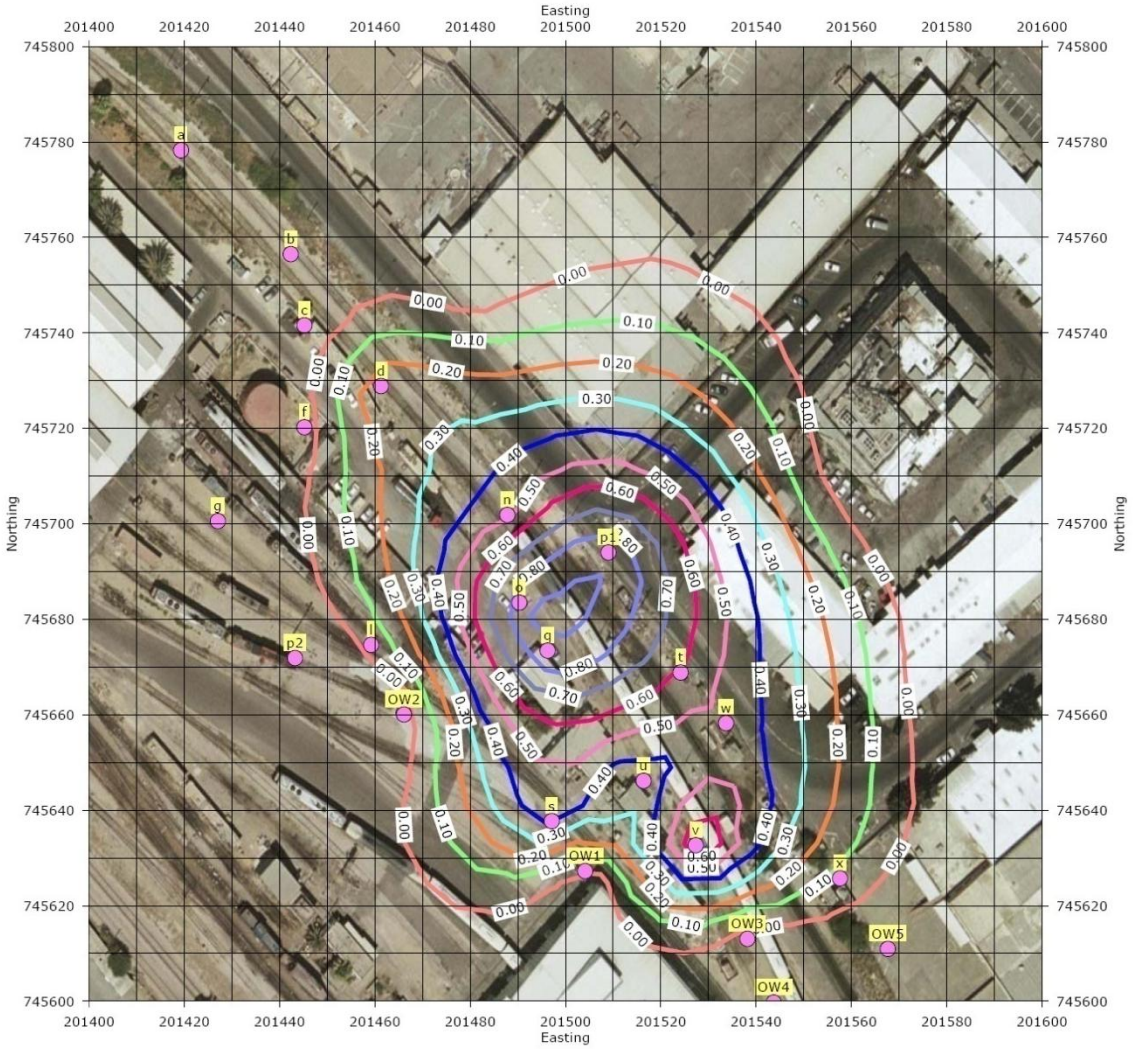

Fig. 2.5. Oil thickness (m) in the fall of year 2005. EWRE (2005), with permission.

2.1.3 Remediation

The remediation system at the site consists of 24 monitoring wells and 7 pumping wells, fig. 2.6.

9 of the monitoring wells are old and 15 are new. Many monitoring wells were destroyed, due to infrastructure work, between the time of the hydrological study and the start of pumping. New wells were therefore drilled in the vicinity of the destroyed wells. A monitoring well consists of a borehole with a diameter of 5 inches (12.7 cm) and a depth of 6 m, or until clay is reached, in which a 2 inch (5.08 cm) diameter pipe is placed. The lower 3 m are perforated and the pipe is surrounded by a gravel pack, see fig. 2.7. Monitoring well measurements are carried out once a month (EWRE, 2007).

In January 2008 seven pumping wells were drilled. A pumping well consists of a borehole with a diameter of 1 m and a depth of 6 m or less if the clay layer is reached. In each well a 14-16 inch (~40 cm) pipe is installed and surrounded by a gravel pack, see fig. 2.8. "Passive pumping" is used – meaning the wells are left to fill with oil and then depleted. Oil pumping was originally performed every two weeks. The pumps operate with compressed air. Only oil is removed, no water is pumped at the site. A problem with clogging exists (Bensabat, 2009).

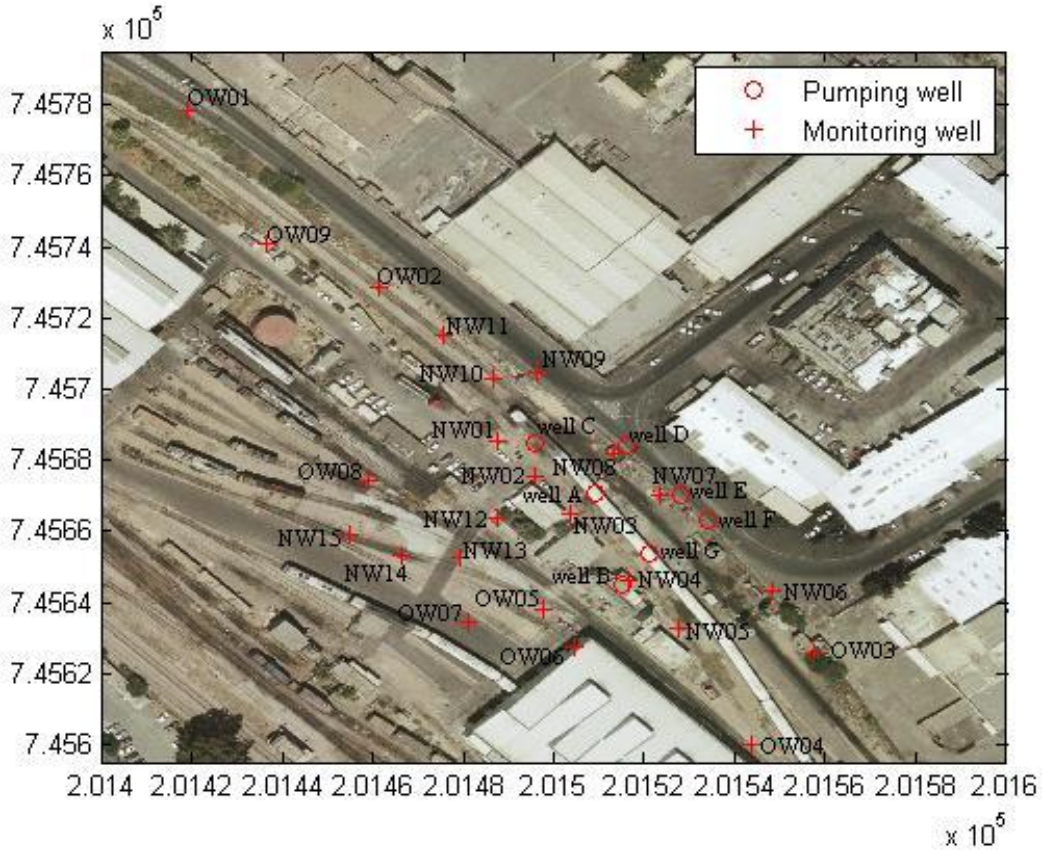

Fig. 2.6. Monitoring and pumping well locations. Wells with names starting with OW and NW are monitoring wells and well A to well G are pumping wells.

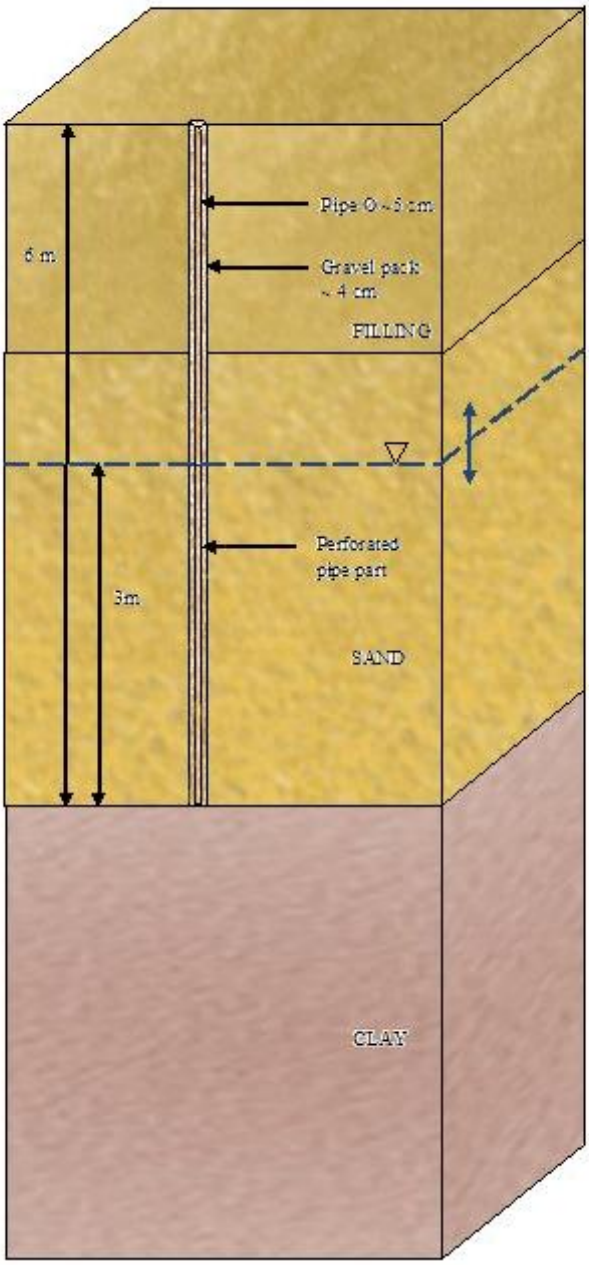

Fig. 2.7. Schematic picture of a monitoring well

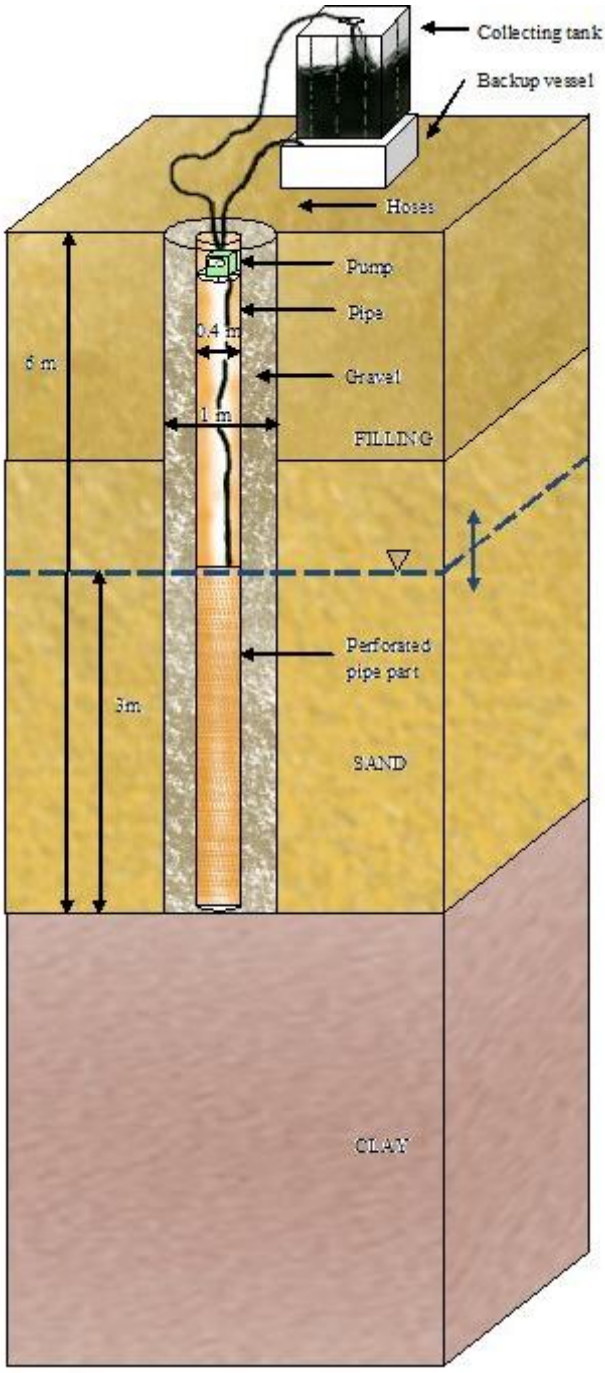

Fig. 2.8. Schematic picture of a pumping well

Measurements are made manually and time series exist for water level and oil level measurements (Bensabat, 2009). From this oil thickness values were calculated. Measurements from monitoring wells are available for the year 2006 (one measurement) and for the period 2008-2009, see fig. 2.9 and 2.10. Pumping well measurements have been made for the period 2008-2009, see fig. 2.11. For NAPL recovery from the pumping wells see fig. 2.12. Well measurements give a mean groundwater table elevation of ~0.8 m above sea level.

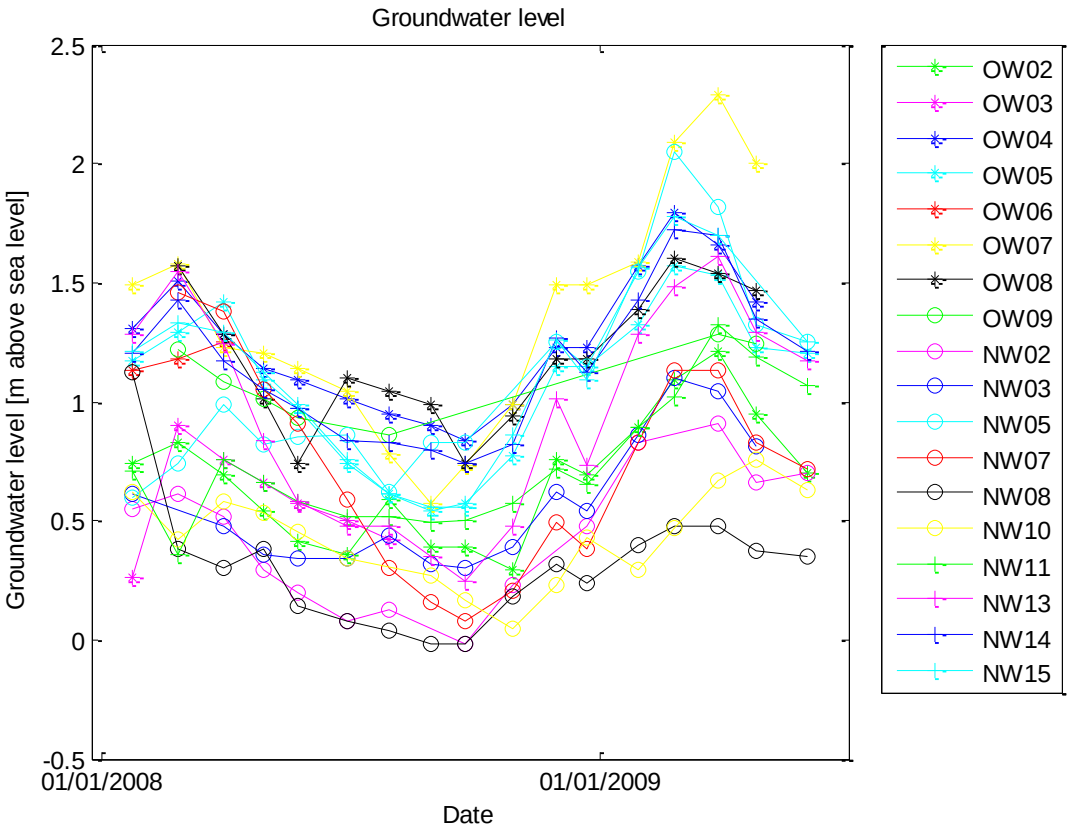

Fig. 2.9 Groundwater level in monitoring wells.

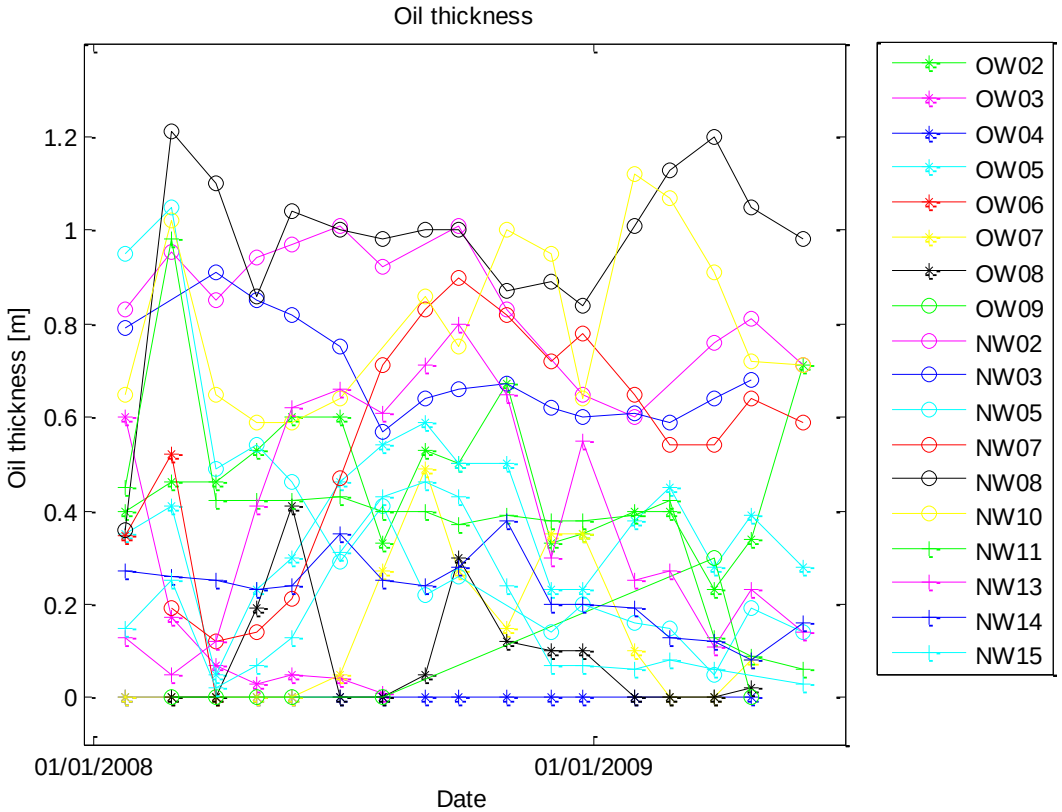

Fig. 2.10 Oil thickness in monitoring wells.

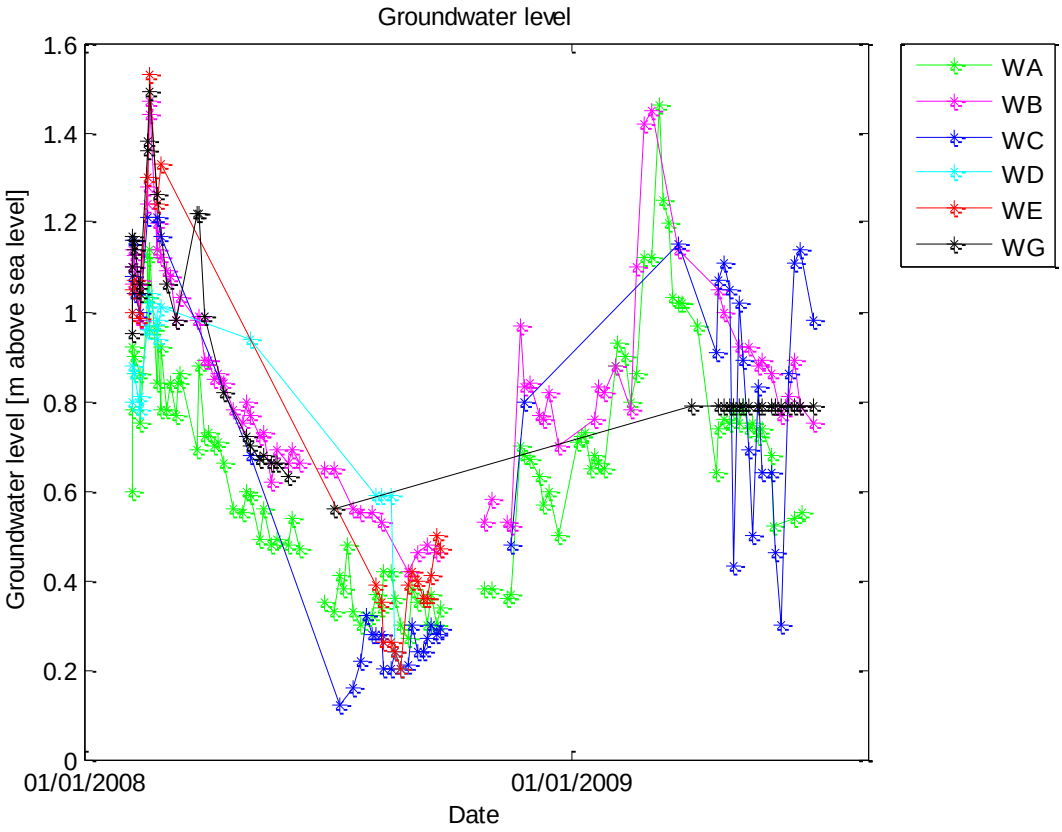

Fig. 2.11. Groundwater level in pumping wells. Well F not included.

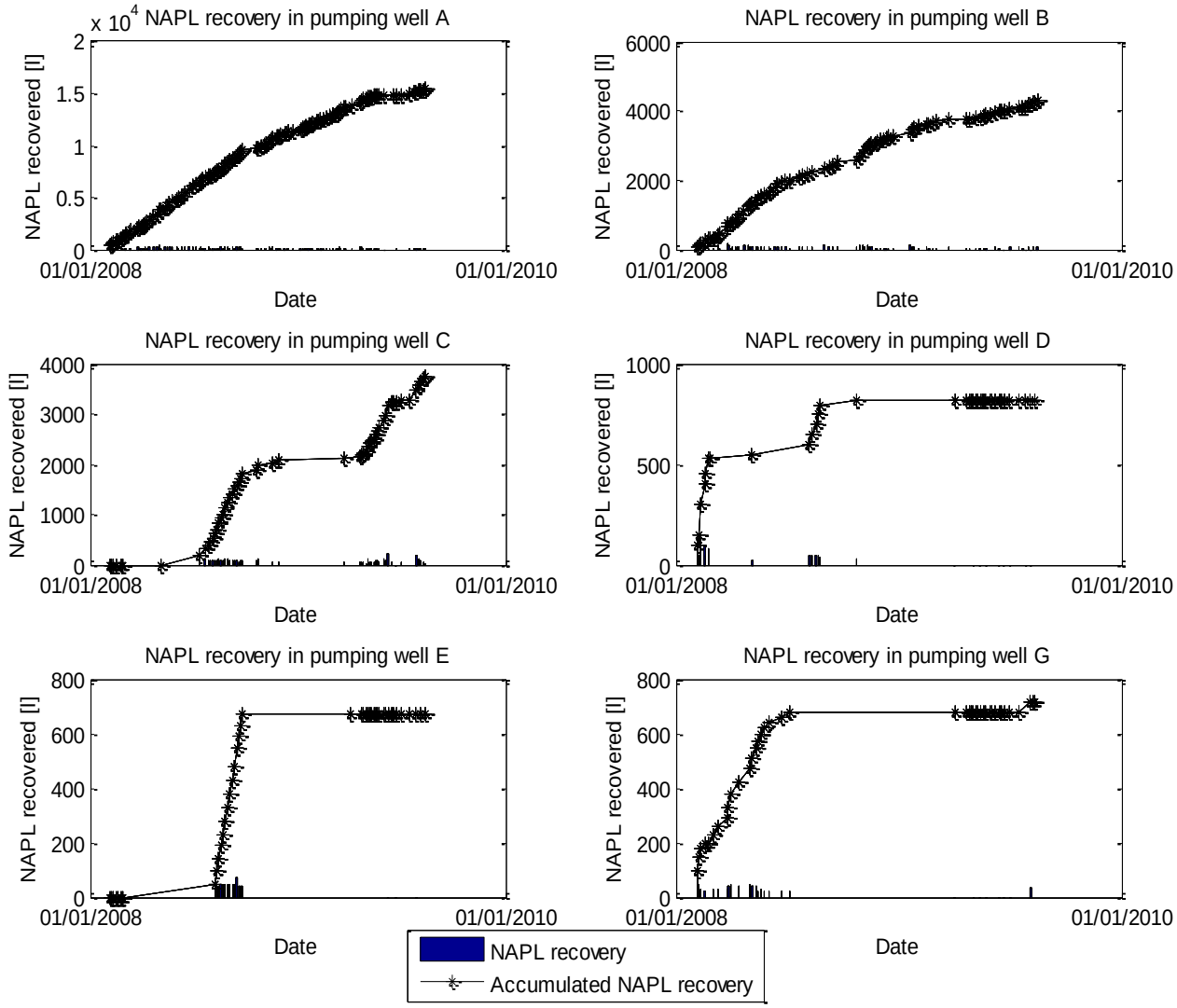

Fig. 2.12. NAPL recovery and accumulated NAPL recovery from pumping wells. As no NAPL has been recovered in well F this well is not shown.

2.2 TMVOC

This chapter is a description of some essential parts of the TMVOC model. As the model is quite comprehensive the whole model with all of its equations cannot be presented here. Parts of greater importance for this work have therefore been selected. The reference for this chapter, when not otherwise stated, is the "TMVOC manual" by Pruess & Battistelli (2002).

TMVOC is a simulation program, written in FORTRAN 77, for three-phase (aqueous, gas and NAPL) non-isothermal multicomponent flow in saturated-unsaturated heterogeneous media. The simulator has its roots in TOUGH2 but is modified to suit volatile organic chemicals.

Mass components considered by TMVOC are water, non-condensible gases and volatile organic chemicals which can be found in the gas, aqueous and NAPL phase. Local chemical and thermal equilibrium exists between phases, although mass transport between these (e.g. dissolution, evaporation and condensation) occur and optionally also biodegradation and adsorption of chemicals dissolved in the aqueous phase. Phase combinations that can occur are gas only, water only, NAPL only, gas and water, gas and NAPL, water and NAPL and finally gas, water and NAPL. In the model the gas phase is assumed to be comprised by real gases.

The mass-, or energy, balance for a component in the model is shown in eq. 1, where κ is the mass component, M is mass, V_n is volume and Γ_n is surface area, **F** is flux of mass/heat, **n** is the normal vector and q represents a source/sink.

$$\frac{d}{dt}\int_{V_n} M^k dV_n = \int_{\Gamma_n} \boldsymbol{F}^k \bullet \boldsymbol{n} d\Gamma_n + \int_{V_n} q^k dV_n \qquad \text{(eq. 1)}$$

The mass transport between phases is driven by a force to equalize the chemical potential. For each component the proportion of mole fraction in the phases corresponds to the equilibrium constants.

Darcy's law (for multiphase flow) expressing advection, eq. 2, and molecular diffusion are used to calculate transport.

$$\boldsymbol{F}_\beta = -k\frac{k_{r\beta}\rho_\beta}{\mu_\beta}\left(\nabla P_\beta - \rho_\beta \boldsymbol{g}\right) \qquad \text{(eq. 2)}$$

For each phase (β) the mass flux ($\boldsymbol{F}$) depend upon the absolute and relative permeability (k and $k_{r\beta}$), density (ρ_β), viscosity (μ_β) and pressure (P_β) of the phase as well as the acceleration of gravity ($\boldsymbol{g}$). If non-isothermal mode is used heat conduction and convection are also considered by the model, where conductivity (C) given by eq. 3 is dependent upon liquid saturation (S_l) and formation heat conductivity under liquid saturated (CWET) and desaturated (CDRY) conditions.

$$C(S_l) = CDRY + \sqrt{S_l \times [CWET - CDRY]} \qquad \text{(eq. 3)}$$

TMVOC uses temperature to calculate solubility (Henry's coefficient) of chemicals, gases and chemical vapors in the aqueous phase and water in the NAPL phase. Solubility of gases in the NAPL phase is however presumed to be temperature independent (constant Henry's coefficient). Solubility (x_w^g) for non-condensable gases (g) in water is calculated from eq. 4 using Henry's coefficient (K_H) and pressure (P_g).

$$P_g = K_H x_w^g \qquad \text{(eq. 4)}$$

One of the alternatives for pressure-temperature and volume relationship is given by the Soave-Redlich-Kwong equation of state, here showed for a multicomponent gas mixture eq. 5.

$$Z^3 - Z^2 + \left(\frac{a_m P}{R^2 T^2} - \frac{b_m P}{RT} - \left(\frac{b_m P}{RT}\right)^2\right) Z - \frac{a_m P}{R^2 T^2}\frac{b_m P}{RT} = 0 \qquad \text{(eq. 5)}$$

The parameters are the real gas compressibility factor (largest Z root), pressure (P), absolute temperature (T) and universal gas constant (R). a_m and b_m given by eq. 6 and eq. 7 are functions of the mole fraction in the gas phase (x_g^κ).

$$a_m = \left(\sum_\kappa x_g^\kappa \, (a_\kappa)^{1/2}\right)^2 \qquad \text{(eq. 6)}$$

$$b_m = \sum_\kappa x_g^\kappa \, b_\kappa \qquad \text{(eq. 7)}$$

Where $a_\kappa = f(P_{c\kappa}, T_{c\kappa}, R, T, \omega_\kappa)$ and $b_\kappa = f(P_{c\kappa}, T_{c\kappa}, R)$, i.e. functions of critical pressure (P_c), critical temperature (T_c) and Pitzer's acentric factor (ω).

TMVOC also calculates and takes into consideration enthalpy, gas heat capacity, viscosity (e.g. calculated according to Yaws equation) and saturated vapor pressure (calculated according to the Wagner or Antoine equations).

The last term in eq. 1 handles sinks and sources and different types exist. The types used for this work are deliverability wells (pumps), heat injection or production (temperature changes) and fluid injection (pollution spill). A deliverability well's phase production rate is given by eq. 8. An alternative can be chosen for which the pumped fluid phase composition will be the same as the phase composition in the producing element. This is done by replacing $k_{r\beta}/\mu_\beta$ with the phase saturation (S_β) in equation 8.

$$q_\beta = \frac{k_{r\beta}}{\mu_\beta}\rho_\beta \times PI \times \left(P_\beta - P_{wb}\right) \quad \text{if } P_\beta > P_{wb} \qquad \text{(eq. 8)}$$

P_{wb} is flowing bottomhole pressure and PI is productivity index, which can be derived from layer thickness (Δz_l), permeability (k), grid block radius (r_e), well radius (r_w) and skin factor (s), eq. 9.

$$(PI)_l = \frac{2\pi(k\Delta z_l)}{ln(r_e/r_w)+s-1/2} \qquad \text{(eq. 9)}$$

As the grid blocks in the model have a rectangular shape, an effective radius is calculated using eq. 10.

$$r_e = \sqrt{\Delta x \times \Delta y/\pi} \qquad \text{(eq. 10)}$$

The permeability of specific grid blocks can be altered, using permeability modification coefficients (ξ), eq. 11. k_{ROCKS} is the original block permeability and $k_{modified}$ is the permeability obtained after the modification. If this function is used the capillary pressure is divided by the square root of the permeability modification coefficient.

$$k_{modified} = k_{ROCKS} \times \xi \qquad \text{(eq. 11)}$$

TMVOC provide some standard capillary pressure functions and relative permeability functions.

In this work water retention is described by the van Genuchten (1980) capillary pressure-saturation function as presented by Parker et al. (1987). Capillary pressure between the gas and the water phase (P_{cgw}), between the NAPL and the water phase (P_{cnw}), and between the gas and the NAPL phase (P_{cgn}), are given by eq. 12-14 respectively. These are functions of effective water saturation ($\bar{S}_w$) and effective total liquid saturation ($\bar{S}_L$). Where effective means that residual water saturation is excluded when calculating the relative saturation. The other parameters are water density (ρ_w), acceleration of gravity (g), parameters describing the retention curve shape (α, n and m (m=1-1/n)) and scaling factors (β).

$$P_{cgw} = -\frac{1}{\beta_{nw}} \times \frac{\rho_w g}{\alpha} \left(\bar{S}_w^{-1/m} - 1\right)^{1/n} - \frac{1}{\beta_{gn}} \times \frac{\rho_w g}{\alpha} \left(\bar{S}_L^{-1/m} - 1\right)^{1/n} \quad \text{(eq. 12)}$$

$$P_{cnw} = P_{cgw} - P_{cgn} \quad \text{(eq. 13)}$$

$$P_{cgn} = -\frac{1}{\beta_{gn}} \times \frac{\rho_w g}{\alpha} \left(\bar{S}_L^{-1/m} - 1\right)^{1/n} \quad \text{(eq. 14)}$$

The scaling factor enables a scaling of the capillary pressure–saturation functions, obtained for a two fluid phase system, to a three phase system. This can be accomplished under the assumption of the following wetting order, water>NAPL>air, a rigid media, negligible fluid-solid interference and a monotonic saturation path, i.e. no hysteresis (Parker et al., 1987). The scaling procedure presented by Fagerlund et al. (2006), eq. 15-17, is used. The scaling factors are determined by the interfacial tension (σ). Ref stands for reference fluids, i.e. the two phase system fluids, usually air and water.

$$\beta_{gn} = \frac{\sigma_{ref}}{\sigma_{gn}} \quad \text{(eq. 15)}$$

$$\beta_{nw} = \frac{\sigma_{ref}}{\sigma_{nw}} \quad \text{(eq. 16)}$$

$$\beta_{gw} = \frac{\sigma_{ref}}{\sigma_{nw} + \sigma_{gn}} \quad \text{(eq. 17)}$$

The relative permeability functions used are described by a modified version of Stone's first three-phase method given by eq. 18-20. Where k_{rx} is relative permeability to x=water (w), air (g) and NAPL (n). The parameters are water saturation (S_w), residual water saturation (S_{wr}), residual NAPL saturation (S_{nr}), gas saturation (S_g), residual gas saturation (S_{gr}) and an empirical parameter (n).

$$k_{rw} = \left[\frac{S_w - S_{wr}}{1 - S_{wr}}\right]^n \quad \text{(eq. 18)}$$

$$k_{rn} = \left[\frac{1 - S_g - S_w - S_{nr}}{1 - S_g - S_{wr} - S_{nr}}\right] \left[\frac{1 - S_{wr} - S_{nr}}{1 - S_w - S_{nr}}\right] \left[\frac{(1 - S_g - S_{wr} - S_{nr})(1 - S_w)}{1 - S_{wr}}\right]^n \quad \text{(eq. 19)}$$

$$k_{rg} = \left[\frac{S_g - S_{gr}}{1 - S_{wr}}\right]^n \quad \text{(eq. 20)}$$

TMVOC discretizes space and time using an integral finite difference method (IFDM) and first-order backward finite difference respectively. The linear equation solver used in this

work is a stabilized bi-conjugate gradient solver, one of five available solvers in the model. Newton-Raphson iteration is used when solving the system of equations.

TMVOC requires input data on space discretization (MESH/GRID), soil (ROCKS) and chemical (CHEMP) properties, solver to be used as well as initial and boundary conditions. If sinks or sources (GENER) exist, these of course have to be specified. Further details about the input data is given in the following sections.

2.3 MODEL IMPLEMENTATION

2.3.1 Chemical composition of the pollution

Implementing a polluting chemical, in this case diesel, into the TMVOC model was done by describing its chemical properties in the input file (CHEMP field). As the composition of the diesel at the site is unknown a "standard" diesel composition was sought. Analyses have shown diesels to exhibit large compositional variations (Sjögren et al., 1995 and Joo et al., 1998). The variations depend on oil origin and refinement processes. Two approaches were used – describing diesel as a multicomponent mixture and describing diesel as one component.

Diesel is a multicomponent mixture and it is not feasible to include all diesel components in a model. In accordance with the report by Gustafson et al. (1997) a method was used in which constituents were divided into subgroups sharing resembling physical and chemical qualities, table 2.2. For the division Equivalent Carbon number (EC), which is determined by a components boiling point, was used. All the subgroups then represent the mixture in the model.

Table 2.2. Appropriate fractions according to Gustafson et al. (1997).

EC Range	Classification
5-6	Aliphatics
>6-8	
>8-10	
>10-12	
>12-16	
>16-35	
Benzene(6.5)	Aromatics
Toluene (7.6)	
>8-10	
>10-12	
>12-16	
>16-21	
>21-35	

Diesel constituents and weight percentages as reported by Gustafson et al. (1997) after communication with BP are presented in Appendix A, table A1. This composition is incomplete and the constituents represent a maximum of only 35 weight percentage of the total diesel composition, table 2.3. However no detailed description of a more complete diesel composition was found so the "standard" diesel was constructed from these maximum weight percentages.

The constituents were grouped into the proposed subgroups, see table A1 in Appendix A, and the EC average (eq. 21) for each subgroup was calculated, table 2.3.

$$EC\ average = \frac{EC_1 \times max\ weig\ ht\ percent\ _1 + EC_2 \times max\ weig\ ht\ percent\ _2 + \ldots + EC_n \times max\ weig\ ht\ percent\ _n}{max\ weig\ ht\ percent\ _1 + max\ weig\ ht\ percent\ _2 + \ldots + max\ weig\ ht\ percent\ _n} \quad \text{(eq. 21)}$$

Where $EC_{1,\ldots,n}$ are the individual EC numbers of the constituents in a subgroup and max weight $percent_{1,\ldots,n}$ are the individual maximum weight percentages of the constituents in the subgroup.

A component with an EC number approximately equal to the EC average of the subgroup was then chosen to represent the entire subgroup, table 2.3, in accordance with Fagerlund and Niemi (2007). E.g. in this case fraction 8 having an EC average of 8.78 is represented by o-xylene with an EC number of 8.81.

Table 2.3. Subgroups, fraction numbers, weight percentages, EC averages and representative components.

		Weight percentage in diesel [%]				
EC Range subgroups	Fraction number	Min	Max	Mean	EC average	Representative component (EC)
>6-8	1	0.1	0.1	0.1	8	n-Octane (8)
>8-10	2	0.47	1.69	1.08	9.71	n-Decane (10)
>10-12	3	1.57	4.8	3.185	11.52	n-Dodecane (12)
>12-16	4	5.51	11.4	8.455	14.52	n-Pentadecane (15)
>16-35	5	4.45	9.02	6.735	18.77	n-Nonadecane (19)
Benzene(6.5)	6	0.003	0.1	0.0515	6.5	Benzene (6.5)
Toluene (7.6)	7	0.007	0.7	0.3535	7.58	Toluene (7.58)
>8-10	8	0.176	1.609	0.8925	8.78	o-Xylene (8.81)
>10-12	9	0.044	0.872	0.458	11.58	Naphthalene (11.69)
>12-16	10	0.822	4.17	2.496	13.65	1-Methylnaphthalene (12.99)
>16-21	11	0.0341	0.527	0.2805	18.71	Phenanthrene (19.36)
>21-35	12	0.0005	0.0228	0.0116	22.77	Fluoranthene (21.85)
Sum		13.19	35.01	24.10		

The component having the EC number closest to the EC average of fraction 10 was 1,5-dimethylnaphthalene (EC=13.87). But as this chemical is not included in the list presented by Reid et al. (1987), the next closest component, 1-methylnaphthalene, was instead used as the representative component for the fraction.

To approximate a complete diesel composition the incomplete diesel composition of table 2.3 was compared to the composition presented by Kolev (2007), table 2.4. Fractions 1 to 5 (27.01 weight percentage) contain alkanes and are equal to paraffin. The remaining fractions (8.00075 weight percentage) contain both naphthalene and aromates and are therefore treated as a collective.

Table 2.4. Diesel composition (Kolev, 2007).

	Mass percent [%]
Paraffin	45.6
Naphthalene	25.6
Aromates	28.6

The missing 65 weight percentage was divided between the fractions in such a way that the composition in table 2.4 was obtained. The assumption was made that the calculated EC averages still were representative for the subgroups.

Benzene and toluene being the only constituents in their respective fraction were kept at their reported max weight percentages. Fractions 1 to 5 should comprise 45.6 weight percentage and fractions 6 to 12 should comprise 54.4 (100-45.6) weight percentage. New weight percentage values were calculated using eq. 22 for fraction 1 to 5 and eq. 23 for fraction 8 to 12.

$$New\ weight\ percentage\ = weight\ percentage\ \times \frac{45.6}{27.01} \qquad \text{(eq. 22)}$$

$$New\ weight\ percentage\ = weight\ percentage\ \times \frac{(54.4-0.1-0.7)}{(8.00075-0.1-0.7)} \qquad \text{(eq. 23)}$$

0.1 and 0.7 are weight percentage of benzene and toluene respectively.

The assumed new composition can be seen in table 2.5.

Table 2.5. Diesel fractions and their weight percentage.

Fraction number	Representative component	Calculated new weight percentage [%]
1	n-Octane	0.17
2	n-Decane	2.85
3	n-Dodecane	8.10
4	n-Pentadecane	19.25
5	n-Nonadecane	15.23
6	Benzene	0.1
7	Toluene	0.7
8	o-Xylene	11.98
9	Naphthalene	6.49
10	1-Methylnaphthalene	31.04
11	Phenanthrene	3.92
12	Fluoranthene	0.17
Sum		100

To make the simulations less time consuming fraction 1 and 12, which constitute a small part of the total composition, were neglected. Phenanthrene was also excluded due to lack of data. The chemical properties of the representative components used by TMVOC are shown in Appendix A, table A2 to A4.

A second approach to implement diesel into the model was to let the mixture be represented by one component. Diesel constituents exhibit a range of different chemical properties (e.g. boiling points) and an approximation must therefore be attempted. According to Kolev (2007) diesel, if represented as one component, could be considered to have the properties seen in Appendix A, table A5. The remaining parameters were assumed to equal those of o-xylene, which have shown to be the most stable to simulate of the large component fractions.

2.3.2 Soil

Soil properties were implemented in the TMVOC model by specifying parameter values in the input file (ROCKS field). Starting estimations can be seen in table 2.6. In the model simplifications had to be made. Since the groundwater table always is located in the sand layer it is probably unnecessary to include the clay layer in the model. The clay layer, having a much smaller conductivity than sand, was implemented as a no-flow-boundary, making clay properties redundant. Neglecting the clay layer should also make the simulations less time consuming. The filling was assumed to have similar properties as sand and therefore the model was simplified to one layer of sand. Only sand properties were therefore needed to be put into the model. As no field or laboratory measurements of retention or hydraulic conductivity for the actual soil were available properties were estimated from a soil retrieved from the UNSODA Access database. In table 2.6 the starting point for the soil search is shown. A sand with a saturated conductivity of approximately 2 m/h (4800 cm/d) and an effective porosity of 0.25 was sought. The closest match was UNSODA soil no. 2584, a sand from Schachen exhibiting a saturated hydraulic conductivity of 4924.8 cm/d and a porosity of 0.284. For this sand laboratory measurements on a drying cycle containing 6 water retention and 4 hydraulic conductivity values were available (Nemes et al., 1999).

Table 2.6. Starting estimations (Bensabat, 2009).

	Effective porosity [-]	Saturated conductivity to water [m/h]	Anisotropy ratio [-]
Filling	0.25	2	1
Sand	0.25	2	1
Clay	0.06	0.0001	1

The soil from the UNSODA database was then applied as the model sand. The computer code RETC (van Genuchten et al., 1991), providing nonlinear least-squares optimization, was used to estimate α and n, for eq. 12-14, from known retention and hydraulic conductivity measurement values for a van Genuchten function and Mualem model. α and n are parameters describing the shape of the water retention curve. A simultaneous fit of water retention and hydraulic conductivity data was conducted. In- and output files can be seen in Appendix B. Initial values of residual water content (θ_r), saturated water content (θ_s), empirical parameters (α, n, m, l) and saturated hydraulic conductivity (K_s) had to be estimated for the RETC run. Some values were retrieved from an article by Carsel & Parrish (1988). K_s and θ_s (assuming it equals porosity) were taken directly from UNSODA. Residual saturation for water in sand (S_r) was chosen to be 0.10 (Mercer & Cohen, 1990) giving θ_r=0.0284. The final fitted parameters are shown in table 2.7.

Table 2.7. RETC result for estimation of van Genuchten and Mualem parameters. r^2 equal to 1 is a perfect fit to observations, here r^2=0.94.

Residual water content [-]	θ_r	0.0284
Saturated water content [-][A]	θ_s	0.284
Empirical parameter [cm^{-1}]	α	0.12134
Empirical parameter [-]	n	2.08699
Empirical parameter [-][B]	m	0.52084
Empirical parameter [-][B]	l	0.5
Saturated hydraulic conductivity[A] [cm/d]	K_s	4924.8

A UNSODA (Nemes et al. 1999). **B** l was assumed to be 0.5 and m=1-1/n.

To be able to use the capillary pressure – saturation functions obtained from the UNSODA sand, which is a two fluid phase (air and water) system, in the model the function had to be scaled to a three phase (air, water and NAPL) system. The scaling was achieved by using the scaling factor as described in eq. 15 and 16 for NAPL-water and air-NAPL systems. Scaling parameters were calculated with eq. 24 and 25.

$$\beta_{gn} = \frac{\sigma_{ref}}{\sigma_{gn}} = \frac{0.0728\ Nm^{-1}}{0.025\ Nm^{-1}} = 2.912 \qquad \text{(eq. 24)}$$

$$\beta_{nw} = \frac{\sigma_{ref}}{\sigma_{nw}} = \frac{0.0728\ Nm^{-1}}{0.050\ Nm^{-1}} = 1.456 \qquad \text{(eq. 25)}$$

Where σ_{nw}=0.05 Nm^{-1} and σ_{gn}=0.025 Nm^{-1} are the interfacial tension and surface tension for diesel respectively at 20 °C (Mercer & Cohen, 1990) and σ_{ref}=0.0728 Nm^{-1} at 20 °C (The Engineering ToolBox, 2005), air and water being the reference fluids.

In the relative permeability functions, eq. 18-20, n is an empirical constant between 2 and 3 (McCray & Falta, 1997), here chosen to be 3. Residual NAPL saturation was approximated to 0.15 (Mercer & Cohen, 1990). This is however a value based on diesel residual saturation in an unspecified soil. Tortuosity factor for binary diffusion was set to 0, which makes TMVOC apply the Millington and Quirk model to calculate tortuosity as a function of porosity and saturation.

Atmospheric properties were included in the model. The values for the atmosphere parameters were taken from an example in the TMVOC guide (Pruess & Battistelli, 2002, p. 108) and then slightly altered to suit the specific model. The capillary pressure and relative permeability functions are different to the ones used for the soil. Zero capillary pressures (P_{cgn} and P_{cgw}) were chosen and the relative permeability was described by a modified version of Stone's first three-phase method.

Complete input data for soil properties can be seen in Appendix C, table C.

2.3.3 Temperature

TMVOC can be used in isothermal mode or taking into account temperature changes in the model's soil profile. For simulations in isothermal mode, as was the case for the 3D model, a constant temperature of 20 °C in the whole model was assumed. However in real life the air temperature varies between 8 °C and 40 °C during the year, effecting the soil temperature and potentially e.g. the viscosity of chemicals. This was tested in a radially symmetric single well model.

Incorporating the yearly temperature fluctuations into the model was done by time-dependent Dirichlet boundary conditions. Sinks and sources were placed in each atmospheric boundary grid block to accomplish time-dependent boundary conditions. Large volume boundary grid blocks ($V=10^{50}$ m^3) with small nodal distances ($D=10^{-9}$ m) can be used to make the influence on the boundary grid blocks from other grid blocks negligible and to prevent alterations of their thermodynamic parameters (Pruess & Battistelli, 2002).

Heat was injected into or produced from the atmospheric grid blocks using sinks or sources of the type HEAT. The temperature (T) is given by eq. 26, where T_0 is start temperature and the second term is the temperature change.

$$T = T_0 + \frac{dT}{dt}\Delta t \qquad \text{(eq. 26)}$$

Sinks and sources were implemented into the TMVOC model through the GENER field were sink or source grid placement and energy rate (GX) were specified. The energy needed to raise the temperature ($E_{\Delta T}$) was calculated knowing the grid block volume (V), rock grain density (DROK), temperature change (ΔT), rock grain specific heat (SPHT) and porosity (ϕ) eq. 27.

$$E_{\Delta T} = V \times DROK \times SPHT \times \Delta T \times (1 - \phi) \qquad \text{(eq. 27)}$$

The required energy was then divided by the time during which the temperature change occur to acquire the energy rate (GX) in J/s.

Average temperature variation during a year is shown in table 2.8. These temperatures are for a depth of 10 cm but they are here used for the atmospheric grid blocks. The yearly mean temperature is 20.42 °C. A simplified temperature fluctuation can be represented by the function in fig. 2.13. The heat conductivity in the model is interpolated using eq. 3.

Table 2.8. Mean temperatures for a depth of 10 cm calculated from temperatures in table 2.1.

	Jan	Feb	Mar	Apr	May	Jun	Jul	Aug	Sep	Oct	Nov	Dec
Mean T [°C]	12.95	13.1	15.05	18.75	21.7	24.95	27.05	27.5	25.8	23.25	19.05	15.05
~	13	13	15	19	22	25	27	28	26	23	19	15

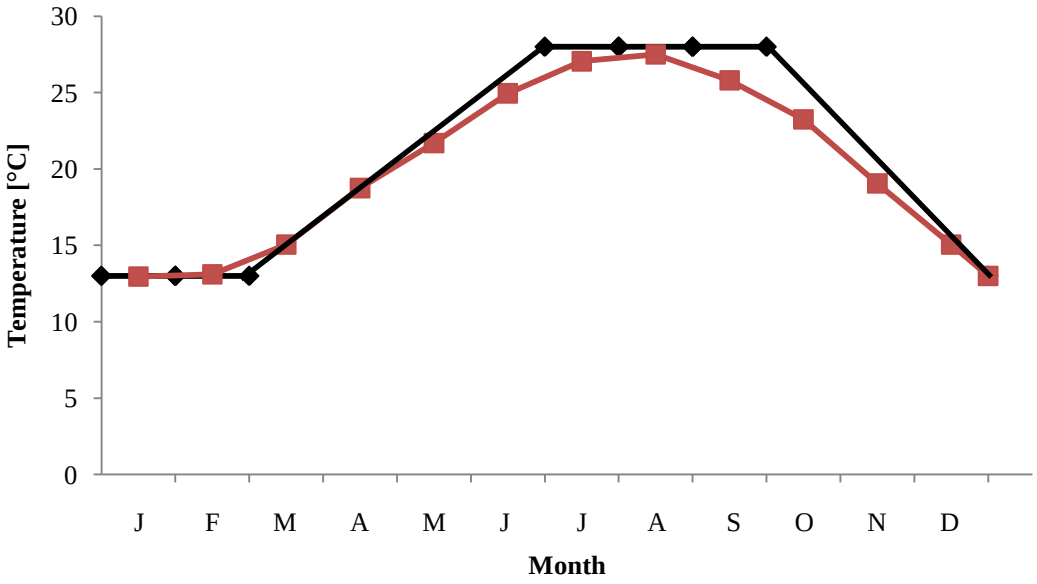

Fig. 2.13. Temperature fluctuation: temperature average (red) and simplified temperature function (black). For the simplified function the temperature is constant during January-February and July-September and otherwise increasing or decreasing at constant rates.

2.3.4 Groundwater table

A static groundwater table can be implemented in a model by assigning an appropriate pressure (so that atmospheric pressure is obtained at the wanted groundwater level) to grid blocks and then locking them by making them inactive. A fluctuating groundwater level can be created by placing sinks and sources (GENER field) in boundary grid blocks and with these inject water alternatively change the pressure profile. This creates a time-dependent Dirichlet boundary condition. The volumes and nodal distances were the same as the one's used to accomplish varying temperature.

The inactive element method is more computational effective (Pruess & Battistelli, 2002) so a static groundwater table was used in the large 3D-model. A changing groundwater level was however tested in a radially symmetric single well model. Only fluctuation in the form of vertical displacement was wanted simultaneously over the area being studied. A vertical migration was obtained by making the water phase pressure at the bottom boundary grid block change with time.

A grid with large volume bottom grid blocks and reversed connections between the bottom grid blocks and the ones directly above these was used. This made the model treat the bottom grid blocks as if they were connected to the top of the next bottom grid block, achieving the effect seen in fig. 2.14, still keeping the depth right although not the volume. The pressure in the profile is then determined by the pressure in the large volume "bottom" grid blocks.

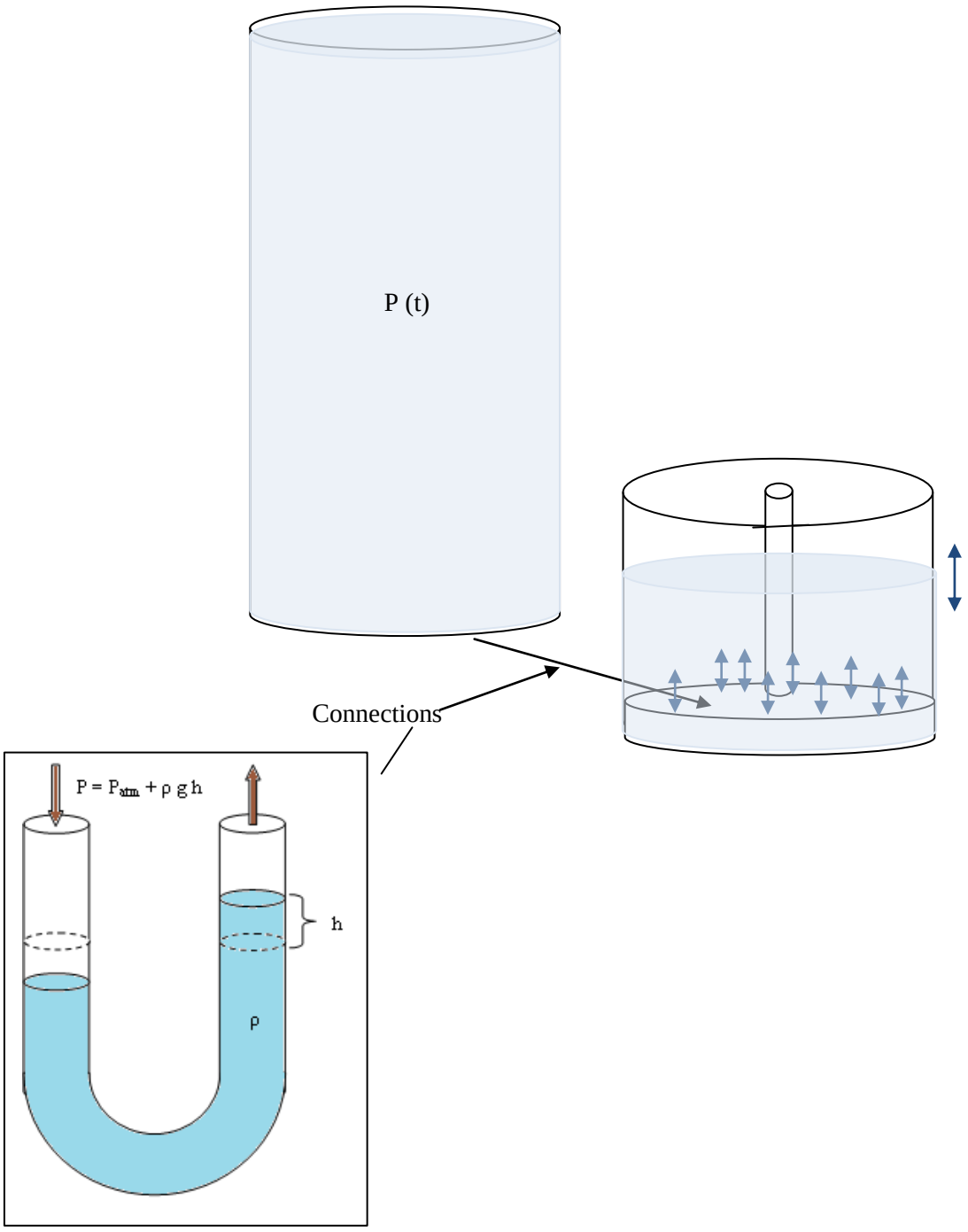

Fig. 2.14. Fluctuating groundwater table concept.

The pressure in the large volume "bottom" grid blocks was changed step wise, using multiple step wise simulations with new initial pressure conditions (INCON) for each simulation.

A simplified groundwater table fluctuation function, with the highest elevation in May and lowest elevation in September (see section 2.1.1 Location) and piece wise constant rise and fall between these points, see fig 2.15, was used. The groundwater level was assumed to fluctuate around a depth of 3 m (±0.75 m), see table 2.9.

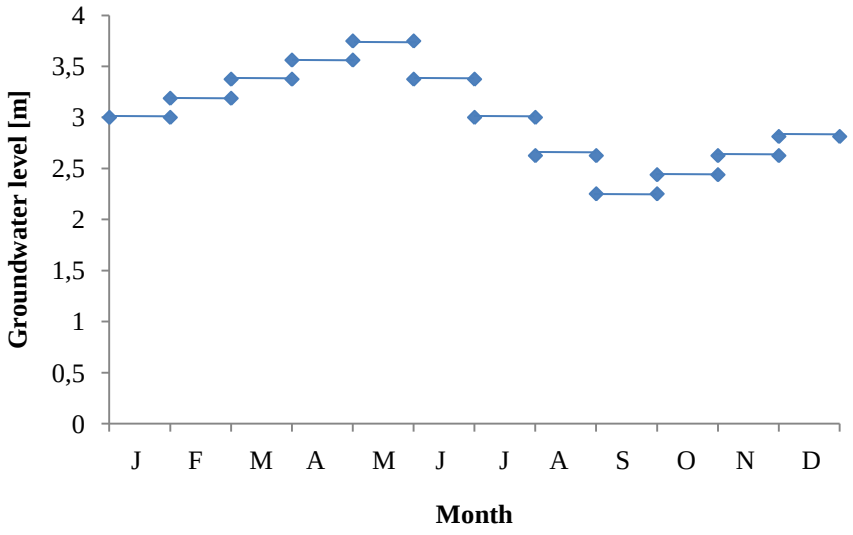

Fig. 2.15. Groundwater level simplified as a piece wise constant function.

Table.2.9. Groundwater level and corresponding pressure in the large volume "bottom" grid blocks.

Month	Groundwater level [m]	Pressure [Pa]
J	3	1.25767E+05
F	3.1875	1.27602E+05
M	3.375	1.29437E+05
A	3.5625	1.31273E+05
M	3.75	1.33108E+05
J	3.375	1.29437E+05
J	3	1.25767E+05
A	2.625	1.22097E+05
S	2.25	1.18427E+05
O	2.4375	1.20262E+05
N	2.625	1.22097E+05
D	2.8125	1.23932E+05

2.3.5 Remediation system

The pumping wells were implemented as sinks in the TMVOC model (GENER field). To imitate the pumping wells on site, the option of deliverability wells against a flowing bottomhole pressure was chosen.

Two options exist when pumping, letting the pumped fluid composition be determined by the relative mobilities of phases in the source element (MOP(9)=0) or letting the pumped fluid phase composition be the same as the phase composition in the producing element i.e. the element containing the well (MOP(9)=1). The first alternative was chosen. As only NAPL phase is pumped in real life, only NAPL phase should be pumped in the model and therefore the TMVOC code had to be altered slightly to accomplish this.

A change was made in subroutine PHASD. The following line:

```
C-----COMPUTE MASS FLOW RATE.

FF((N-1)*NPH+NP)=FF((N-1)*NPH+NP)*PIN*DELP
```

was substituted by:

```
C-----COMPUTE MASS FLOW RATE.

      IF(NP.EQ.1.OR.NP.EQ.2) THEN

       FF((N-1)*NPH+NP)=0.

      ELSE

       FF((N-1)*NPH+NP)=FF((N-1)*NPH+NP)*PIN*DELP

      END IF
```

This prevents outflow of gas and water phase in the deliverability wells. But dissolved gas and water in the NAPL phase are still permitted to flow out as in real life.

As the wells are screened (have intake) from a depth of 3 to 6 m, the sinks (deliverability wells) were placed in the bottom six grid blocks, at each well location. These layers had a thickness of 0.5 m, see section 2.4.1 Grid. To simplify the model the impermeable construction of the wells was neglected in the 3D model. This could possible contribute to some differences from real life pumping as NAPL could be pumped through areas which should be impermeable. This makes inflow from above and not just from the well sides possible.

Table 2.10 shows the TMVOC input data for the 3D-model deliverability wells. Bottomhole pressure (P_{wb}) was assumed to equal atmospheric pressure. Table 2.11 shows parameters for calculating productivity index (PI) in accordance with eq. 9.

Table 2.10. TMVOC input data for pumping wells in the 3D-grid.

	TMVOC name	
Number of open layers	LTAB	6
Option for sink	TYPE	DELV
Productivity index PI [m^3]	GX	2.6E-11[A]
Bottomhole pressure P_{wb} at the center of the topmost producing layer [Pa]	EX	1.013E+5
Thickness of layer [m]	HG	0.5

A Calculated according to eq. 9, the same for all six grid blocks.

Table 2.11. Parameters for calculating PI for the 3D-grid.

Permeability [m^2]	K	1.0E-11
Layer thickness [m]	Δz_l	0.5
Effective grid block radius [m]	r_e	2.821[A]
Well radius [m]	r_w	0.5
Skin factor [-]	S	0

A Calculated according to eq. 10 and an area of 5x5 m^2.

The skin factor (s) accounts for the pressure drop due to drilling inflicted permeability change around the wellbore. A skin factor of zero would correspond to a zero permeability change. The skin factor can be calculated with Hawkins formula eq. 28 (Ahmed & McKinney, 2005).

$$S = \left(\frac{k}{k_s} - 1\right) \ln \frac{r_s}{r_w} \qquad \text{eq. 28}$$

Where k is permeability, k_s is permeability in the skin zone (permeability effected zone) and r_s is the skin zone radius. The soil outside the well radius was assumed not to be impacted and therefore to have the same permeability as undisturbed soil. This assumption was however not based on any measurements.

As NAPL thickness in the ground does not equal NAPL thickness in a well, no "monitoring wells" in the form of print outs of phase composition at monitoring well locations were implemented. For the purpose of comparison with real life measurements they would be misleading. Instead pumped volume was chosen for the comparison of historical and model values.

The productivity index in the radially symmetric model was assumed to equal 2.09E-11.

2.4 SIMULATION SCHEME

2.4.1 Grid

The area modeled is 180 m x 130 m centered around a hypothetical line source, fig. 2.16. This constitutes a rectangle with corner coordinates shown in table 2.12. One of the rectangle's corner coordinates was used as point (0,0) in an new coordinate system, oriented in an angel of approximately 56° from the first coordinate system. Fig. 2.16 shows the area in the new coordinate system and the placement of the line source and pumping wells.

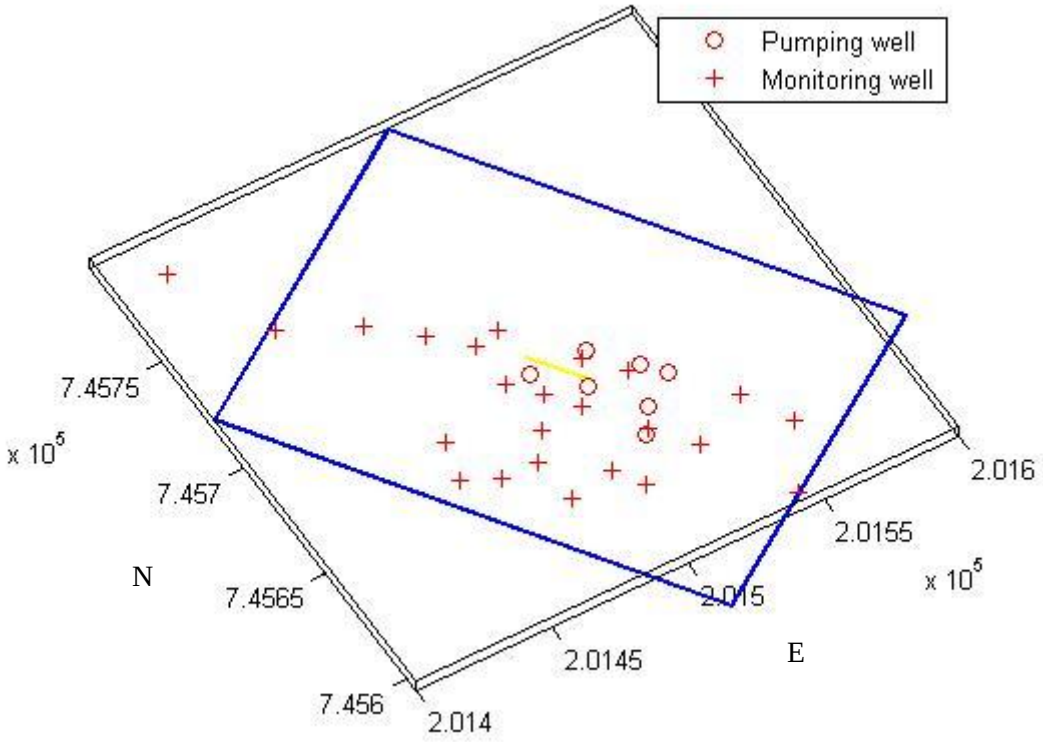

Fig. 2.16. Modeled area (blue rectangle) and hypothetical line source (yellow line).

Table 2.12. Corner coordinates of the model area.

Easting	Northing
201401.0963	745720.0691
201508.6511	745793.0894
201502.2014	745571.1471
201609.7562	745644.1674

The model is a rectangular box (180 m x 130 m x 6 m), with a depth of 6 m.

A grid was created to represent the site. In the vertical (z-)direction the grid spacing had the following distribution: a 0.001 m top grid block followed by twelve 0.5 m grid blocks, fig. 2.17. There were a total of 13 grid blocks in the z-direction.

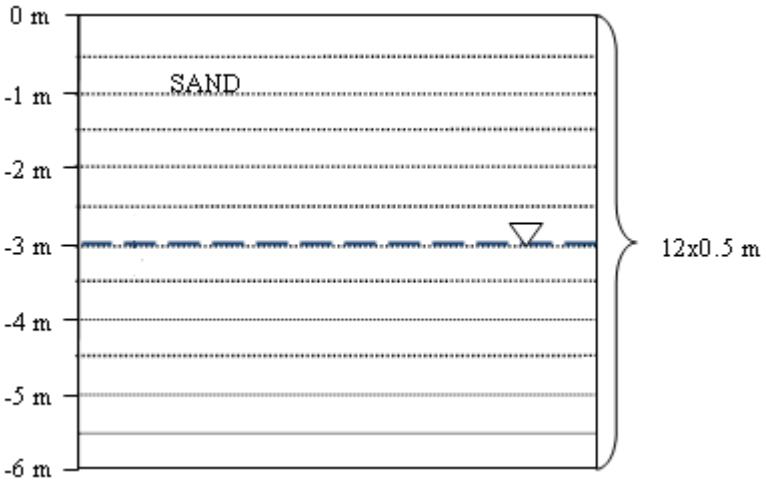

Fig. 2.17. Grid spacing in the vertical direction. The top grid block is not shown.

In the x-direction the grid spacing was (20) 5 m grid blocks around the line source and pumping wells, (4) 10 m grid blocks on both side of those and 0.001 m boundary grid blocks at each end, fig. 2.18. In the x-direction there were a total of 30 grid blocks.

In the y-direction the grid spacing was (14) 5 m grid blocks around the line source and pumping wells, outside these were (3) 10 m grid blocks, fig. 2.18. In the y-direction there were a total of 20 grid blocks.

Total number of grid blocks in the model was 7800.

For the single well simulation a radially symmetric model was used. Two different grids were created for this, one with large volume boundary grid blocks on top and at the bottom and one with small volume boundary grid blocks on top and no extra bottom grid blocks. The mesh with small volume boundary grid blocks was used for static groundwater table simulations using the inactive element method. The mesh with large volume boundary blocks was used for fluctuating groundwater and temperature condition simulations.

The radially symmetric grid for static temperature and groundwater level simulations:

In the vertical direction the grid spacing had the following distribution: a zero volume top grid block followed by twelve 0.5 m grid blocks. In the horizontal direction the grid spacing was a 0.5 m radius followed by ten cylinders with radiuses increasing with 2.5 m up to a total of 25.5 m. The total number of grid blocks in the model was 143, see fig. 2.19.

The radially symmetric grid for fluctuating temperature and groundwater level simulations:

In the vertical direction the grid spacing had the following distribution: a 1.E50 m top grid block followed by twelve 0.5 m grid blocks and a bottom grid block of 1.E50 m. The connection between the large bottom grid block and the one directly above this was reversed, making it function as if the large volume grid block was connected to the top of the small grid block. In the horizontal direction the grid spacing was a 0.5 m radius followed by ten cylinders with radiuses increasing with 2.5 m up to a total of 25.5 m. The total number of grid blocks in the model was 154, see fig. 2.19.

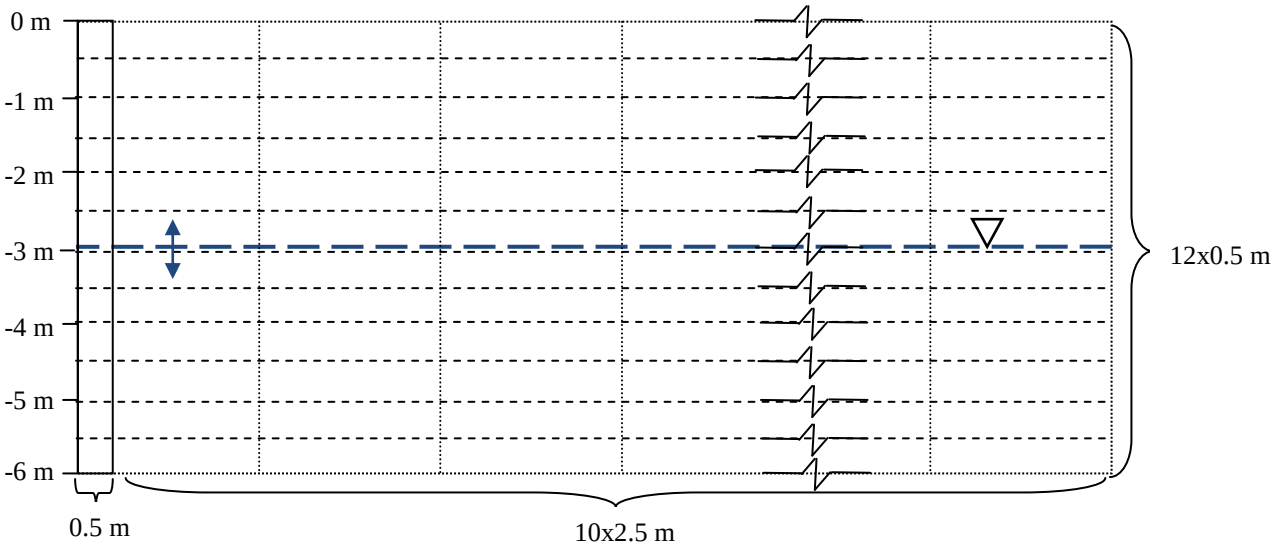

Fig. 2.19. Grid spacing in the radially symmetric model. The top grid blocks or extra bottom grid blocks are not shown.

The input files used to create the three grids can be seen in Appendix D.

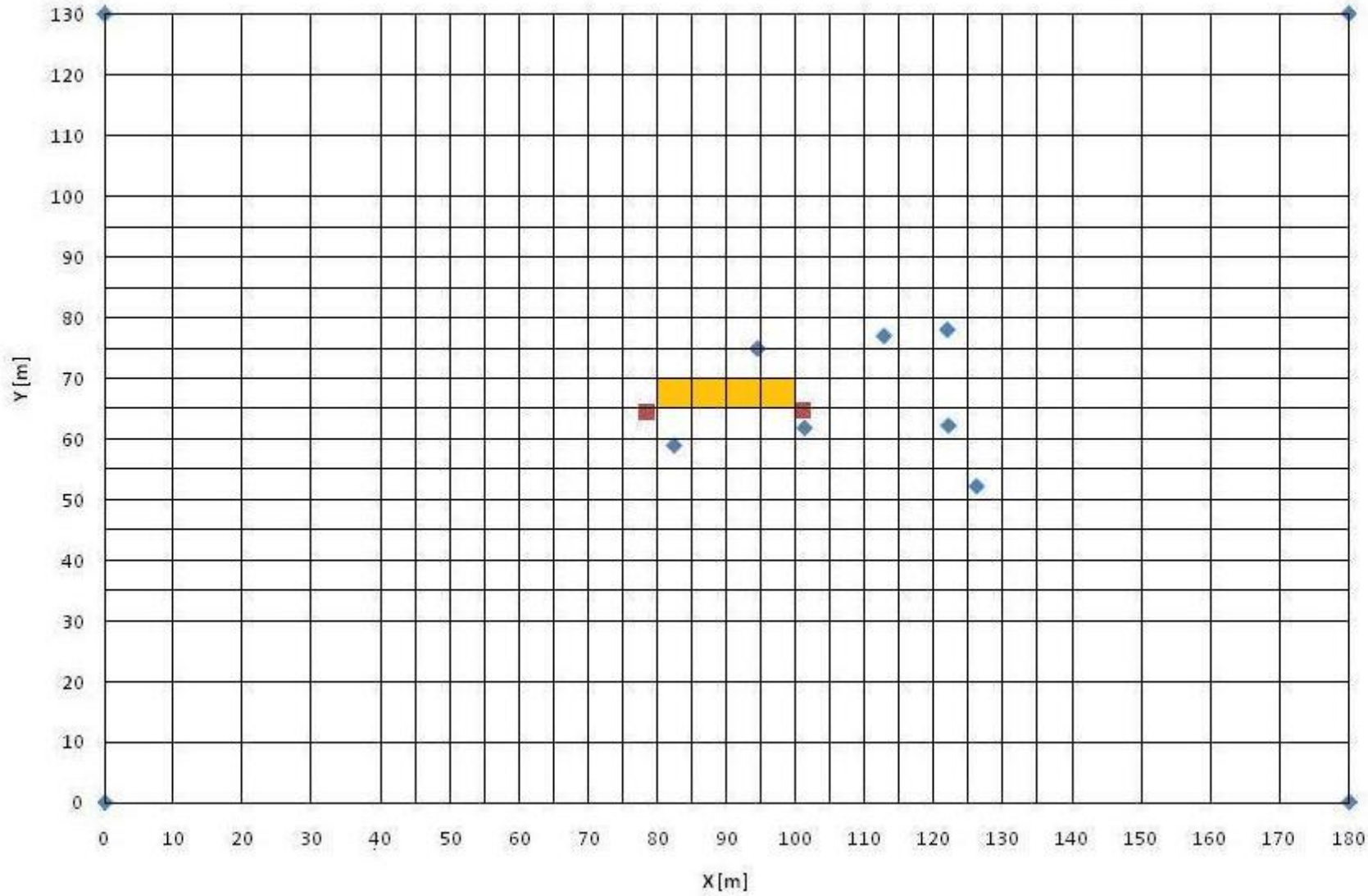

Fig. 2.18. The 3D-grid seen from above and placement of pumping wells (blue squares), endpoints of hypothetical line source (red squares) and injection grid blocks (yellow). Corner coordinates are shown as blue squares. Boundary grid blocks in the x-direction are not shown.

2.4.2 Single well simulation

A single well simulation was carried out to test the impact of model simplifications. Three scenarios were modeled, multicomponent versus one-component diesel spill, a fluctuating temperature versus a constant temperature and a fluctuating groundwater table versus a static groundwater table. The effect on pumped NAPL was compared.

The radially symmetric grid presented in the previous section was used for these simulations. For the first scenario small volume boundary grid blocks were used while for the last two scenarios large volume boundary grid blocks were used. For all scenarios a boundary condition for the outer boundary was set up, placing the groundwater table at a depth of 3 m. Then a steady state simulation was performed for the whole model to obtain initial conditions for the following simulations.

Multicomponent versus one-component "diesel"

For this simulation the top row atmospheric grid blocks were made inactive (locked). A pollution event was simulated. The pollution (multicomponent alternatively one-component diesel) was injected into the second from above inner boundary grid block i.e. at the centre just below the atmospheric grid block. The injection volume was 467 m^3 and the injection time was 30 years, see APPENDIX E. This was followed by two years of pumping, see APPENDIX E.

Fluctuating versus static temperature

An identical NAPL (one-component diesel) injection into the same grid block as for the previous simulations was simulated in this scenario. This was followed by two years of pumping. For the fluctuating temperature scenario the temperature was fluctuating only during the pumping simulation, see APPENDIX E. The simulation was carried out in 9 steps, table 2.13. An example of a heat injection calculation is shown in table 2.14.

Table 2.13. Simulation steps for fluctuating temperature.

Step	Month	Temperature	Start time [s]	End time [s]
1	May-June	20°C => 28°C	0.00000E+00	5.25600E+06
2	July-Sept	28 °C	5.25600E+06	1.31400E+07
3	Oct-Dec	28°C => 13°C	1.31400E+07	2.10240E+07
4	Jan-Feb	13°C	2.10240E+07	2.62800E+07
5	Mars-June	13°C => 28°C	2.62800E+07	3.67920E+07
6	July-Sept	28°C	3.67920E+07	4.46760E+07
7	Oct-Dec	28°C => 13°C	4.46760E+07	5.25600E+07
8	Jan-Feb	13°C	5.25600E+07	5.78160E+07
9	Mars-Apr	13°C => 20°C	5.78160E+07	6.30720E+07

Table 2.14. Calculation of heat needed to raise the temperature from 20 to 28 °C (step 1). dT=8 °C and rock grain density=2680 kg/m^3 . The rock grain specific heat for the atmospheric grid blocks was set to 50000 J/kg °C this is a model trick to exclude these large volume blocks from the global material balances.

Grid block	Volume [m^3]	Total weight [kg]	Porosity [-][A]	Energy needed to rise temp [J][B]	Time for temp rise [s]	[J/s]
A1 1	7.8540E+49	2.1049E+53	2.84E-01	6.0284E+58	5.2560E+06	1.1469E+52
A1 2	2.7490E+51	7.3673E+54	2.84E-01	2.1100E+60	5.2560E+06	4.0145E+53
A1 3	6.6760E+51	1.7892E+55	2.84E-01	5.1242E+60	5.2560E+06	9.7492E+53
A1 4	1.0600E+52	2.8408E+55	2.84E-01	8.1361E+60	5.2560E+06	1.5480E+54
A1 5	1.4530E+52	3.8940E+55	2.84E-01	1.1153E+61	5.2560E+06	2.1219E+54
A1 6	1.8460E+52	4.9473E+55	2.84E-01	1.4169E+61	5.2560E+06	2.6958E+54
A1 7	2.2380E+52	5.9978E+55	2.84E-01	1.7178E+61	5.2560E+06	3.2682E+54
A1 8	2.6310E+52	7.0511E+55	2.84E-01	2.0194E+61	5.2560E+06	3.8421E+54
A1 9	3.0240E+52	8.1043E+55	2.84E-01	2.3211E+61	5.2560E+06	4.4161E+54
A1 10	3.4160E+52	9.1549E+55	2.84E-01	2.6220E+61	5.2560E+06	4.9885E+54

A The same atmosphere and soil as in the 3D-model was used except an atmospheric porosity of 0.284 (as for the soil) was assumed. This because a porosity of 0.999 (even with a very large volume) would result in a small atmospheric "rock volume" and therefore the area inside the boundaries would influence the atmosphere, draining it of energy. This would result in a very small temperature rise. Using the smaller porosity the atmospheric boundary would have a large enough volume to be negligible effected by the inner domain, and thereby function as a temperature setting boundary. **B** Calculated using eq. 27.

Fluctuating versus static groundwater table

The result from the previous spill simulation was used as initial condition. Two years of pumping was simulated. For the fluctuating groundwater table simulation the pressure in the "bottom" boundary grid blocks were changed at each step during the pumping simulations. A total of 24 simulations were used for the two years of pumping, table 2.15.

Table 2.15. Simulation steps for fluctuating groundwater level.

Step	Month	Start time [s]	End time [s]	Pressure [Pa]	Groundwater level [m]
1	J	0.00000E+00	2.62800E+06	1.25767E+05	3
2	F	2.62800E+06	5.25600E+06	1.27602E+05	3.1875
3	M	5.25600E+06	7.88400E+06	1.29437E+05	3.375
4	A	7.88400E+06	1.05120E+07	1.31273E+05	3.5625
5	M	1.05120E+07	1.31400E+07	1.33108E+05	3.75
6	J	1.31400E+07	1.57680E+07	1.29437E+05	3.375
7	J	1.57680E+07	1.83960E+07	1.25767E+05	3
8	A	1.83960E+07	2.10240E+07	1.22097E+05	2.625
9	S	2.10240E+07	2.36520E+07	1.18427E+05	2.25
10	O	2.36520E+07	2.62800E+07	1.20262E+05	2.4375
11	N	2.62800E+07	2.89080E+07	1.22097E+05	2.625
12	D	2.89080E+07	3.15360E+07	1.23932E+05	2.8125
13	J	3.15360E+07	3.41640E+07	1.25767E+05	3
14	F	3.41640E+07	3.67920E+07	1.27602E+05	3.1875
15	M	3.67920E+07	3.94200E+07	1.29437E+05	3.375
16	A	3.94200E+07	4.20480E+07	1.31273E+05	3.5625
17	M	4.20480E+07	4.46760E+07	1.33108E+05	3.75
18	J	4.46760E+07	4.73040E+07	1.29437E+05	3.375
19	J	4.73040E+07	4.99320E+07	1.25767E+05	3
20	A	4.99320E+07	5.25600E+07	1.22097E+05	2.625
21	S	5.25600E+07	5.51880E+07	1.18427E+05	2.25
22	O	5.51880E+07	5.78160E+07	1.20262E+05	2.4375
23	N	5.78160E+07	6.04440E+07	1.22097E+05	2.625
24	D	6.04440E+07	6.30720E+07	1.23932E+05	2.8125

2.4.3 Historical simulation

A historical simulation was performed to investigate if the assumptions made about the origin and volume of the spill were in alignment with the volume of NAPL recovered through pumping. This also functioned as a test of whether the assumptions made in the model about e.g. soil properties were reasonable. An assumption was made that the pollution originated from a line source with endpoints (201498.6, 745691.4) and (201511.4, 745672.9), fig. 2.20. An estimation of the volume leaked oil is 1400 m^3 and the leakage is assumed to have been in progress for 30 years.

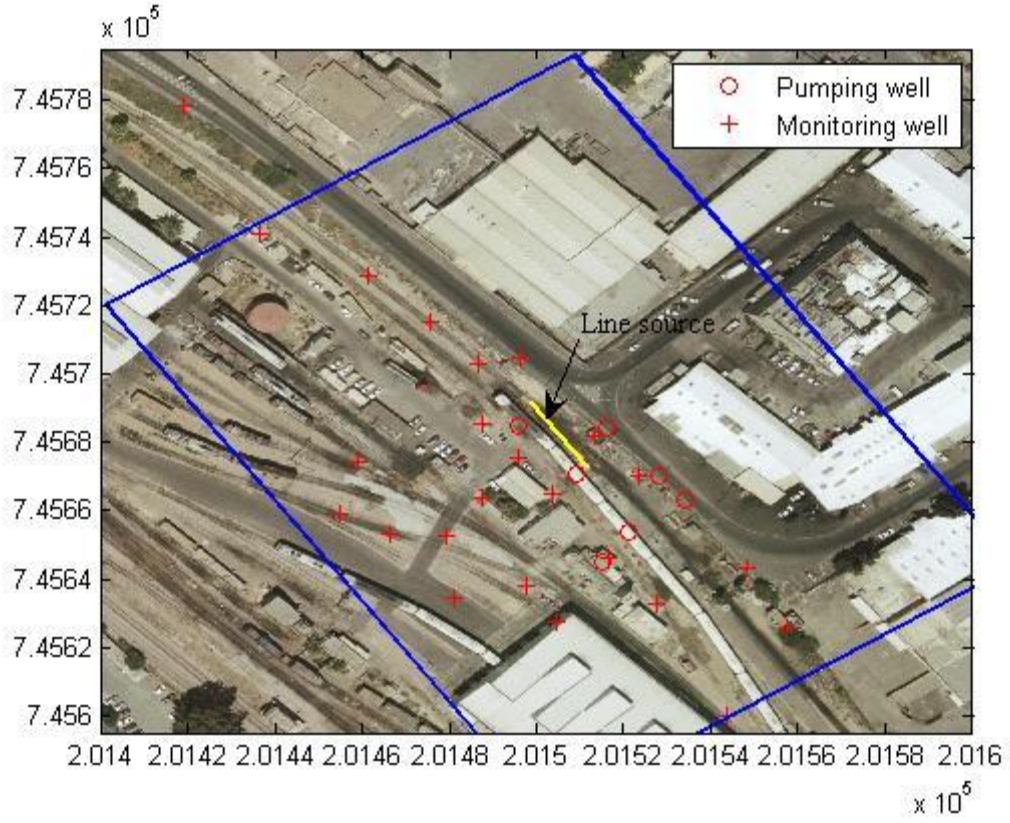

Fig. 2.20. Hypothetical line source.

The simulation was performed in four steps, first boundary conditions were simulated, then steady state conditions for the whole model was obtained, which served as initial conditions for the following spill scenario and last pumping well operation was simulated. The 3D-grid was used and a static groundwater level was assumed for these simulations.

Simulation of boundary conditions

Boundary conditions for the four corners in the rectangular box model were set up. A gravity-capillary simulation (air and water) was performed just for the corner elements, one corner at the time. The top grid element and the bottom element (used for locking the groundwater table) were made inactive.

In the simulation a static groundwater level was used and the groundwater table was placed at a depth of 3 m. The pressure to assign the nodal point of the groundwater table locking grid block (located 2.75 m below the groundwater table) was calculated using eq. 29.

$$P = P_{atm} + \rho \times g \times h \qquad \text{eq. 29}$$

Where P_{atm} is atmospheric pressure (101300 Pa), ρ is the water density (997.65 kg/m^3), g is the gravitational acceleration vector (9.81 m/s^2) and h is the distance from the groundwater table to the element node (2.75 m). A pressure of 1.28214E+05 Pa was assigned to the grid block, fixing the groundwater table at the right elevation.

For these simulations the energy balance was excluded and an assumption of no diffusion was made. The input file is shown in Appendix F. The boundary conditions at the other three corners were set up in the same manner.

Then the boundary conditions for the two short sides of the rectangular box were set up. For each side the previous simulation results for the two corners nearest to the side were used. The corner grid blocks and the top row (atmospheric condition) grid blocks were inactivated. The short sides were set to have static conditions, making it possible for NAPL to flow across these boundaries, out of the model. No diffusion was assumed to occur. The input file is shown in Appendix F. The models long sides were no-flow boundaries.

Steady state simulation

A simulation was performed to obtain steady state conditions for the whole model. The short side grid blocks and top grid blocks (atmospheric condition) were made inactive and result from the previous simulations was used as values for the locked sides. No diffusion was assumed to occur. The input file is shown in Appendix F.

Simulation of spill scenario

A 30 years continuous spill from a 22 m long line source was simulated. The one component "diesel" version was used. The NAPL was injected using four injection sources, one for each grid block and chemical. The injections were made into 4 grid blocks with nodes at a depth of 0.25 m, second grid block from above i.e the first non-atmospheric grid blocks. The location can be seen in fig. 2.18. Due to the grid discretization the line source is only 20 m long and covers a 100 m^2 (4 squares of 5 m x 5 m) large area. The injection rate for the chemical can be seen in table 2.16. The input file is shown in Appendix F. A spill with half the volume was also tested for comparison reasons, table 2.16.

Table. 2.16. Spill scenario information.

Spill volume [m^3]	1400	700
Density [kg/m^3]	833.69	833.69
Spill mass [kg]	1167166	583583
Number of injection elements	4	4
Injection time [years]	30	30
Injection rate in each element [kg/s]	3.0842E-04	1.5421E-04

Simulation of pumping

The almost two year (2008-2009) historical pumping regime was simulated using six deliverability wells, see fig. 2.18 and section 2.3.5 Remediation system. No impermeable well construction was taken into consideration. The result from the spill simulation was used as starting conditions. A printout of pumping rates (moles/s) was made once a week and from this accumulated NAPL recovery was calculated.

2.4.4 Simulation of the current pumping regime

The future NAPL recovery using the same pumping regime as present was simulated to estimate the remediation time needed and the effects on NAPL distribution. The six active pumps were let to operate as before. The simulation was started from where the historical pumping simulation ended. Here a spill volume of 700 m^3 and spill time of 30 years was assumed, as this gave the best agreement in the previous simulation.

3. RESULTS

3.1 SINGLE WELL SIMULATION

Multicomponent versus one-component "diesel"

Multicomponent diesel often turned out to lead to convergence failure during NAPL-injection simulation, so the one-component diesel was used in the 3D-model. The benzene, toluene and o-xylene fractions functioned well to inject together. For simulations with decane, dodecane, n-pentadecane, nonadecane and 1-methylnaphthalene convergence failure often arose in grid blocks at the groundwater table. A small spill of six components (decane, dodecane, benzene, toluene, o-xylene and naphthalene) could be simulated, these components are however not the largest groups when it comes to weight percentage. For the smaller spill the six-component diesel resulted in a slightly higher NAPL volume than the one-component diesel (40 m^3 compared to 39 m^3), fig. 3.1. The one-component diesel was more soluble. The result from the one-component diesel spill and pumping simulation is shown in fig. 3.1.

Fig. 3.1

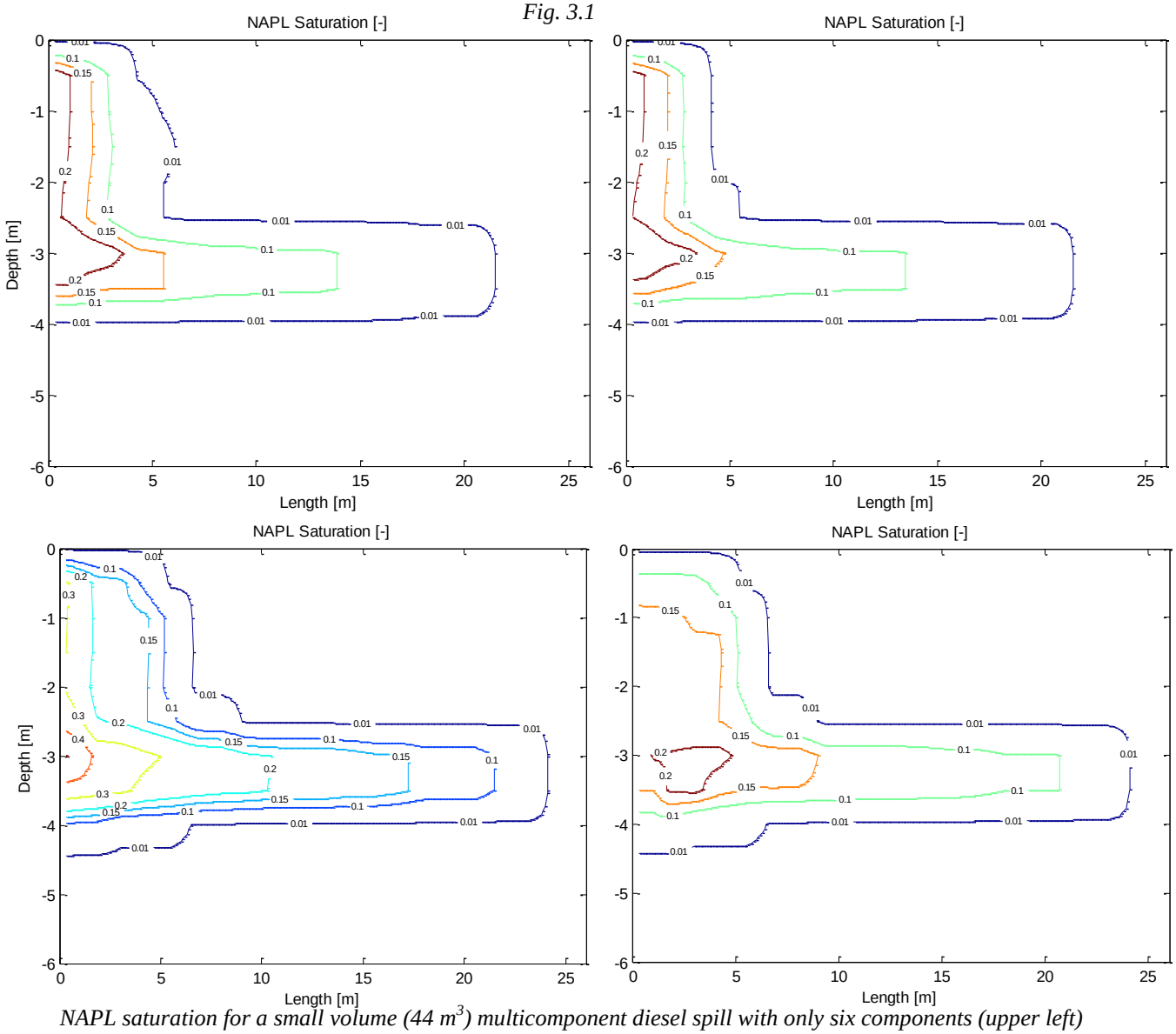

NAPL saturation for a small volume (44 m^3) multicomponent diesel spill with only six components (upper left) and one-component diesel of the same volume (upper right). NAPL saturation for the larger volume pollution after 30 years of spill at the (lower left) and the same spill after two years of pumping (lower right).

Fluctuating versus static temperature

The results from simulations of pumping under static temperature conditions and fluctuating temperature conditions showed only small differences. The changing temperature profile can be seen in fig. 3.2. The effect on NAPL distribution is shown in fig. 3.3 and the effect on pumped NAPL in fig. 3.4.

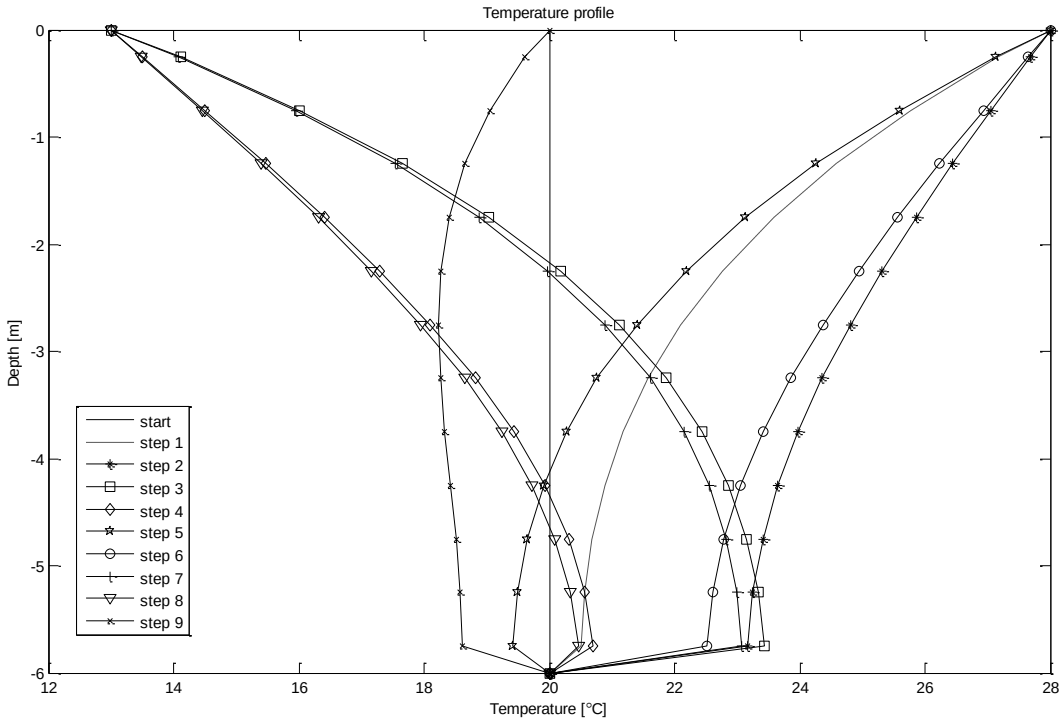

Fig. 3.2. Temperature profile for column 5 in the model at start and at the end of each simulation step. The bottom was locked at 20 °C (mean temperature).

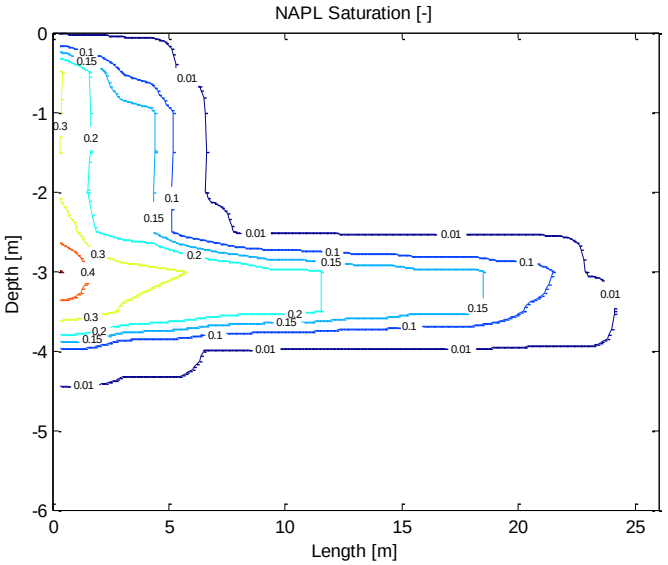

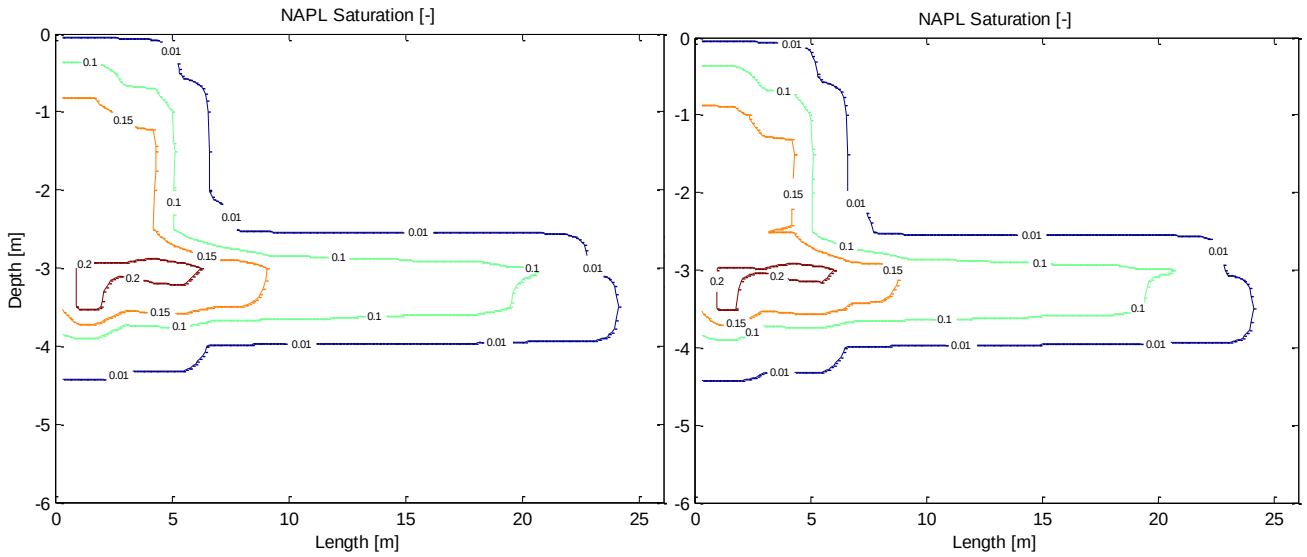

Fig. 3.3 NAPL saturation after 30 years of spill (previous side). NAPL saturation after two years of pumping with constant temperature (left) and with fluctuating temperature (right).

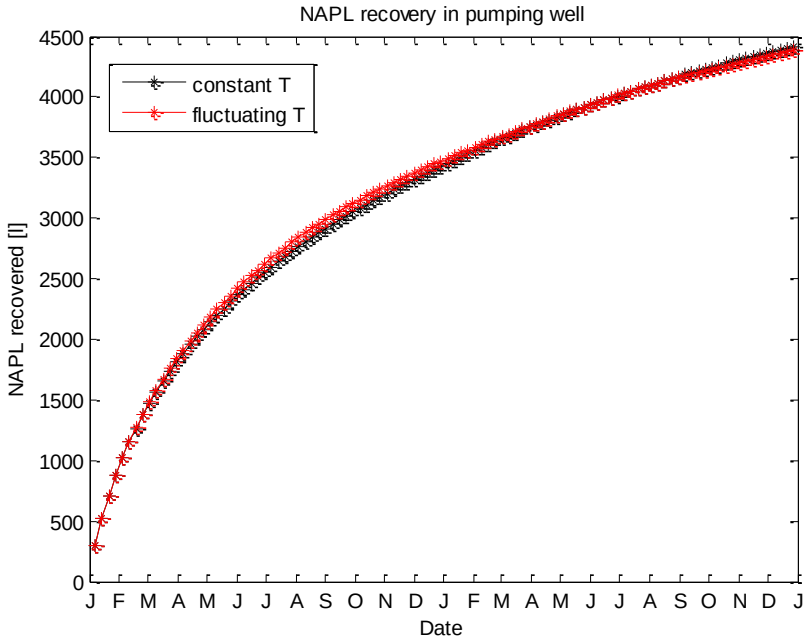

Fig. 3.4 Accumulated NAPL recovery after two years of pumping. The difference between the constant and fluctuating temperature simulation results is small.

Fluctuating versus static groundwater table

The results from simulations of pumping with a static groundwater level and a fluctuating groundwater level showed great differences. The effect on NAPL distribution is shown in fig. 3.5-3.6 and the effect on pumped NAPL in fig. 3.7-3.8.

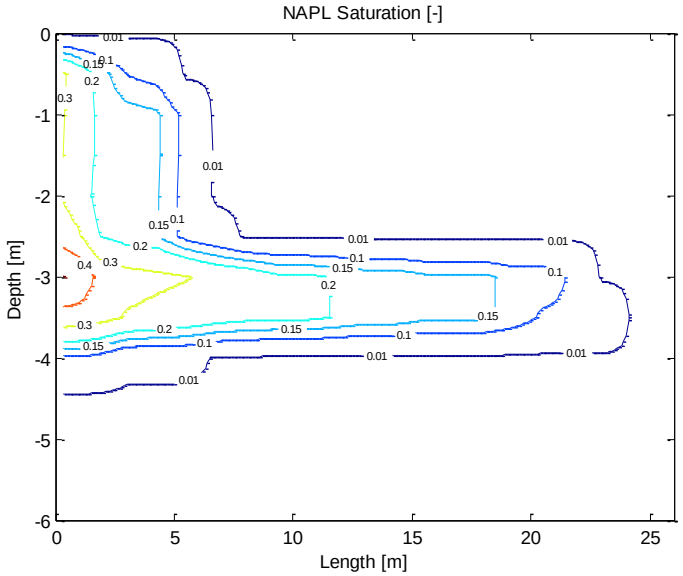

Fig. 3.5 NAPL saturation after 30 years of spill.

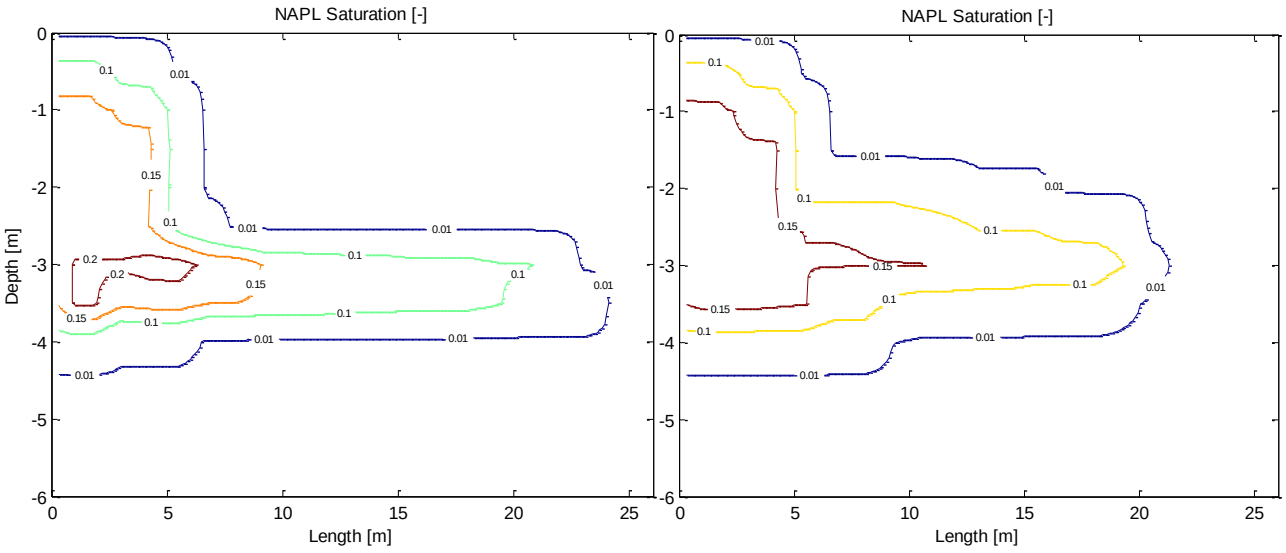

Fig. 3.6 NAPL saturation after two years of pumping with constant groundwater level (left) and with fluctuating groundwater level (right). The right figure shows enhanced spreading of the NAPL over a larger region.

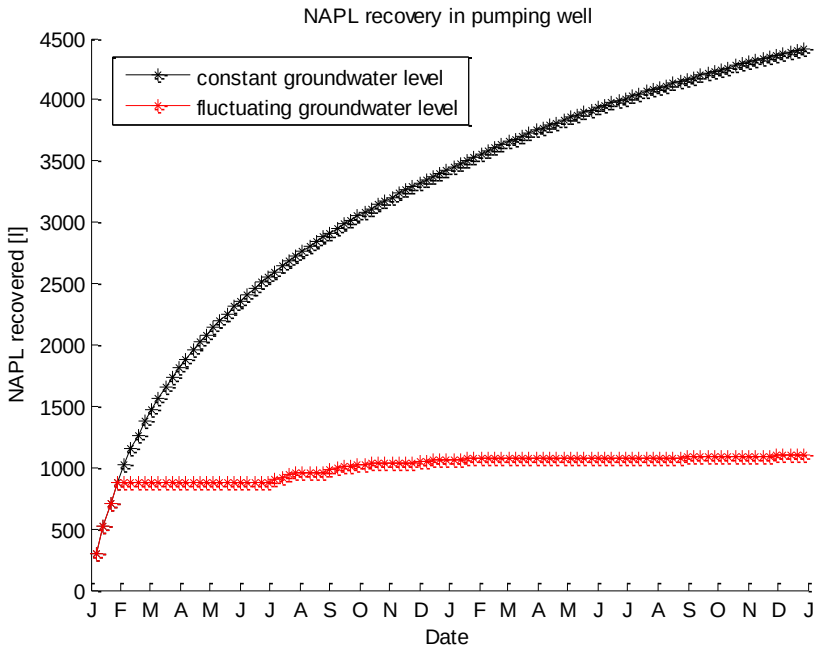

Fig. 3.7 Accumulated NAPL recovery after two years of pumping. The fluctuating groundwater level simulation resulted in a much smaller accumulated NAPL recovery volume than the static groundwater level simulation.

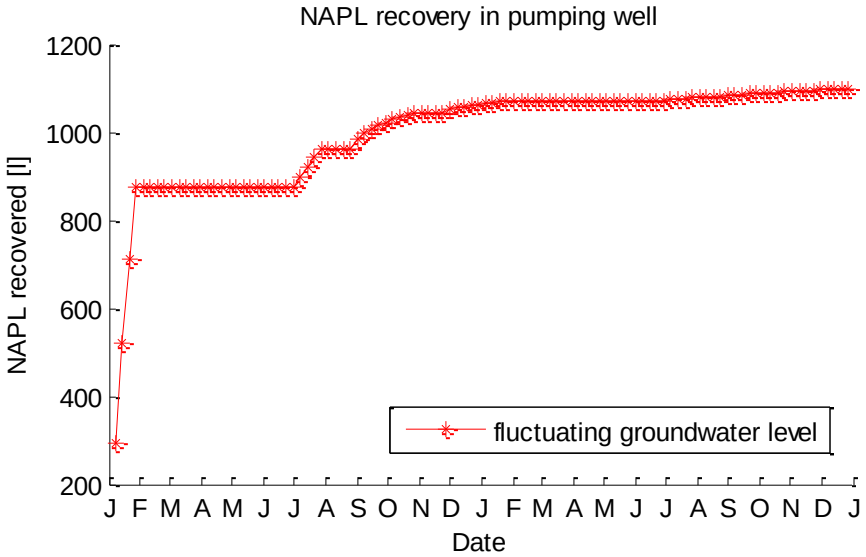

Fig. 3.8 A closer look at the accumulated NAPL recovery after two years of pumping with a fluctuating groundwater level. The accumulated NAPL recovery exhibit a terrace pattern.

3.2 HISTORICAL SIMULATION

Simulation of boundary conditions

Results from the boundary condition simulations are shown in fig. 3.8-3.10. The groundwater table is at an elevation of 3 m.

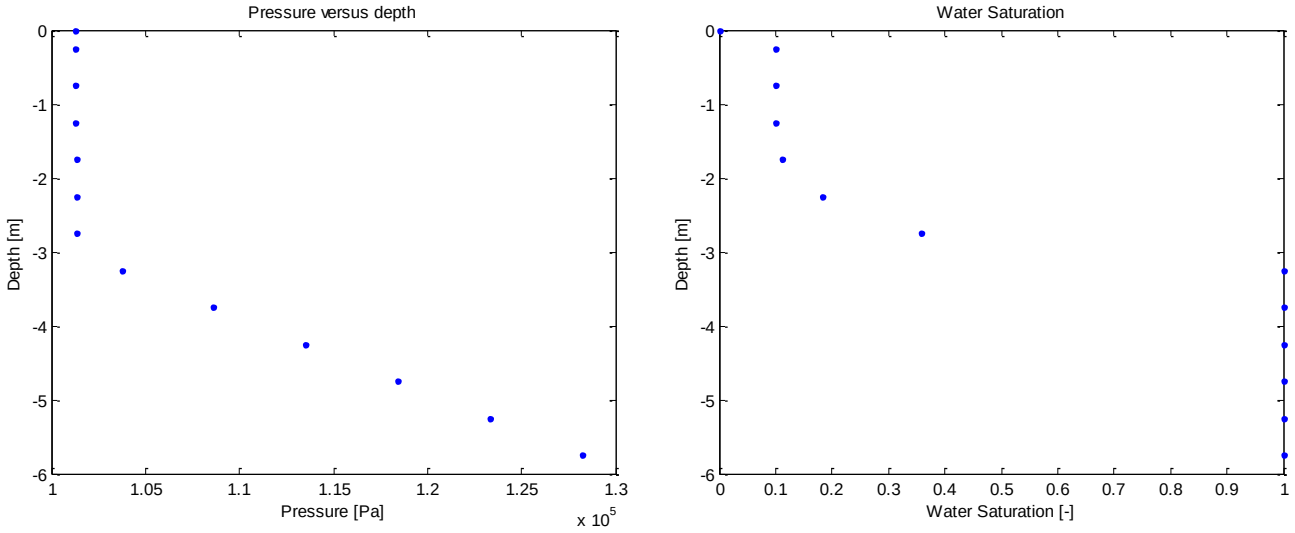

Fig. 3.8. Pressure curve (left) and water saturation (right) for the corner boundaries.

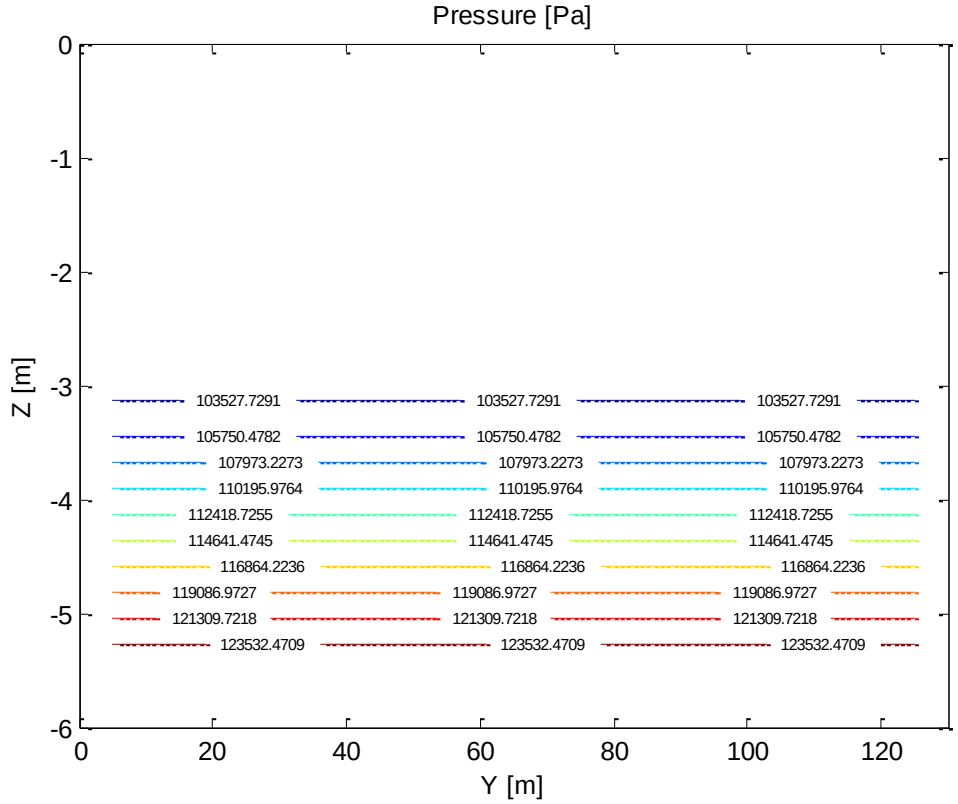

Fig. 3.9. Pressure curve for the side boundaries.

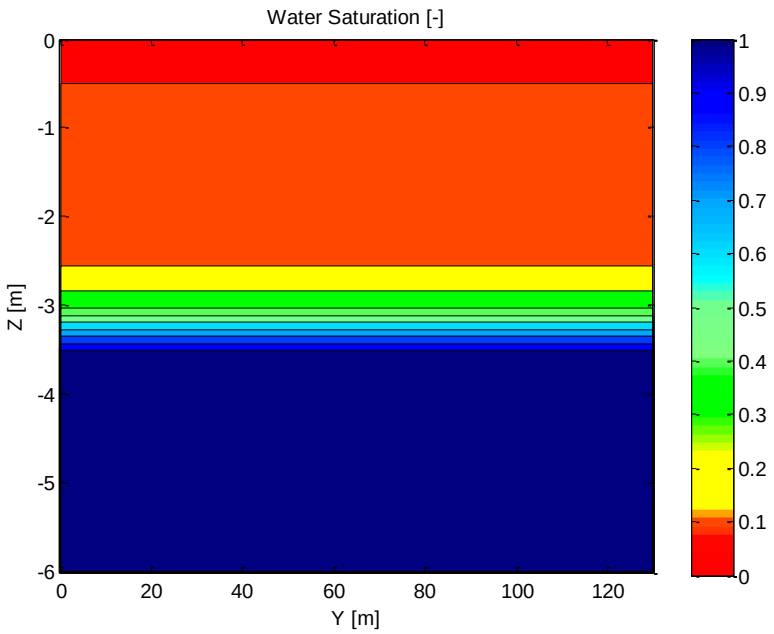

Fig. 3.10. Water saturation profile for side boundaries.

Steady state simulation

The result from the steady state simulation is shown in fig. 3.11.

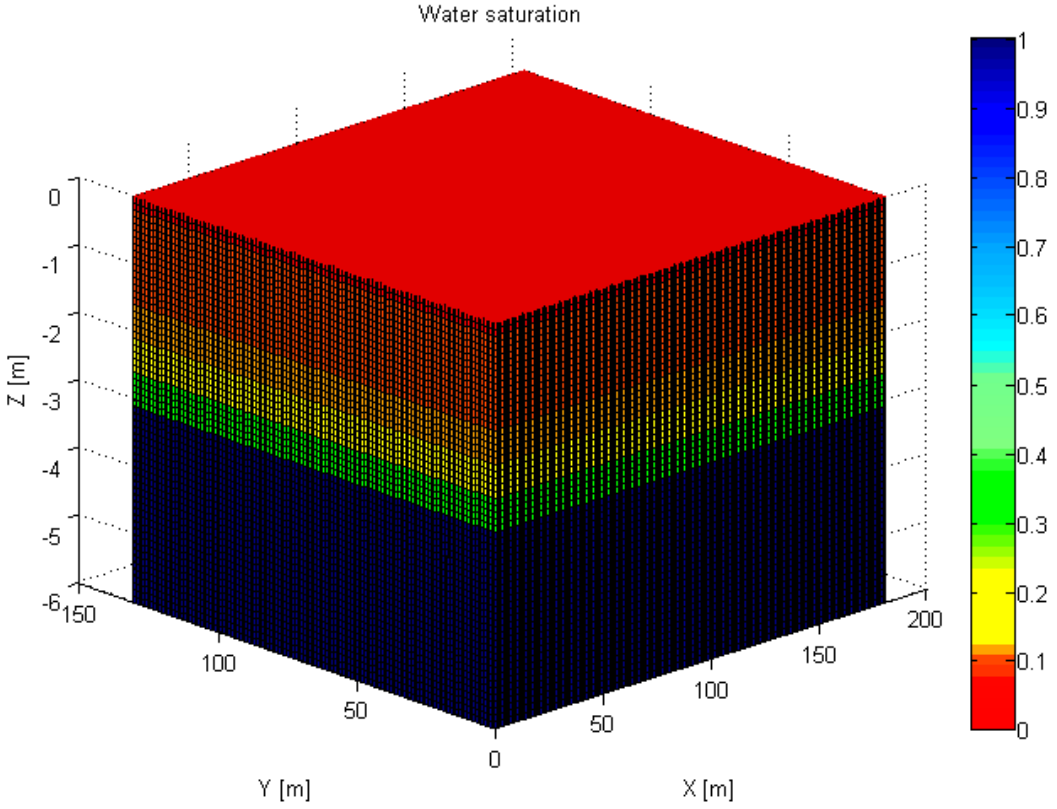

Fig. 3.11. Water saturation profile for the whole 3D-model obtained through steady state simulation. Residual saturation is 0.1 and this is also the lowest saturation possible in the profile as the steady state simulation was initiated at fully saturated conditions.

Simulation of spill scenario

The result from the spill scenario simulation (1400 m^3) is shown in fig. 3.12-3.14.

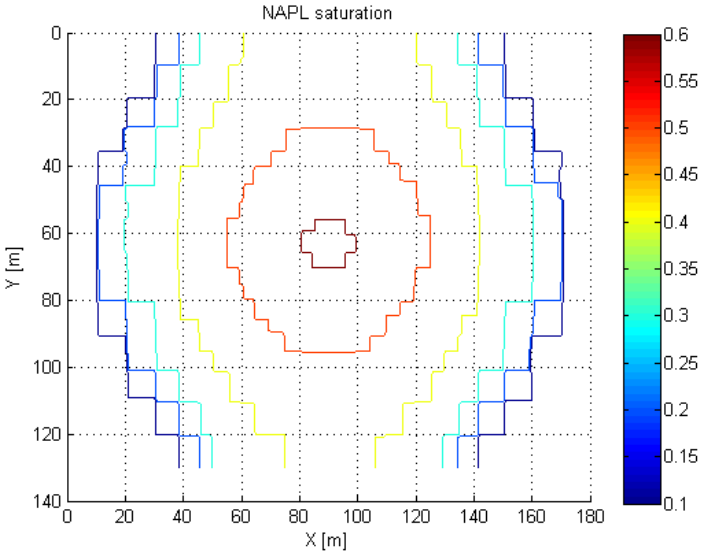

Fig. 3.12. NAPL saturation in 3D- model. Slice at z=-3.5 m.

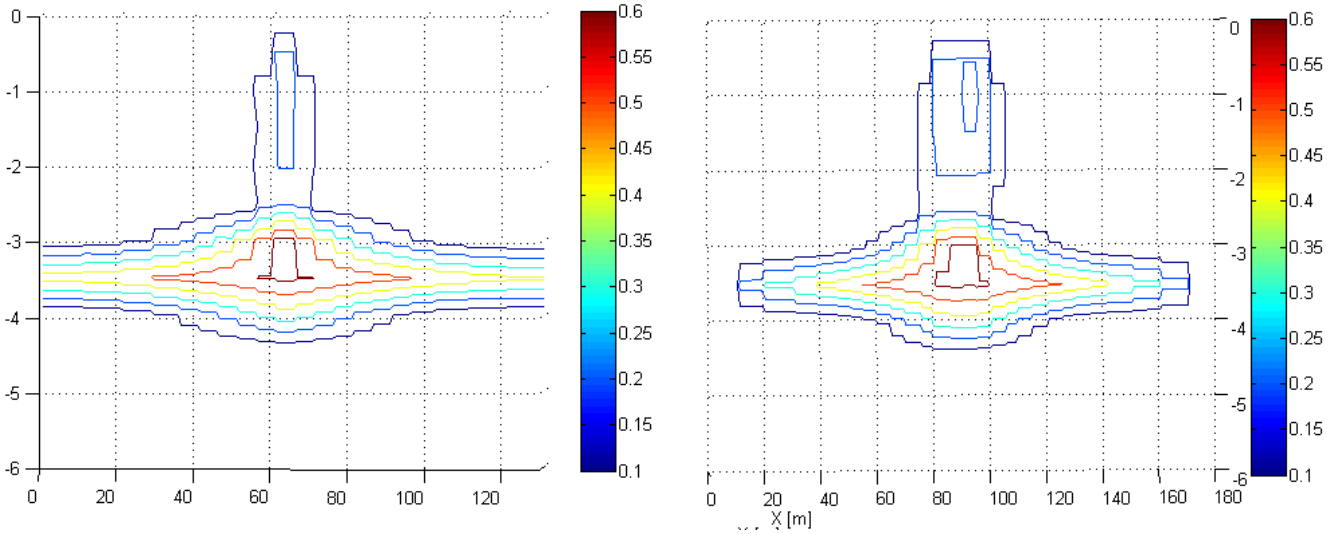

Fig. 3.13. NAPL saturation in 3D-model. Slice at x=90 (left) and at y=65 (right).

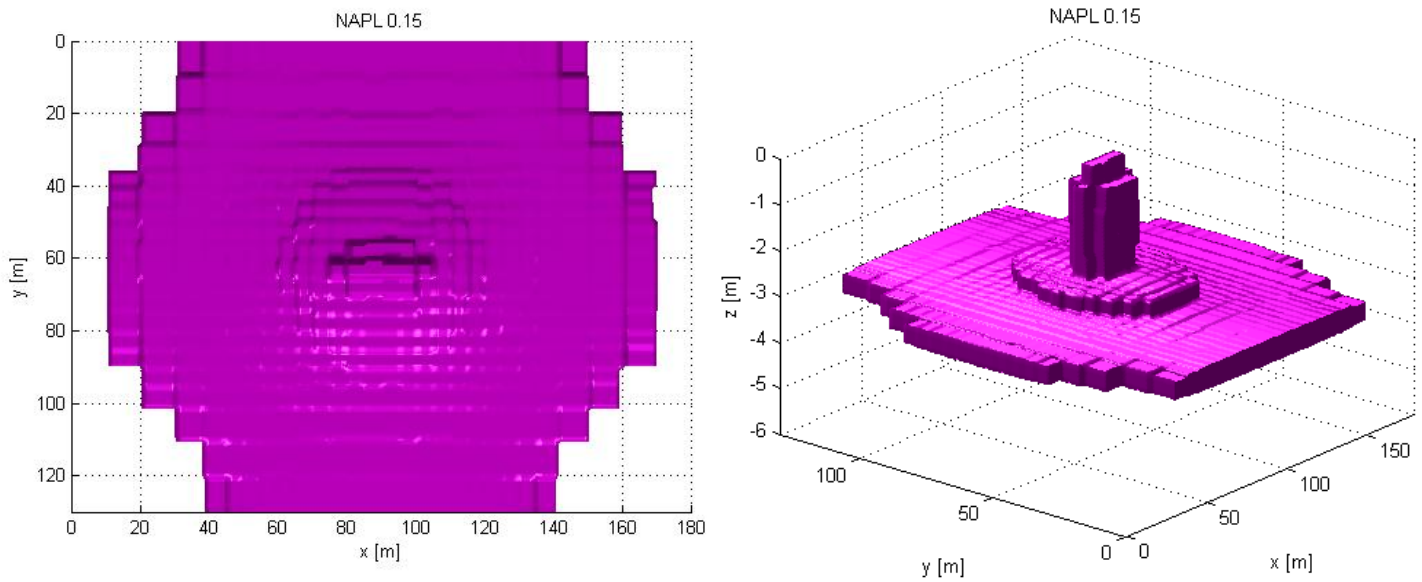

Fig. 3.14. Isosurface of NAPL residual saturation in the 3D- model.

The result from the 700 m^3 spill scenario can be seen in fig. 3.15 and 3.16.

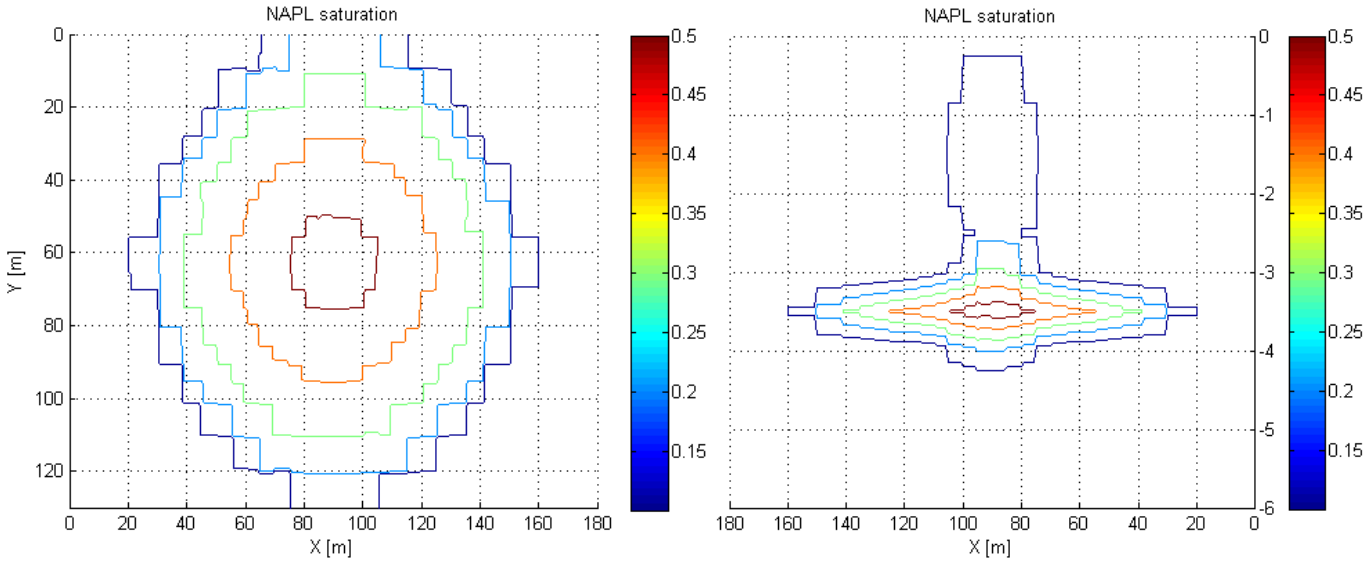

Fig. 3.15. NAPL saturation in 3D- model (700 m^3 spill). Slice at z=-3.5 m (left) and at y=65 (right).

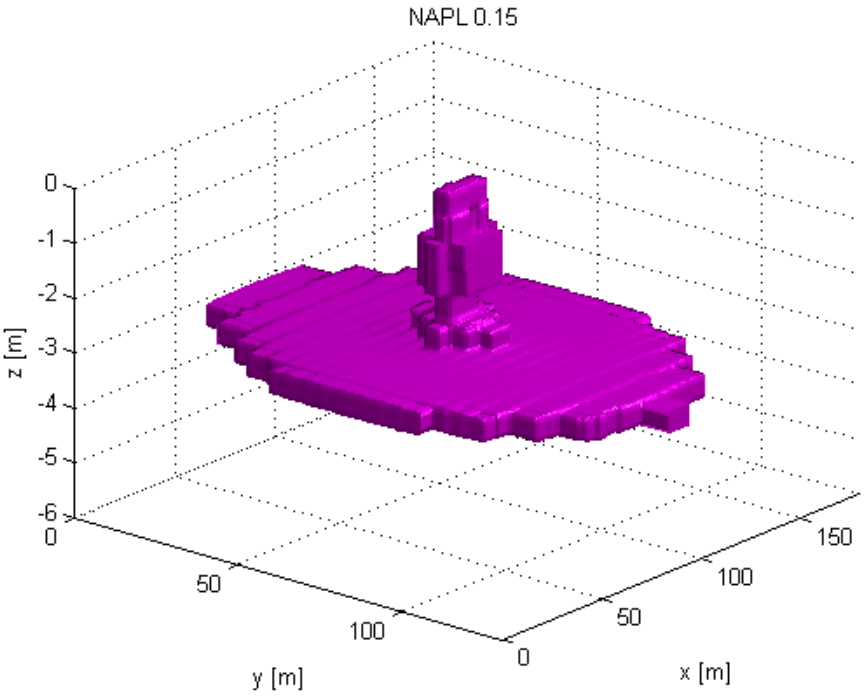

Fig. 3.16. Isosurface of NAPL residual saturation in the 3D- model (700 m^3 spill).

Simulation of pumping

The results from the pumping simulation, fig. 3.17, showed large discrepancies to measured volumes of pumped NAPL. The pumping simulation starting from the 1400 m^3 spill scenario gave a much higher accumulated NAPL recovery for all wells than observed, while pumping simulations starting from the 700 m^3 spill scenario showed good agreement with observed accumulated NAPL recovery in well A and well B (wells without terrace shape).

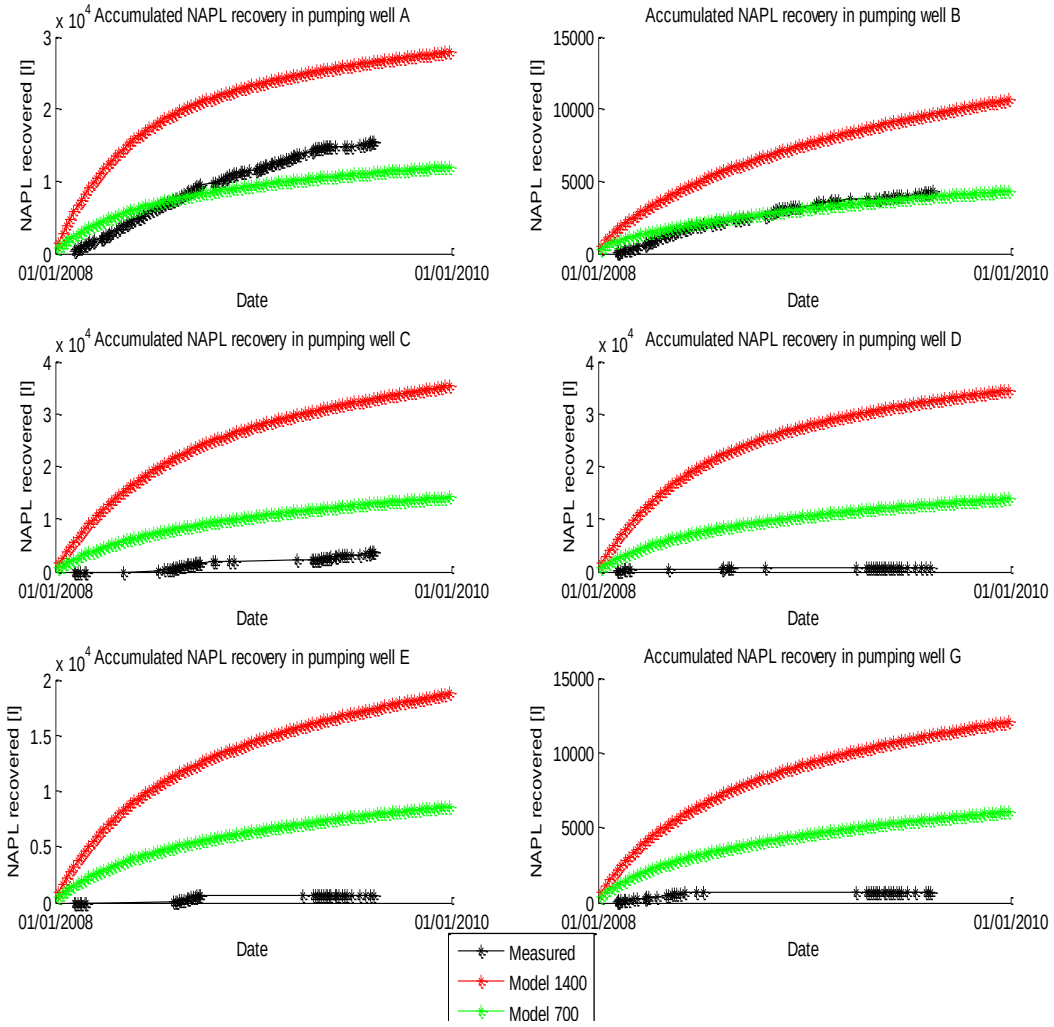

Fig. 3.17. Accumulated NAPL recovery in the model (red 1400 m^3 spill and green 700 m^3spill) and measured (black). The pumped NAPL volume was obtained from the production rate (moles/s) retrieved from simulations, time interval (one week), density and molecular weight.

The effect of pumping on NAPL distribution can be seen in fig. 3.18-3.20.

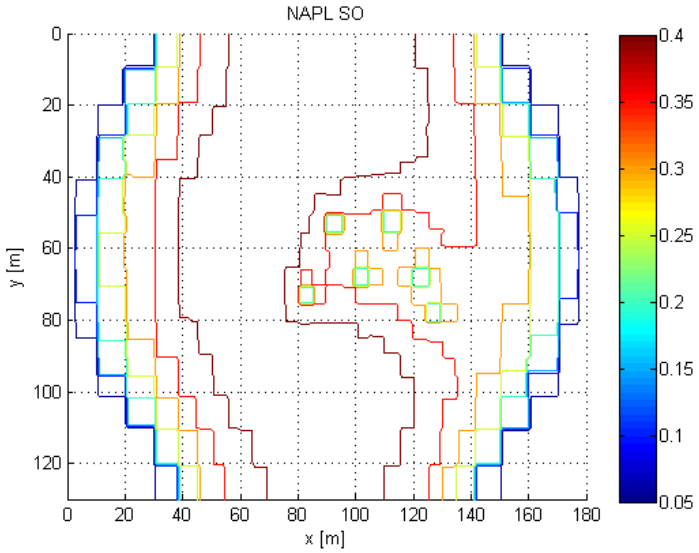

Fig. 3.18. NAPL saturation in the 3D-model after 2 years of pumping (1400 m^3 spill). Slice at z=-3.5 m.

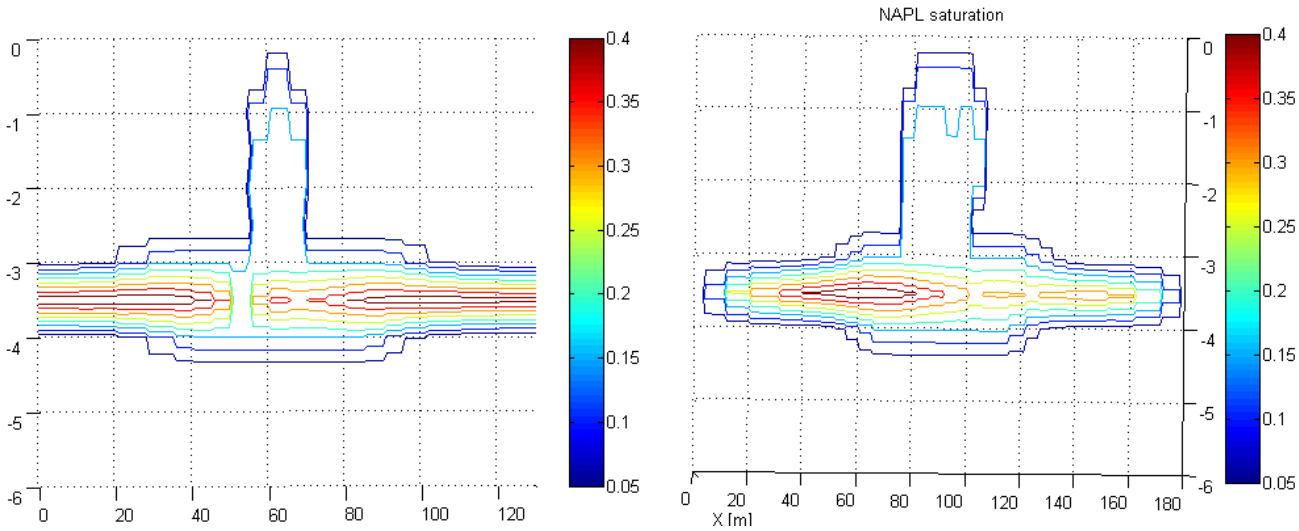

Fig. 3.19. NAPL saturation in the 3D-model after 2 years of pumping (1400 m^3 spill). Slice at x=90 (left) and at y=65 (right).

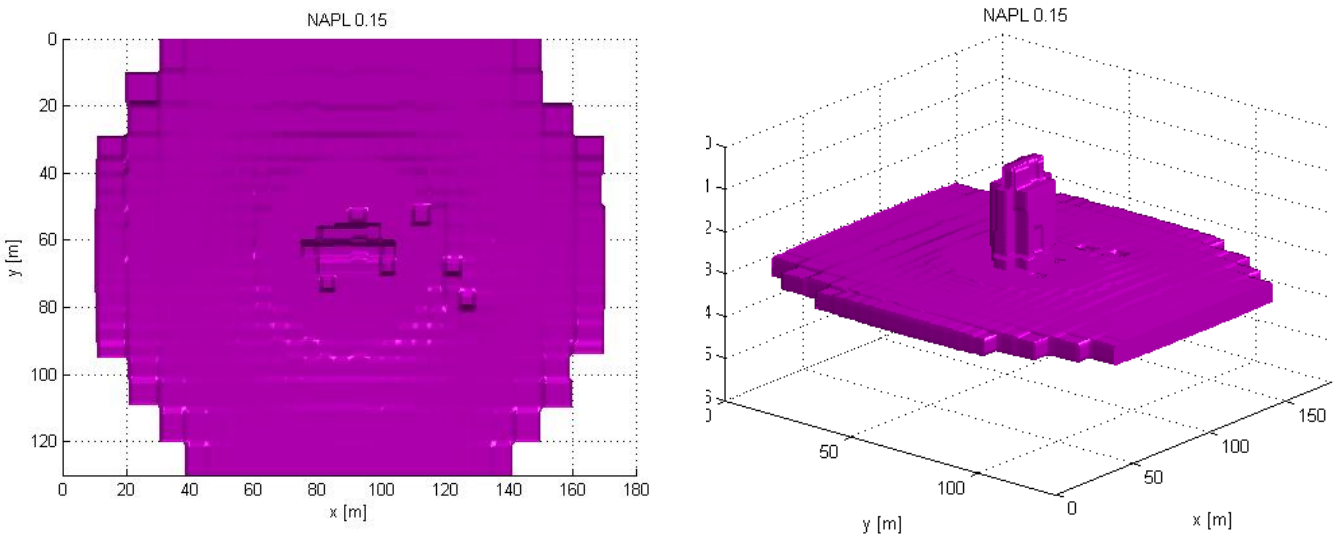

Fig. 3.20. Isosurface of NAPL residual saturation in the 3D-model (1400 m^3 spill).

The effect of pumping on NAPL distribution for the smaller spill can be seen in fig. 3.21

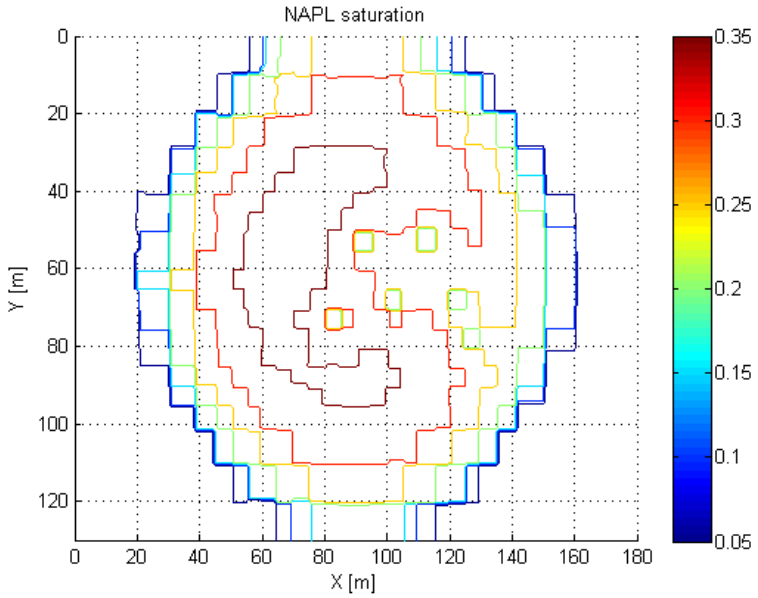

Fig. 3.21. NAPL saturation in the 3D-model after 2 years of pumping (700 m^3 spill). Slice at z=-3.5 m.

3.3 SIMULATION OF THE CURRENT PUMPING REGIME

The result from the simulation of future NAPL recovery in the model using the same pumping regime as present is shown in fig. 3.22. A decrease in inflow of NAPL to the wells with time can be seen in fig. 3.23. The plotted results start after the 2 year historical pumping simulation. At this time 591 m^3 NAPL still remained in the model.

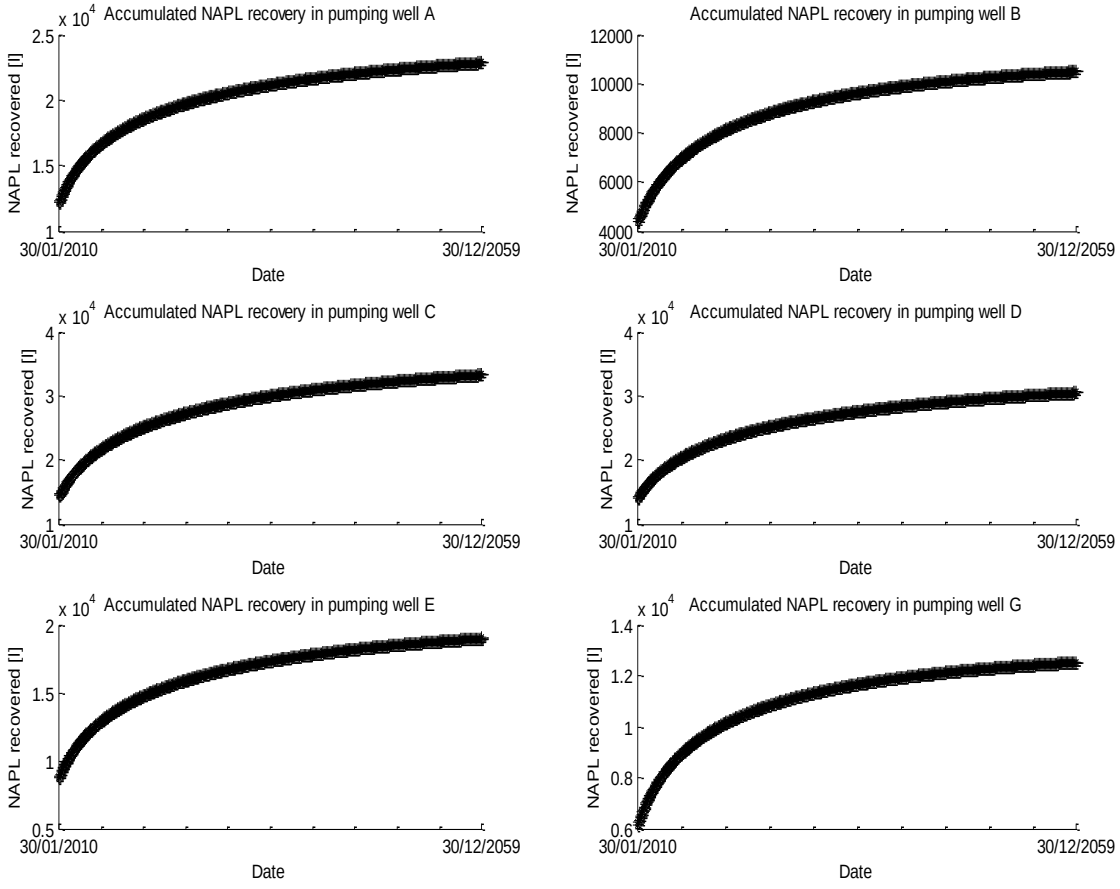

Fig. 3.22. Future accumulated NAPL recovery in the model.

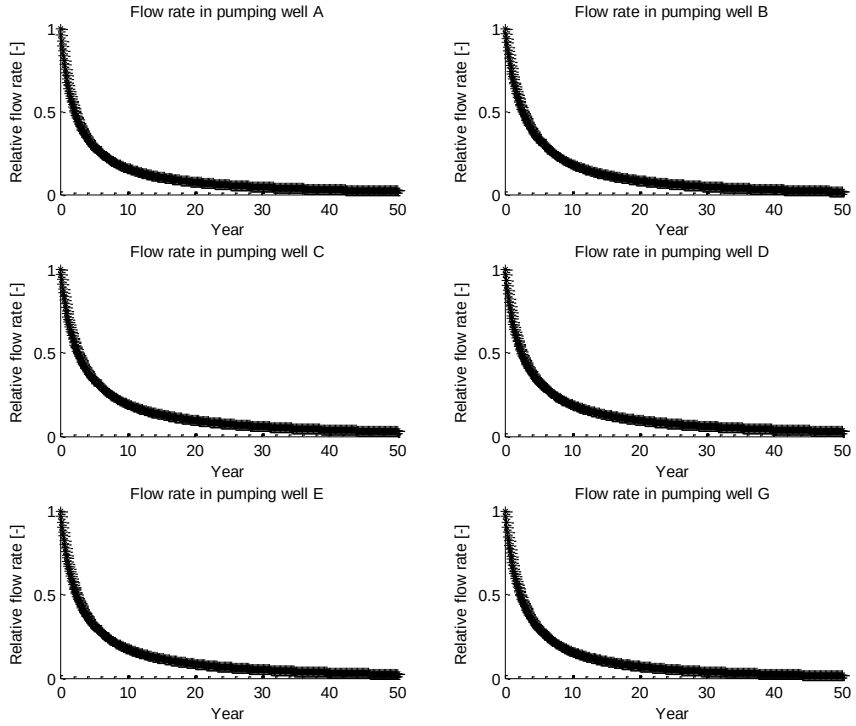

Fig. 3.23.Relative NAPL flow rates in the wells. After 2.5 years the remediation effectiveness was halved.

The NAPL volume in the model declined very slowly, fig. 3.24.

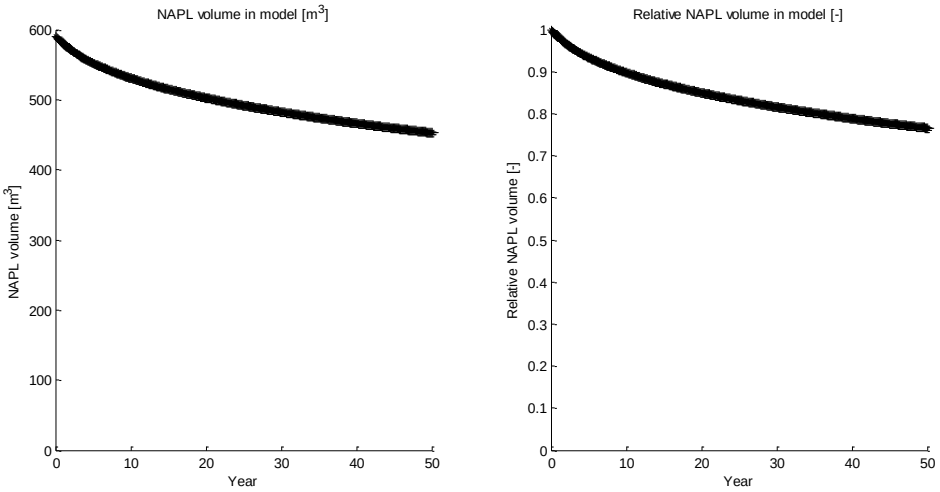

Fig. 3.24. Model NAPL volume and relative NAPL volume (compared to the start volume for the current pumping regime simulation).

During the 50 years simulated pumping 70 m^3 NAPL was recovered, 18 m^3 of this amount during the first 2.5 years of the simulated period. The historical pumping simulation showed a NAPL recovery of 59 m^3. Adding the results from the two simulations indicated that approximately 20 percent of the original NAPL spill was recovered after 52 years of pumping.

The simulation indicated that an estimation of remediation time by this TMVOC model is very long and probably determined by how the well NAPL flow rates decrease, while the NAPL volume gets distributed over a large area and decrease in volume very slowly. At residual saturation the NAPL can't be pumped out.

Effects on NAPL distribution are shown in fig. 3.25 and fig. 3.26.

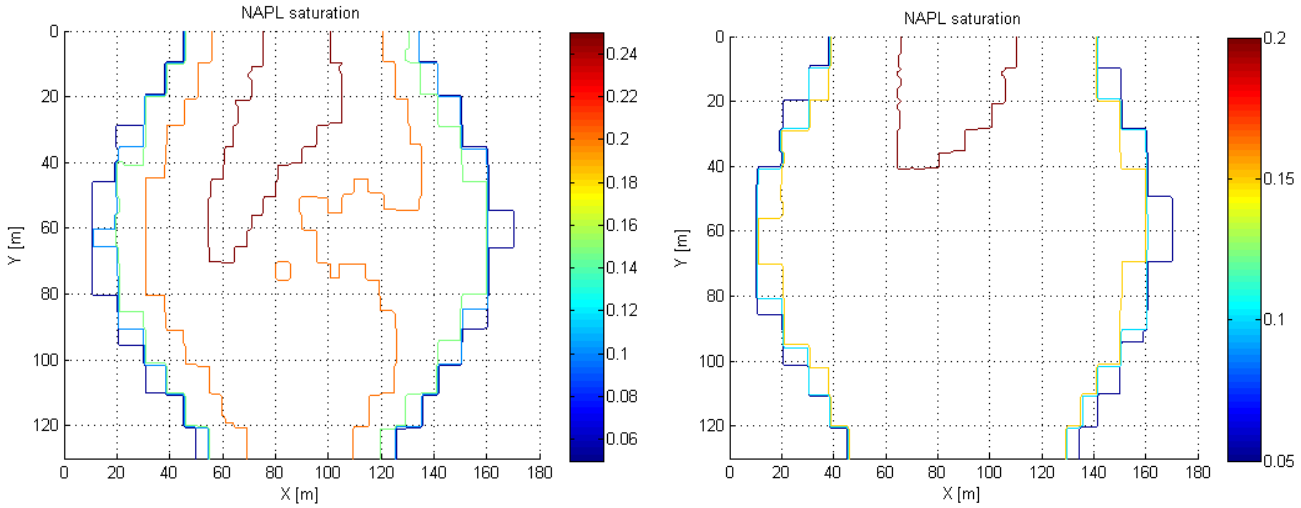

Fig. 3.25. Model future NAPL saturation distribution after 15 years of current pumping regime simulation (left) and 50 years (right).

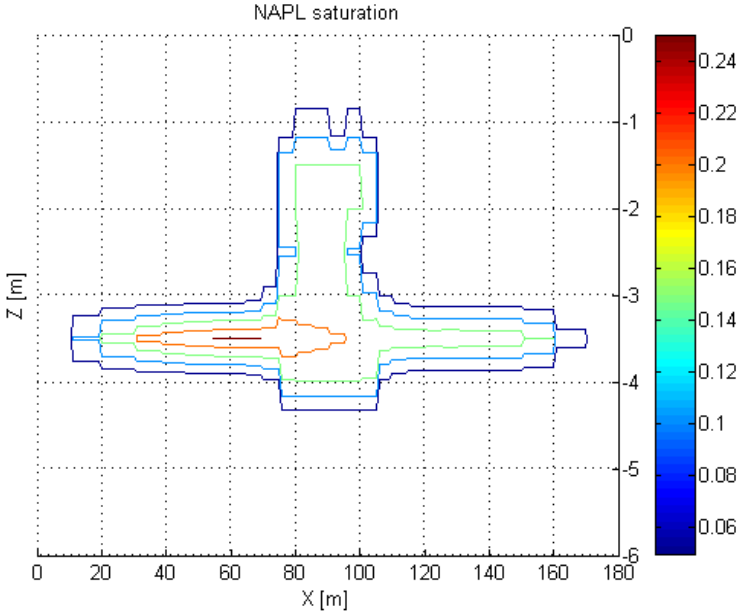

Fig. 3.26. NAPL distribution after 15 years of NAPL recovery according to the current pumping regime. Slice at y=65. Highest saturation at the opposite side of the pumping wells.

.

4. DISCUSSION

In this work both single-component multiphase model as well as a multicomponent multiphase model were used. The simulations with the multicomponent model can be seen as very preliminary ones, with an objective to take a relatively seldom used model into use. The preliminary simulations with the multicomponent multiphase model had significant convergence problems and simulation of the entire spill spreading period could not be completed as convergence failure occurred before that. The reason for this convergence failure can be for example that the nine components had very different properties, e.g. solubilities ranging from 10^{-4} to 10^{-12}. Benzene, toluene and o-xylene functioned well to inject together in all grids and soils tested. These chemicals have similar properties. For decane, dodecane, n-pentadecane, nonadecane and 1-methylnaphthalene convergence failure often arose in grid blocks at the groundwater table. In common for these are that their viscosity function is described by only two parameters, they have low solubility and simulation failure arises when their densities are specified. A small spill of six components (decane, dodecane, benzene, toluene, o-xylene and naphthalene) could be simulated. These components are however not the largest groups when it comes to weight percentage of the diesel. The program does not seem to have problem with the number of chemicals specified. Convergence failure could also possible depend on the grid. Further studies should address these issues.

The small multicomponent diesel spill (decane, dodecane, benzene, toluene, o-xylene and naphthalene) simulation gave similar result as the one-component diesel spill simulation. This result was expected as the largest constituent amount in the multicomponent spill was that of o-xylene the same chemical that the one-component diesel was largely based on.

The preliminary simulations addressing the effect of seasonal temperature variations did not show significant temperature dependence. As these simulations were based on an assumed heat conductivity (unknown heat conductivity for the soil at the site) it would be of interest to try to obtain site specific parameters for new simulations which possibly would show a different result. It could not be excluded that temperature fluctuations have a large impact on NAPL migration and distribution in reality even though the model showed little impact. In reality temperature is suspected to influence the NAPL recovery. Further studies could attempt to match the simulation results to observations in more detail.

The single well simulations showed groundwater level fluctuations to be of great importance for simulation results. A terrace shaped accumulated NAPL recovery curve developed due to the fact that the groundwater table, and therefore also the NAPL, was vertically displaced away from the well, retarding or preventing the NAPL inflow. This occurs when the groundwater table elevation is above the well intake. The curve shape in the single well simulation fig. 3.8 is quite similar to the curve shape of well C-G in fig. 2.12.

In the historical pumping simulations the difference between the simulated pumped NAPL volume and the measured volume could depend on the amount of NAPL injected into the model, where the source of leakage is located in the model, the time during which this occur and how this agree with reality. The difference in the simulated pumped NAPL volume and the real measured volume could also arise from inaccurate assumptions in the model e.g. regarding any of the chemical or soil parameters. Further studies of interest would be to test different values for some of the model parameters e.g. conductivity and residual saturation. The result from these simulations would serve as a sensitivity analysis. The uncertainty in the soil parameters could be minimized by conducting an own retention curve survey on a soil sample from the site.

The one-component diesel used in the model was based on average component and o-xylene properties and is probably quite different from real diesel, and with it follows another movement of the spill in the ground.

The results from the historical pumping simulations could indicate that the spill could be less than the estimated 1400 m^3, perhaps around 700 m^3. This is based on the poor agreement between the 1400 m^3 spill pumping simulation and the measured pumped volumes for all wells. The simulated historical pumping of a 700 m^3 spill (injected during 30 years) on the contrary showed good comparison with measured values for well A and B, but overestimated the recovery in the remaining wells (C,D,E and G). This overestimation could be due to the fact that the 3D-model does not simulate seasonal changes in the groundwater level. Such seasonal changes, as showed in the radially symmetric model, can result in a much smaller accumulated NAPL recovery and a characteristic terrace shaped accumulated NAPL recovery curve for the wells concerned. Why these wells could be more affected by changes in the elevation of the water table than well A and B could possibly depend on differences in local lithology or construction of the wells. The model assumed a homogeneous sand layer which may not in a satisfactory way describe the vicinity of the remaining wells, which seem to be more subjected to the changes in groundwater level. A possible solution for making well C, D, E and G pump more NAPL could be to pump more water from the wells creating a depression cone, lowering the groundwater table and thereby facilitating the NAPL lens to flow into the wells more easily, irrespective of seasonal changes. This is of course only a possible solution if surrounding structures allow for such a strain and there is enough space.

Other explanations for the discrepancies between measured and simulated pumped NAPL in well C, D, E and G could be clogging or pipes and underground structures that are not featured in the model but that could have a potentially great effect on the groundwater flow. General discrepancies can also be caused by the model assuming the soil to be a homogenous sand layer while the actual soil has conductive boulders.

It could however not be excluded that the spill volume is larger, in the vicinity of 1400 m^3. The lack of a fluctuating groundwater level, uncertainties in parameters and other assumptions made in the 3D-model could explain differences in simulated and measured recovered NAPL.

To simplify the model the impermeable construction of the wells was neglected. This could possible contribute to some differences from real life pumping as NAPL could be pumped through areas that would otherwise be impermeable. This makes inflow from above and not just from the well sides possible.

The history of the spill cannot be simulated with 100% certainty, but simulations can show the effect of different assumptions concerning spill location, amount and timeframe on the result e.g. spreading of the NAPL lens. The validity of the input parameters is of great importance. In this case existing pumping measurements from the site could be used for comparison with simulated pumping result and gave guidance in probable amount of spill.

The time needed for the pumping remediation was hard to estimate, because of the uncertainty in the spill volume, the location and time the leakage has occurred. Assuming a spill of 700 m^3 during a period of 30 years, future pumping was simulated. The results from these simulations show that the remediation time would be long due to the fast decreasing mobility of the NAPL phase. After 2.5 years the flow rate was halved and the highest NAPL saturation could be found at the opposite side of the pumping wells in the model. The model indicated

that a large percentage of the original NAPL spill could be distributed over a large area at near residual saturation and decrease in volume very slowly. The NAPL recovery would therefore be relatively small. The accuracy of these results also depends on the validity of the assumed soil and chemical parameters as discussed above. The simulated NAPL volume remaining in the model depended not only on the recovered pumped NAPL, but some NAPL also left the model by crossing the static boundaries (the short sides of the model).

The simulation results in this thesis are based on models for which many parameters are estimated (where site specific parameters were unknown) and the results are therefore not surprisingly quite different from "real" measurements made on site. But the models presented can serve as a base for further studies and can be improved by incorporating more site specific parameters. A future improvement of the 3D-model could be to incorporate a fluctuating groundwater table as the effect of a changing groundwater table on the NAPL distribution was shown to be of great importance in the simulation. Another improvement would be to choose a finer discretized grid, especially in the vertical direction. This would make it possible to capture the varying thickness of the NAPL lens and thereby obtain a better understanding of the NAPL distribution in the soil. A finer grid would also result in longer computational time. One could also choose to set all the sides of the model as static boundaries, making it possible for the NAPL phase to flow out in all directions, perhaps more in accordance to reality than no-flow boundaries.

Other things of interest to simulate could be to study the impact of trenches (between the wells) on the remediation time. A fine grid (5 m x 5 m is too coarse) able to capture the trenches is then necessary. It could also be of interest to study how pumping of groundwater and creation of a depression cone would impact the NAPL lens and the remediation time.

5. CONCLUSIONS

The history of the spill was simulated and results from the historical pumping simulation indicated that the spill volume could be less than the estimated 1400 m^3, perhaps around 700 m^3, assuming a leakage time of 30 years. The historical pumping simulation of a 700 m^3 (30 years) diesel spill showed good agreement with measured values for well A and B, but overestimated the recovery in the remaining wells (C,D,E and G). This overestimation could be due to the fact that the 3D-model does not take seasonal changes in the groundwater level into consideration.

Assuming a spill of 700 m^3 during a period of 30 years, future pumping was simulated. The results from these preliminary simulations show that the remediation time would be long due to a rapid decrease in NAPL flow rates. After 2.5 years the flow rate was halved and the highest NAPL saturation found at the opposite side of the pumping wells in the model. The model indicates that the NAPL volume could be distributed over a large area at near residual saturation and NAPL recovery could therefore be relatively small.

The simulation results should be seen as preliminary in character. A major focus in this work has been to take in use a new multicomponent-multiphase modeling approach. Subsequently not as much effort was invested in parameter sensitivity studies and as parameters are first estimates the results are therefore not surprisingly different from field observations. But the models presented can serve as a base for further studies and can be improved by incorporating more site specific parameters.

REFERENCES

Ahmed, T., & McKinney, P. (2005). *Advanced Reservoir Engineering.* Elsevier.

Akron. (2009, February 10). *The Department of Chemistry at the University of Akron*. Retrieved September 9, 2009, from The Chemical Database: http://ull.chemistry.uakron.edu/

Aylward, G., & Findlay, T. (2002). *SI Chemical Data* (fifth ed.). Milton, Australia: John Wiley & Sons.

Battistelli, A. (2006). Modeling Organic Spills in Coastal Sites with TMVOC V.2.0. *Proceedings, TOUGH Symposium, May 15-17, 2006* (pp. 1-8). Berkeley, California: Lawrence Berkeley National Laboratory.

Bensabat, J. (2009, July 27). Environmental and Water Resources Engineering (EWRE). (K. Rasmusson, & M. Rasmusson, Interviewers) Haifa, Israel.

Carsel, R. F., & Parrish, R. S. (1988). Developing Joint Probability Distributions of Soil Water Retention Characteristics. *Water Resources Research , Vol. 24* (5), 755-769.

CHERIC. (1995-2009). *Pure Component Properties.* Retrieved September 9, 2009, from CHERIC-Chemical Engineering Research Information Center: http://www.cheric.org/kdb/kdb/hcprop/showprop.php?cmpid=19

Domenico, P. A., & Schwartz, F. W. (1998). *Physical and Chemical Hydrogeology* (second ed.). New York: John Wiley & Sons, Inc.

EWRE. (2007). *בתת בסולר הזיהום תמונת עידכון - בחיפה ישראל רכבת של המוסכים מתחם של הקרקע [The oil pollution in the underground in the Israeli train area located in Haifa]*. Haifa: EWRE.

EWRE. (2005). *התהום במי דלק עדשת לאיתור הידרולוגי סקר -ישראל רכבת של המוסכים מתחם, חיפה –מזרח [Hydrology survey in order to find the oil in the aquifer located in the Israeli railroad compound Haifa East]*. Haifa: EWRE.

Fagerlund, F. F., Niemi, A., & Odén, M. (2006). Comparison of relative permeability-fluid saturation-capillary pressure relations in the modelling of non-aqueous phase liquid infiltration in variably saturated, layered media. *Advances in Water Resources , Vol. 29*, 1705-1730.

Fagerlund, F., & Niemi, A. (2007). A partially coupled, fraction-by-fraction modelling approach to the subsurface migration of gasoline spills. *Journal of Contaminant Hydrology , Vol. 89*, 174-198.

Fetter, C. W. (1999). *Contaminant Hydrogeology* (second ed.). Upper Saddle River, New Jersey, United States of America: Prentice Hall inc., Simon & Schuster.

Gustafson, J. B., Griffith Tell, J., & Orem, D. (1997). *Selection of Representative TPH Fractions Based on Fate and Transport Considerations, Vol. 3, Total Petroleum Hydrocarbon Criteria Working Group Series.* Amherst, Massachusetts: Amherst Scientific Publishers.

IMS. (2007). *Israel Meteorological Service*. Retrieved July 28, 2009, from http://www.ims.gov.il/IMS/CLIMATE

Joo, Y., Fotinich, A., & Dhir, V. K. (1998). Remediation of Contaminated Soil with Diesel by Soil Venting Technique. *KSME International Journal , Vol. 12* (6), 1174-1183.

Kaluarachchi, J. J., Parker, J. C., & Lenhard, J. (1990). A numerical model for areal migration of water and light hydrocarbon in unconfined aquifers. *Advances in Water Resources , Vol. 13* (1), 29-40.

Kolev, N. I. (2007). *Multiphase Flow Dynamics 3: Turbulence, Gas Absorption and Release, Diesel Fuel Properties.* Berlin, Heidelberg, Germany: Springer-Verlag Berlin Heidelberg, [Electronic Resource].

Landolt-Börnstein. (1999). Landolt-Börnstein - Group IV Physical Chemistry. *Vapor Pressure and Antoine Constants for Hydrocarbons, and S, Se, Te, and Halogen Containing Organic Compounds , Vol. 20 A*(ISSN 1616-9557 online, SpringerLink 2006, June 16). Springer-Verlag.

McCray, J. E., & Falta, R. W. (1997). Numerical Simulation of Air Sparging for Remediation of NAPL Contamination. *Ground Water , Vol. 35* (1), 99-110.

Mercer, J. W., & Cohen, R. M. (1990). A review of immiscible fluids in the subsurface: properties, models, characterization and remediation. *Journal of Contaminant Hydrology , Vol. 6*, 107-163.

Moridis, G. (1994, November). VOC data sets prepared by George Moridis. *voc.dat* . Lawrence Berkeley Laboratory.

Nemes, A., Schaap, M. G., & Leij, F. J. (1999). *UNSODA version 2.0, Database of Unsaturated Soil Hydraulic Properties*. Retrieved August 10, 2009, from United States Department of Agriculture, Agricultural Research Service, Products and Services: http://www.ars.usda.gov/Services/docs.htm?docid=8967

Parker, J. C., Lenhard, R. J., & Kuppusamy, T. (1987). A Parametric Model of Constitutive Properties Governing Multiphase Flow in Porous Media. *Water Resources Research , Vol. 23* (4), 618-624.

Pruess, K., & Battistelli, A. (2002). *TMVOC, A Numerical Simulator for Three-Phase Non-isothermal Flows of Multicomponent Hydrocarbon Mixtures in Saturated-Unsaturated Heterogeneous Media.* LBNL-49375. Berkeley, CA: Lawrence Berkeley National Laboratory.

Reid, R. C., Prausnitz, J. M., & Poling, B. E. (1987). *The Properties of Gases & Liquids* (fourth ed.). New York: McGraw-Hill.

Sjögren, M., Li, H., Rannug, U., & Westerholm, R. (1995). A Multivariate Statistical Analysis of Chemical Composition and Physical Characteristics of Ten Diesel Fuels. *Fuel , Vol. 74* (7), 983-989.

The Engineering ToolBox. (2005). Retrieved August 17, 2009, from Water Surface Tension: http://www.engineeringtoolbox.com/water-surface-tension-d_597.html

van Genuchten, M. T. (1980). A Closed-form Equation for Predicting the Hydraulic Conductivity of Unsaturated Soils. *Soil Science Society of America Journal , Vol. 44*, 892-898.

van Genuchten, M. T., Leij, F. J., & Yates, S. R. (1991). *The RETC Code for Quantifying the Hydraulic Functions of Unsaturated Soils, EPA/600/2-91/065.* U.S. Department of Agriculture, Agricultural Research Service, Riverside, California. Oklahoma: U.S. Environmental Protection Agency.

Vargaftik, N. B. (1975). *Tables on the Thermophysical Properties of Liquids and gases* (second ed.). Washington D.C., N.W., United States of America: Hemisphere Publishing Corporation.

Wong, J. H., Lim, C. H., & Nolen, G. L. (1997). *Design of remediation systems.* Boca Raton, Florida, United States of America: CRC Press LLC.

APPENDIX A

Table A1. Diesel composition (Gustafson et al., 1997). If minimum and maximum values were provided the mean value was calculated by us. If a value is shown in the comment field this was the value range from the source and the value in the mean column was chosen for the calculations. Components with a question mark in the EC column were not used when dividing into subgroups because the EC number was not presented in the source. The color code shows which subgroups the components were assigned to. Aliphatic fractions have the following color code lilac EC >6-8, pink EC >8-10, dark green EC >10-12, blue EC >12-16, grey EC >16-35. Aromatics have the following color code light brown Benzene EC=6.5, yellow Toluene EC=7.58, magenta EC >8-10, light green EC>10-12, orange EC>12-16, dark brown EC>16-21 and red EC >21-35.

			Weight percentage [%]			
	Component	**EC**	**Min**	**Max**	**Mean**	**Comment**
Straight chain alkanes	n-Octane	8			0.1	
	n-Nonane	9	0.19	0.49	0.34	
	n-Decane	10	0.28	1.2	0.74	
	n-Undecane	11	0.57	2.3	1.435	
	n-Dodecane	12	1	2.5	1.75	
	n-Tridecane	13	1.5	2.8	2.15	
	n-Tetradecane	14	0.61	2.7	1.655	
	n-Pentadecane	15	1.9	3.1	2.5	
	n-Hexadecane	16	1.5	2.8	2.15	
	n-Heptadecane	17	1.4	2.9	2.15	
	n-Octadecane	18	1.2	2	1.6	
	n-Nonadecane	19	0.7	1.5	1.1	
	n-Eicosane	20	0.4	1	0.7	
	n-Heneicosane	21	0.26	0.83	0.545	
	n-Docosane	22	0.14	0.44	0.29	
	n-Tetracosane	24			0.35	
Branched chain alkanes	3-Methylundecane	?	0.09	0.28	0.185	
	2-Methyldodecane	?	0.15	0.52	0.335	
	3-Methyltridecane	?	0.13	0.3	0.215	
	2-Methyltetradecane	?	0.34	0.63	0.485	
Alkyl Benzenes	Benzene	6.5	0.003	0.1	0.0515	
	Toluene	7.58	0.007	0.7	0.3535	
	Ethylbenzene	8.5	0.007	0.2	0.1035	
	o-Xylene	8.81	0.001	0.085	0.043	
	m-Xylene	8.6	0.018	0.512	0.265	
	p-Xylene	8.61	0.018	0.512	0.265	
	Styrene	8.83			0.002	<0.002
	1-Methyl-4-isopropylbenzene	10.13	0.003	0.026	0.0145	
	1,3,5-Trimethylbenzene	9.62	0.09	0.24	0.165	
	n-Propylbenzene	9.47	0.03	0.048	0.039	
	Isopropylbenzene	9.13			0.01	<0.01
	n-Butylbenzene	10.5	0.031	0.046	0.0385	

	Biphenyl	?	0.01	0.12	0.065	
Naphtheno-Benzenes	Fluorene	16.55	0.034	0.15	0.092	
	Fluoranthene	21.85	7.0E-07	0.02	0.0100004	
	Benz(b)fluoranthene	30.14	3.0E-07	1.94E-04	9.715E-05	
	Benz(k)fluoranthene	30.14	3.0E-07	1.95E-04	9.765E-05	
	Indeno (1,2,3,-cd) pyrene	35.01	1.0E-06	9.7E-05	4.9E-05	
Alkyl Naphthalenes	Naphthalene	11.69	0.01	0.8	0.405	
	1-Methylnaphthalene	12.99	0.001	0.81	0.4055	
	2-Methylnaphthalene	12.84	0.001	1.49	0.7455	
	1,3-Dimethylnaphthalene	14.77	0.55	1.28	0.915	
	1,4-Dimethylnaphthalene	14.6	0.11	0.23	0.17	
	1,5-Dimethylnaphthalene	13.87	0.16	0.36	0.26	
Polynuclear Aromatics	Anthracene	19.43	3.0E-06	0.02	0.0100015	
	2-Methyl anthracene	20.73	1.5E-05	0.018	0.0090075	
	Phenanthrene	19.36	2.7E-05	0.3	0.1500135	
	1-Methylphenanthrene	20.73	1.1E-05	0.024	0.0120055	
	2-Methylphenanthrene	?	0.014	0.18	0.097	
	3-Methylphenanthrene	?	1.3E-05	0.011	0.0055065	
	4 & 9-Methylphenanthrene	?	1.0E-05	0.034	0.017005	
	Pyrene	20.8	1.8E-05	0.015	0.007509	
	1-Methylpyrene	?	2.4E-06	0.00137	6.862E-04	
	2-Methylpyrene	?	3.7E-06	0.00106	5.319E-04	
	Benz(a)anthracene	26.37	2.1E-06	6.7E-04	3.361E-04	
	Chrysene	27.41			4.5E-05	
	Triphenylene	26.61			3.3E-04	
	Cyclopenta(cd)pyrene	?	2.0E-06	3.65E-05	1.925E-05	
	1-Methyl-7-isopropylphenanthrene	?	1.5E-06	0.00399	0.0019958	
	3-Methylchrysene	?			0.001	<0.001
	6-Methylchrysene	?			5.0E-04	<0.0005
	Benz(a)pyrene	31.34	5.0E-06	8.4E-4	4.225E-04	
	Benz(e)pyrene	31.17	5.4E-06	2.4E-4	1.227E-04	
	Perylene	31.34			1.0E-04	<0.0001
	Benz(ghi)perylene	34.01	9.0E-07	4.0E-05	2.045E-05	
	Picene	?	4.0E-07	8.3E-05	4.17E-05	

Table A2. Chemical data for representative components (Reid et al., 1987).

	TMVOC name	n-Decane	n-Dodecane	n-Pentadecane	n-Nonadecane	Benzene
Chemical critical temperature [K]	TCRIT	617.7	658.2	707.0	756.0	562.2
Chemical critical pressure [bar]	PCRIT	21.2	18.2	15.2	11.1	48.9
Chemical critical compressibility [-]	ZCRIT	0.249	0.24	0.230	0.209[F]	0.271
Pitzer's acentric factor [-]	OMEGA	0.489	0.575	0.706	0.827	0.212
Chemical dipole moment [debyes]	DIPOLM	0.0	0.0	-	-	0.0
Chemical normal boiling point [K]	TBOIL	447.3	489.5	543.8	603.1	353.2
Chemical vapor pressure constant	VPA	-8.56523	0.[D]	0.[D]	0.[G]	-6.98273
	VPB	1.97756	6.7931[D]	7.5981[D]	7.5981[G]	1.33213
	VPC	-5.81971	2023.9[D]	2752.3[D]	2752.3[G]	-2.62863
	VPD	-0.29982	-61.1[D]	-40.65[D]	-40.65[G]	-3.33399
Chemical molecular weight [g/mole]	AMWT	142.286	170.340	212.421	268.529	78.114
Chemical ideal gas heat constant	CPA	-0.7913E+01	-0.9328E+01	-0.1192E+02	-0.1549E+02	-0.3392E+02
	CPB	0.9609E+00	0.1149E+01	0.1433E+01	0.1812E+01	0.4739E+00
	CPC	-0.5288E-03	-0.6347E-03	-0.7972E-03	-0.1015E-02	-0.3017E-03
	CPD	0.1131E-06	0.1359E-06	0.1720E-06	0.2205E-06	0.7130E-07
Reference NAPL (liquid) density [kg/m^3]	RHOREF	730.0	748.0	769.0	772.0[H]	885.0
Reference temperature for NAPL density [K]	TDENRF	293.00	293.00	293.00	313.15[H]	289.00
Reference binary diffusivity of VOC in air [m^2/s]	DIFV0	0.500E-05[A]	0.450E-05[A]	0.390E-05[A]	0.310E-05[A]	0.770E-05[J]
Reference temperature for gas diffusivity [K]	TDIFREF	293.15[A]	293.15[A]	293.15[A]	293.15[A]	273.10[J]
Exponent for calculation of chemical diffusivity	TEXPO	1.90[B]	1.90[B]	1.90[B]	1.90[B]	1.52[J]
Liquid NAPL viscosity constant	VLOA	0	0	0	0	0.4612E+01
	VLOB	0	0	0	0	0.1489E+03
	VLOC	0.86	1.37	2.56	4.00	-0.2544E-01
	VLOD	298.15	298.15	298.15	308.15	0.2222E-04
Chemical critical volume [cm^3/mole]	VOLCRIT	603.0	713.0	880.0	1099.5[I]	259.0
Constant for chemical solubility in water [mole fraction]	SOLA	6.584E-09[C]	3.913E-10[C]	1.000E-12[E]	1.000E-12[E]	4.104E-04[C]
	SOLB	0.0	0.0	0.0	0.0	0.0

	SOLC	0.0	0.0	0.0	0.0	0.0
	SOLD	0.0	0.0	0.0	0.0	0.0
Chemical organic carbon partition coefficient K_{oc} [m^3/kg]	OCK	0.194E+03[A]	0.126E+04[A]	0.174E+05[A]	0.933E+06[A]	0.812E-01[A]
Default value for fraction of organic carbon in soil	FOX	0.000	0.000	0.000	0.000	0.000
Decay constant for biodegradation of VOC [s^{-1}]	ALAM	0.0	0.0	0.0	0.0	0.0

A (Gustafson et al., 1997). The reference temperature is in the interval 10-25 °C, here a reference temperature of 20 °C was assumed. **B** Value not found instead an assumption of 1.90 was used. **C** See table B3. **D** (Landolt-Börnstein, 1999). **E** Zero solubility but set to a small value for the simulation to work. **F** (CHERIC, 1995-2009). **G** Assumed to be the same as for n-Pentadecane. **H** (Vargaftik, 1975). **I** Calculated with Joback's method (Reid et al., 1987, p. 14). **J** (Moridis, 1994). **K** (Akron, 2009).

Table A2. Continued.

	TMVOC name	Toluene	o-Xylene	Naphthalene	1-Methylnaphthalene
Chemical critical temperature [K]	TCRIT	591.8	630.3	748.4	772.0
Chemical critical pressure [bar]	PCRIT	41.0	37.3	40.5	36.0
Chemical critical compressibility [-]	ZCRIT	0.263	0.262	0.269	0.234
Pitzer's acentric factor [-]	OMEGA	0.263	0.310	0.302	0.310
Chemical dipole moment [debyes]	DIPOLM	0.4	0.5	0.0	0.5
Chemical normal boiling point [K]	TBOIL	383.8	417.6	491.1	517.9
Chemical vapor pressure constant	VPA	-7.28607	-7.53357	-7.85178	-7.56390
	VPB	1.38091	1.40968	2.17172	1.19577
	VPC	-2.83433	-3.10985	-3.70504	-3.38134
	VPD	-2.79168	-2.85992	-4.81238	-2.86388
Chemical molecular weight [g/mole]	AMWT	92.141	106.168	128.174	142.201
Chemical ideal gas heat constant	CPA	-0.2435E+02	-0.1585E+02	-0.6880E+02	-0.6482E+02
	CPB	0.5125E+00	0.5962E+00	0.8499E+00	0.9387E+00
	CPC	-0.2765E-03	-0.3443E-03	-0.6506E-03	-0.6942E-03
	CPD	0.4911E-07	0.7528E-07	0.1981E-06	0.2016E-06
Reference NAPL (liquid) density [kg/m^3]	RHOREF	867.0	880.0	971.0	1020.0
Reference temperature for NAPL density [K]	TDENRF	293.00	293.00	363.00	293.00
Reference binary diffusivity of VOC in air [m^2/s]	DIFV0	0.880E-05[J]	0.870E-05[A]	0.513E-05[J]	0.570E-05[A]
Reference temperature for gas diffusivity [K]	TDIFREF	303.10[J]	293.15[A]	273.00[J]	293.15[A]

Exponent for calculation of chemical diffusivity	TEXPO	1.41[J]	1.93[J]	1.50[J]	1.90[B]
Liquid NAPL viscosity constant	VLOA	-0.5878E+01	-0.3332E+01	-0.1027E+02	0
	VLOB	0.1287E+04	0.1039E+04	0.2517E+04	0
	VLOC	0.4575E-02	-0.1768E-02	0.1098E-01	3.44[K]
	VLOD	-0.4499E-05	0.1076E-05	-0.5867E-05	293.15[K]
Chemical critical volume [cm^3/mole]	VOLCRIT	316.0	369.0	413.0	462.0
Constant for chemical solubility in water [mole fraction]	SOLA	1.007E-04[C]	3.732E-05[C]	4.357E-06[C]	3.547E-06[C]
	SOLB	0.0	0.0	0.0	0.0
	SOLC	0.0	0.0	0.0	0.0
	SOLD	0.0	0.0	0.0	0.0
Chemical organic carbon partition coefficient K_{oc} [m^3/kg]	OCK	0.234[A]	0.557[A]	0.844[A]	0.217E+01[A]
Default value for fraction of organic carbon in soil	FOX	0.000	0.000	0.000	0.000
Decay constant for biodegradation of VOC [s^{-1}]	ALAM	0.0	0.0	0.0	0.0

A (Gustafson et al., 1997). The reference temperature is in the interval 10-25 °C, here a reference temperature of 20 °C was assumed. **B** Value not found instead an assumption of 1.90 was used. **C** See table B3. **D** (Landolt-Börnstein, 1999). **E** Zero solubility but set to a small value for the simulation to work. **F** (CHERIC, 1995-2009). **G** Assumed to be the same as for n-Pentadecane. **H** (Vargaftik, 1975). **I** Calculated with Joback's method (Reid et al., 1987, p. 14). **J** (Moridis, 1994). **K** (Akron, 2009).

Table A3. Calculation of solubility values presented in table A2.

Component	Solubility [g/l][A]	Molecular Weight [g/mole][B]	Solubility [mole/cm^3]	Solubility mole fraction [-][C]
n-Decane	0.000052	142.29	3.65E-10	6.584E-09
n-Dodecane	0.0000037	170.33	2.17E-11	3.913E-10
n-Pentadecane	0	212.42	0	0.000E+00
n-Nonadecane	0	268.53	0	0.000E+00
Benzene	1.78	78.11	2.28E-05	4.104E-04
Toluene	0.515	92.13	5.59E-06	1.007E-04
o-Xylene	0.22	106.2	2.07E-06	3.732E-05
Naphthalene	0.031	128.19	2.42E-07	4.357E-06
1-Methylnaphthalene	0.028	142.2	1.97E-07	3.547E-06

A (Gustafson et al., 1997). **B** (Reid et al., 1987). **C** A water density of 1 g/cm^3 (Aylward & Findlay, 2002) and a molecular weight of 18.015 g/mole (Reid et al., 1987) corresponding to 0.055509 mol/cm^3 were used when calculating the solubility mole fractions.

Table A4. Diffusion coefficients.

	Diffusion coefficients in different phases [m^2/s]		
	Gas	Aqueous[A]	NAPL[A]
Water	2.E-05[B]	6.E-10	6.E-10
Air	2.E-05[B]	6.E-10	6.E-10
n-Decane	8.0E-06[C]	6.E-10	6.E-10
n-Dodecane	8.0E-06[D]	6.E-10	6.E-10
n-Pentadecane	4.0E-06[E]	6.E-10	6.E-10
n-Nonadecane	4.0E-06[F]	6.E-10	6.E-10
Benzene	9.0E-06[G]	6.E-10	6.E-10
Toluene	8.0E-06[H]	6.E-10	6.E-10
o-Xylene	8.0E-06[I]	6.E-10	6.E-10
Naphthalene	6.0E-06[J]	6.E-10	6.E-10
1-Methylnaphthalene	6.0E-06[K]	6.E-10	6.E-10

A Coefficients for the aqueous and NAPL phase are presumed to be constant in accordance with Pruess & Battistelli (2002). **B** (Pruess & Battistelli, 2002). **C** Approximated value as the value given by Vargaftik (1975), 1.05E-05 m^2/s, is valid at 453.8 K. At moderate temperatures the diffusion coefficient is assumed to be an order smaller, like Benzene. **D** Approximated in accordance to n-Decane. **E** Approximated to be ~3.92E-06 m^2/s, the value given for n-Hexane by Vargaftik (1975). **F** Approximated to be ~3.96E-06 m^2/s, the value given for n-Octadecane by Vargaftik (1975). **G** Closest unity to 8.82E-06 m^2/s, value given by Vargaftik (1975). **H** (Vargaftik, 1975). **I A**pproximated in accordance to Toluene. **J** Closest unity to 6.11E-06 m^2/s, value given by Vargaftik (1975). **K** Approximated in accordance to Naphthalene.

Table A5. Average diesel properties (Kolev, 2007).

	TMVOC name	
Chemical critical temperature [K]	TCRIT	658.4
Chemical critical pressure [bar]	PCRIT	30.0
Chemical critical compressibility [-]	ZCRIT	0.202[A]
Pitzer's acentric factor [-]	OMEGA	0.310[B]
Chemical dipole moment [debyes]	DIPOLM	0.0[C]
Chemical normal boiling point [K]	TBOIL	453.15
Chemical vapor pressure constant	VPA	-7.53357[B]
	VPB	1.40968[B]
	VPC	-3.10985[B]
	VPD	-2.85992[B]
Chemical molecular weight [g/mole]	AMWT	170
Chemical ideal gas heat constant	CPA	-0.1585E+02[B]
	CPB	0.5962E+00[B]
	CPC	-0.3443E-03[B]
	CPD	0.7528E-07[B]
Reference NAPL (liquid) density [kg/m^3]	RHOREF	833.69~834.
Reference temperature for NAPL density [K]	TDENRF	288.15
Reference binary diffusivity of VOC in air [m^2/s]	DIFV0	0.870E-05[B]
Reference temperature for gas diffusivity [K]	TDIFREF	293.15[B]
Exponent for calculation of chemical diffusivity	TEXPO	1.93[B]
Liquid NAPL viscosity constant	VLOA	-0.3332E+01[B]
	VLOB	0.1039E+04[B]
	VLOC	-0.1768E-02[B]
	VLOD	0.1076E-05[B]
Chemical critical volume [cm^3/mole]	VOLCRIT	369.0[B]
Constant for chemical solubility in water [mole fraction]	SOLA	3.732E-05[B]
	SOLB	0.0
	SOLC	0.0
	SOLD	0.0
Chemical organic carbon partition coefficient Koc [m^3/kg]	OCK	0.557[B]
Default value for fraction of organic carbon in soil	FOX	0.000
Decay constant for biodegradation of VOC [s^{-1}]	ALAM	0.0

A Calculated with $Z_c=P_cV_c/RT_c$. **B** Same as for o-Xylene. **C** An assumption of no dipole moment was made.

APPENDIX B

The control file (retc.ctl), the input file for observed data (retcon.in) and the output file (RETC.out) from the RETC parameter fitting.

retc.ctl

```
RETCON.IN

RETC.OUT

RETPLT.OUT

CONPLT.OUT

EXAMPLE: SAND

    3    4    0    0    1    8   50

 WCR  WCS ALPHA  N    M    L  CONDS

    .02840    .28400    .14500   2.68000    .62687    .50000   4924.80000

    0    0    1    1    1    0    0

   1.00000   42
```

retcon.in

```
EXAMPLE 3: FIT OF RETENTION AND CONDUCTIVITY DATA

    1.00 .284 1

   10.00 .239 1

   20.00 .185 1

   40.00 .113 1

   80.00 .085 1

15000.00 .035 1

-1 -1 -1

        10.    82.9400 1

        20.    36.2900 1

        40.    0.6566 1

        80.    0.00769 1
```

RETC.out

```
     ******************************************************************

     *                                                                *

     *     ANALYSIS OF SOIL HYDRAULIC PROPERTIES                      *

     *                                                                *
```

```
*     EXAMPLE: SAND                                                *
*                                                                  *
*     MUALEM-BASED RESTRICTION, M=1-1/N                            *
*     SIMULTANEOUS FIT OF RETENTION AND CONDUCTIVITY DATA          *
*     FIT ON LOG-TRANSFORMED K/D DATA                              *
*     MTYPE= 3     METHOD= 4                                       *
*                                                                  *
********************************************************************

INITIAL VALUES OF THE COEFFICIENTS
==================================
NO      NAME        INITIAL VALUE   INDEX
 1       WCR            .0284         0
 2       WCS            .2840         0
 3      ALPHA           .1450         1
 4        N            2.6800         1
 5        M             .6269         0
 6        L             .5000         0
 7      CONDS        4924.8000         0

WEIGHTING COEFFICIENTS
======================
W1=  1.00000    W2=   .10862     W12=   .10862


NIT     SSQ     ALPHA     N
 0     .08364   .1450  2.6800
 1     .01848   .1177  2.2523
 2     .01749   .1161  2.1712
 3     .01743   .1181  2.1336
 4     .01741   .1195  2.1133
 5     .01740   .1203  2.1020
 6     .01740   .1207  2.0956
 7     .01740   .1210  2.0919
13     .01740   .1213  2.0870
```

CORRELATION MATRIX

==========

	ALPHA	N
	1	2
1	1.0000	
2	-.8260	1.0000

RSQUARED FOR REGRESSION OF OBSERVED VS FITTED VALUES = .93659385

==========

NONLINEAR LEAST-SQUARES ANALYSIS: FINAL RESULTS

==========

				95% CONFIDENCE LIMITS	
VARIABLE	VALUE	S.E.COEFF.	T-VALUE	LOWER	UPPER
ALPHA	.12134	.02380	5.10	.0665	.1762
N	2.08699	.27748	7.52	1.4471	2.7269

OBSERVED AND FITTED DATA

==========

NO	P	LOG-P	WC-OBS	WC-FIT	WC-DEV
1	.1000E+01	.0000	.2840	.2824	.0016
2	.1000E+02	1.0000	.2390	.1871	.0519
3	.2000E+02	1.3010	.1850	.1188	.0662
4	.4000E+02	1.6021	.1130	.0734	.0396
5	.8000E+02	1.9031	.0850	.0499	.0351
6	.1500E+05	4.1761	.0350	.0285	.0065

	P	LOG-P	LOGK-OBS	LOGK-FIT	LOGK-DEV	K-OBS
7	.1000E+02	1.0000	1.9188	2.3269	-.4081	.8294E+02
8	.2000E+02	1.3010	1.5598	1.1959	.3639	.3629E+02
9	.4000E+02	1.6021	-.1827	-.1389	-.0438	.6566E+00
10	.8000E+02	1.9031	-2.1141	-1.5375	-.5765	.7690E-02

SUM OF SQUARES OF OBSERVED VERSUS FITTED VALUES

==========

	UNWEIGHTED	WEIGHTED
RETENTION DATA	.00992	.00992

COND/DIFF DATA .63331 .00747

ALL DATA .64323 .01740

SOIL HYDRAULIC PROPERTIES (MTYPE = 3)

==========

WC	P	LOGP	COND	LOGK	DIF	LOGD
.0300	.8784E+03	2.944	.3631E-06	-6.440	.1837E+00	-.736
.0316	.4642E+03	2.667	.7354E-05	-5.133	.9833E+00	-.007
.0348	.2453E+03	2.390	.1490E-03	-3.827	.5265E+01	.721
.0412	.1295E+03	2.112	.3020E-02	-2.520	.2824E+02	1.451
.0476	.8901E+02	1.949	.1758E-01	-1.755	.7563E+02	1.879
.0540	.6815E+02	1.833	.6143E-01	-1.212	.1525E+03	2.183
.0604	.5533E+02	1.743	.1623E+00	-.790	.2634E+03	2.421
.0667	.4661E+02	1.668	.3594E+00	-.444	.4127E+03	2.616
.0731	.4026E+02	1.605	.7048E+00	-.152	.6049E+03	2.782
.0795	.3543E+02	1.549	.1265E+01	.102	.8447E+03	2.927
.0859	.3160E+02	1.500	.2121E+01	.326	.1137E+04	3.056
.0923	.2850E+02	1.455	.3371E+01	.528	.1487E+04	3.172
.0987	.2592E+02	1.414	.5135E+01	.711	.1901E+04	3.279
.1051	.2373E+02	1.375	.7550E+01	.878	.2386E+04	3.378
.1115	.2185E+02	1.339	.1078E+02	1.033	.2949E+04	3.470
.1179	.2022E+02	1.306	.1501E+02	1.176	.3599E+04	3.556
.1243	.1877E+02	1.274	.2045E+02	1.311	.4346E+04	3.638
.1306	.1749E+02	1.243	.2736E+02	1.437	.5201E+04	3.716
.1370	.1634E+02	1.213	.3602E+02	1.557	.6178E+04	3.791
.1434	.1529E+02	1.184	.4675E+02	1.670	.7292E+04	3.863
.1498	.1434E+02	1.156	.5993E+02	1.778	.8561E+04	3.933
.1562	.1346E+02	1.129	.7598E+02	1.881	.1001E+05	4.000
.1626	.1265E+02	1.102	.9540E+02	1.980	.1166E+05	4.067
.1690	.1190E+02	1.075	.1187E+03	2.075	.1354E+05	4.132
.1754	.1119E+02	1.049	.1466E+03	2.166	.1570E+05	4.196
.1818	.1053E+02	1.022	.1799E+03	2.255	.1817E+05	4.259
.1882	.9897E+01	.996	.2193E+03	2.341	.2103E+05	4.323
.1945	.9299E+01	.968	.2660E+03	2.425	.2434E+05	4.386
.2009	.8726E+01	.941	.3211E+03	2.507	.2820E+05	4.450
.2073	.8175E+01	.913	.3860E+03	2.587	.3273E+05	4.515
.2137	.7642E+01	.883	.4626E+03	2.665	.3810E+05	4.581

.2201	.7122E+01	.853	.5530E+03	2.743	.4453E+05	4.649
.2265	.6611E+01	.820	.6598E+03	2.819	.5234E+05	4.719
.2329	.6106E+01	.786	.7864E+03	2.896	.6199E+05	4.792
.2393	.5602E+01	.748	.9372E+03	2.972	.7417E+05	4.870
.2457	.5093E+01	.707	.1118E+04	3.049	.8997E+05	4.954
.2521	.4571E+01	.660	.1338E+04	3.126	.1113E+06	5.046
.2584	.4026E+01	.605	.1609E+04	3.207	.1415E+06	5.151
.2648	.3440E+01	.537	.1953E+04	3.291	.1881E+06	5.274
.2712	.2780E+01	.444	.2409E+04	3.382	.2705E+06	5.432
.2776	.1958E+01	.292	.3078E+04	3.488	.4689E+06	5.671
.2808	.1392E+01	.144	.3595E+04	3.556	.7645E+06	5.883
.2840	.0000E+00		.4925E+04	3.692		

END OF PROBLEM

==========

APPENDIX C

Table C. Soil and atmospheric properties. The atmospheric properties were taken from examples by Pruess & Battistelli (2002) if not otherwise stated.

	TMVOC name	Sand	Atm
Grain density [kg/m^3]	DROK	2680.[A]	2680.[E]
Porosity [-]	POR	0.284[A]	.999
Absolute permeability [m^2]	PER(1)	1.0E-11[B]	4.0E-09
	PER(2)	1.0E-11[B]	4.0E-09
	PER(3)	1.0E-11[B]	1.0E-09
Formation heat conductivity under fully liquid-saturated conditions [W/m °C]	CWET	3.1	3.1
Rock grain specific heat [J/kg °C]	SPHT	1000.	1000.
Pore compressibility [Pa^{-1}]	COM	0.	0.e-8
Pore expansivity [1/°C]	EXPAN	0.	0.
Formation heat conductivity under desaturated conditions [W/m °C][C]	CDRY	2.85	2.85
Tortuosity factor for binary diffusion	TORTX	0	0.0
Klinkenberg parameter b [Pa^{-1}]	GK	-	-
Fraction of organic carbon [-]	FOCM	0.0	-
Integer for choice of relative permeability function	IRP	6	6
S_{wr} (if IRP=6)	RP(1)	0.10[D]	.600
S_{nr} (if IRP=6)	RP(2)	0.15[D]	.01
S_{gr} (if IRP=6)	RP(3)	0.01[F]	.000
n (if IRP=6)	RP(4)	3.[G]	3.
Integer for choice of capillary pressure function	ICP	8	9
Irreducible wetting fluid saturation, S_{wr} (if ICP=8) [-]	CP(1)	0.10[D]	-
Parameter describing the shape of the saturation-capillary head curve, n (if ICP=8) [-]	CP(2)	2.09[C]	-
Parameter describing the shape of the saturation-capillary head curve, $\alpha\times\beta_{gn}$ (if ICP=8) [m^{-1}]	CP(3)	35.3[C]	-
Parameter describing the shape of the saturation-capillary head curve, $\alpha\times\beta_{nw}$ (if ICP=8) [m^{-1}]	CP(4)	17.7[C]	-

A UNSODA (Nemes et al., 1999). **B** (Wong et al., 1997). **C** from the RETC parameter optimization, Appendix B, or calculated from these values. **D** (Mercer & Cohen, 1990). **E** Chosen to equal the sand grain density. **F** Assumption. **G** (McCray & Falta, 1997).

APPENDIX D

The following MESHMAKER file created the grid for the 3D model.

```
*****
MESHMAKER1----*----2----*----3----*----4----*----5----*----6----*----7----*----8
XYZ


NX        1     0.001
NX        4      10.0
NX       20       5.0
NX        4      10.0
NX        1     0.001
NY        3      10.0
NY       14       5.0
NY        3      10.0
NZ        1     0.001
NZ       12       0.5


ENDFI----1----*----2----*----3----*----4----*----5----*----6----*----7----*----8
```

The following MESHMAKER file created the grid for the radially symmetric model with small boundary grid blocks.

```
*****
MESHMAKER1----*----2----*----3----*----4----*----5----*----6----*----7----*----8
RZ2D
RADII
  12
     0.     0.5     3.0     5.5      8.     10.5     13.     15.5
    18.    20.5     23.     25.5
LAYER
  13
   -0.01     0.5


ENDFI----1----*----2----*----3----*----4----*----5----*----6----*----7----*----8
```

The following MESHMAKER file created the grid for the radially symmetric model with large boundary grid blocks.

```
*****

MESHMAKER1----*----2----*----3----*----4----*----5----*----6----*----7----*----8

RZ2D

RADII

   12

        0.       0.5       3.0       5.5        8.      10.5       13.      15.5

       18.      20.5       23.      25.5

LAYER

   14

     1.E50       0.5       0.5       0.5       0.5       0.5       0.5       0.5

       0.5       0.5       0.5       0.5       0.5     1.E50



ENDFI----1----*----2----*----3----*----4----*----5----*----6----*----7----*----8
```

APPENDIX E

The input file used for the spill simulation is shown below.

```
*spill* ... NAPL spill in unsaturated zone

ROCKS----1----*----2----*----3----*----4----*----5----*----6----*----7----*----8

SAND1    3     2680.      .284   1.0e-11   1.0e-11   1.0e-11       3.1     1000.

        0.        0.      2.85       0.0

    6           .100      0.15      .010      3.00

    8          0.100      2.09      35.3      17.7

SAND2    3     2680.      .284   1.0e-11   1.0e-11   1.0e-11       3.1     1000.

        0.        0.      2.85       0.0

    6           .100      0.15      .010      3.00

    8          0.100      2.09      35.3      17.7

ATM 3    3     2680.      .999   4.0E-09   4.0E-09   1.0E-09       3.1    50000.

     0.e-8        0.      2.85       0.0

    6           .600       .01      .000        3.

    9


CHEMP----1----*----2----*----3----*----4----*----5----*----6----*----7----*----8

    1

DIESEL

     658.4      30.0     0.202     0.310       0.0

     453.2  -7.53357   1.40968  -3.10985  -2.85992

   170.000-.1585E+020.5962E+00-.3443E-030.7528E-07

      834.    288.15 0.870E-05    293.15      1.93

-.3332E+010.1039E+04-.1768E-02 .1076E-05     369.0

 3.732E-05 0.000E+00 0.000E+00 0.000E+00

     0.557     0.000

NCGAS----1----*----2----*----3----*----4----*----5----*----6----*----7----*----8

    1

AIR

SELEC----1----*----2----*----3----*----4----*----5----*----6----*----7----*----8

    0    1


MULTI----1----*----2----*----3----*----4----*----5----*----6----*----7----*----8

    3    3    3    8    2

START----1----*----2----*----3----*----4----*----5----*----6----*----7----*----8

----*----1 MOP: 123456789*123456789*1234 ---*----5----*----6----*----7----*----8
```

```
PARAM----1----*----2----*----3----*----4----*----5----*----6----*----7----*----8
   39999    999910003000000000 4 0000000                1.8
           94.6080e7       -1.                        9.8060
     1.e+1
     1.E-5     1.E02                                1.000E-8                1.e4
    2
             1.010e5              0.9E-7                20.0
SOLVR----1----*----2----*----3----*----4----*----5----*----6----*----7----*----8
5  Z1   O0    8.0e-1    1.0e-7
RPCAP----1----*----2----*----3----*----4----*----5----*----6----*----7----*----8
    6           .100      0.15      .010      3.00
    8          0.100      2.09      35.3      17.7
DIFFU----1----*----2----*----3----*----4----*----5----*----6----*----7----*----8
     2.e-5    6.e-10    6.e-10
     2.e-5    6.e-10    6.e-10
    8.0e-6    6.e-10    6.e-10
GENER----1----*----2----*----3----*----4----*----5----*----6----*----7----*----8
A2  1HC  1                         COM3 4.1123E-04

ENDCY----1----*----2----*----3----*----4----*----5----*----6----*----7----*----8
```

The input file used for the pumping simulation is shown below.

```
*pump* ... NAPL spill in unsaturated zone
ROCKS----1----*----2----*----3----*----4----*----5----*----6----*----7----*----8
SAND1    3     2680.      .284   1.0e-11   1.0e-11   1.0e-11       3.1     1000.
        0.        0.      2.85       0.0
    6           .100      0.15      .010      3.00
    8          0.100      2.09      35.3      17.7
SAND2    3     2680.      .284   1.0e-11   1.0e-11   1.0e-11       3.1     1000.
        0.        0.      2.85       0.0
    6           .100      0.15      .010      3.00
    8          0.100      2.09      35.3      17.7
ATM 3    3     2680.      .999   4.0E-09   4.0E-09   1.0E-09       3.1    50000.
     0.e-8        0.      2.85       0.0
    6           .600       .01      .000        3.
    9
```

```
CHEMP----1----*----2----*----3----*----4----*----5----*----6----*----7----*----8
    1
DIESEL
     658.4      30.0     0.202     0.310       0.0
     453.2  -7.53357   1.40968  -3.10985  -2.85992
   170.000-.1585E+020.5962E+00-.3443E-030.7528E-07
      834.    288.15 0.870E-05    293.15      1.93
-.3332E+010.1039E+04-.1768E-02 .1076E-05     369.0
 3.732E-05 0.000E+00 0.000E+00 0.000E+00
     0.557     0.000
NCGAS----1----*----2----*----3----*----4----*----5----*----6----*----7----*----8
    1
AIR
SELEC----1----*----2----*----3----*----4----*----5----*----6----*----7----*----8
    0    1


MULTI----1----*----2----*----3----*----4----*----5----*----6----*----7----*----8
    3    3    3    8
START----1----*----2----*----3----*----4----*----5----*----6----*----7----*----8
----*----1 MOP: 123456789*123456789*1234 ---*----5----*----6----*----7----*----8
PARAM----1----*----2----*----3----*----4----*----5----*----6----*----7----*----8
40 39999    999910003000000000 4 0000000                1.8
           63.0720e6       -1.                       9.8060
     1.e+1
     1.E-5     1.E02                                1.000E-8               1.e4
    2
             1.010e5              0.9E-7                 0.0                          20.0
SOLVR----1----*----2----*----3----*----4----*----5----*----6----*----7----*----8
5  Z1   O0    8.0e-1    1.0e-7
RPCAP----1----*----2----*----3----*----4----*----5----*----6----*----7----*----8
    6           .100      0.15      .010      3.00
    8          0.100      2.09      35.3      17.7
DIFFU----1----*----2----*----3----*----4----*----5----*----6----*----7----*----8
     2.e-5    6.e-10    6.e-10
     2.e-5    6.e-10    6.e-10
    8.0e-6    6.e-10    6.e-10
GENER----1----*----2----*----3----*----4----*----5----*----6----*----7----*----8
```

```
AD  1WEL 1                    6     DELV   2.09E-11                 0.5
AC  1WEL 1                          DELV   2.09E-11                 0.5
AB  1WEL 1                          DELV   2.09E-11                 0.5
AA  1WEL 1                          DELV   2.09E-11                 0.5
A9  1WEL 1                          DELV   2.09E-11                 0.5
A8  1WEL 1                          DELV   2.09E-11   1.013E5       0.5

ENDCY----1----*----2----*----3----*----4----*----5----*----6----*----7----*----8
```

The input file used for simulating pumping with fluctuating temperature (step 1) is shown below.

```
*heat* ... NAPL spill in unsaturated zone
ROCKS----1----*----2----*----3----*----4----*----5----*----6----*----7----*----8
SAND1    3     2680.      .284   1.0e-11   1.0e-11   1.0e-11       3.1     1000.
        0.        0.      2.85       0.0
    6           .100      0.15      .010      3.00
    8          0.100      2.09      35.3      17.7
SAND2    3     2680.      .284   1.0e-11   1.0e-11   1.0e-11       0.0    50000.
        0.        0.      0.00       0.0
    6           .100      0.15      .010      3.00
    8          0.100      2.09      35.3      17.7
ATM 3    3     2680.      .284   4.0E-09   4.0E-09   1.0E-09       3.1    50000.
     0.e-8        0.      2.85       0.0
    6           .600       .01      .000        3.
    9

CHEMP----1----*----2----*----3----*----4----*----5----*----6----*----7----*----8
    1
DIESEL
     658.4      30.0     0.202     0.310       0.0
     453.2  -7.53357   1.40968  -3.10985  -2.85992
   170.000-.1585E+020.5962E+00-.3443E-030.7528E-07
      834.    288.15 0.870E-05    293.15      1.93
-.3332E+010.1039E+04-.1768E-02 .1076E-05     369.0
 3.732E-05 0.000E+00 0.000E+00 0.000E+00
     0.557     0.000
NCGAS----1----*----2----*----3----*----4----*----5----*----6----*----7----*----8
    1
```

```
AIR
SELEC----1----*----2----*----3----*----4----*----5----*----6----*----7----*----8
    0    1


MULTI----1----*----2----*----3----*----4----*----5----*----6----*----7----*----8
    3    4    3    8
START----1----*----2----*----3----*----4----*----5----*----6----*----7----*----8
----*----1 MOP: 123456789*123456789*1234 ---*----5----*----6----*----7----*----8
PARAM----1----*----2----*----3----*----4----*----5----*----6----*----7----*----8
   39999    999910003000000000 4 0000000                1.8
            5.2560e6       -1.                       9.8060
     1.e+1
     1.E-5     1.E02                                1.000E-8               1.e4
    2
             1.010e5              0.9E-7               20.0
SOLVR----1----*----2----*----3----*----4----*----5----*----6----*----7----*----8
5  Z1   O0    8.0e-1    1.0e-7
RPCAP----1----*----2----*----3----*----4----*----5----*----6----*----7----*----8
    6           .100      0.15      .010      3.00
    8          0.100      2.09      35.3      17.7
DIFFU----1----*----2----*----3----*----4----*----5----*----6----*----7----*----8
     2.e-5    6.e-10    6.e-10
     2.e-5    6.e-10    6.e-10
    8.0e-6    6.e-10    6.e-10
GENER----1----*----2----*----3----*----4----*----5----*----6----*----7----*----8
A1  1TEM 1                         HEAT 1.1469E+52
A1  2TEM 2                         HEAT 4.0145E+53
A1  3TEM 3                         HEAT 9.7492E+53
A1  4TEM 4                         HEAT 1.5480E+54
A1  5TEM 5                         HEAT 2.1219E+54
A1  6TEM 6                         HEAT 2.6958E+54
A1  7TEM 7                         HEAT 3.2682E+54
A1  8TEM 8                         HEAT 3.8421E+54
A1  9TEM 9                         HEAT 4.4161E+54
A1 10TEM10                         HEAT 4.9885E+54
AD  1WEL 1                   6     DELV   2.09E-11                0.5
AC  1WEL 1                         DELV   2.09E-11                0.5
```

```
AB  1WEL 1                          DELV   2.09E-11                0.5

AA  1WEL 1                          DELV   2.09E-11                0.5

A9  1WEL 1                          DELV   2.09E-11                0.5

A8  1WEL 1                          DELV   2.09E-11   1.013E5      0.5


ENDCY----1----*----2----*----3----*----4----*----5----*----6----*----7----*----8
```

APPENDIX F

The input file used for setting up one of the corner boundaries is shown below.

```
*prep* ... boundary conditions

ROCKS----1----*----2----*----3----*----4----*----5----*----6----*----7----*----8

SAND1    3     2680.      .284   1.0e-11   1.0e-11   1.0e-11       3.1     1000.

        0.        0.      2.85       0.0

    6           .100      0.15      .010      3.00

    8          0.100      2.09      35.3      17.7

SAND2    3     2680.      .284   1.0e-11   1.0e-11   1.0e-11       3.1     1000.

        0.        0.      2.85       0.0

    6           .100      0.15      .010      3.00

    8          0.100      2.09      35.3      17.7

ATM 3    3     2680.      .999   4.0E-09   4.0E-09   1.0E-09       3.1    50000.

     0.e-8        0.      2.85       0.0

    6           .600       .01      .000        3.

    9


CHEMP----1----*----2----*----3----*----4----*----5----*----6----*----7----*----8

    0

NCGAS----1----*----2----*----3----*----4----*----5----*----6----*----7----*----8

    1

AIR

SELEC----1----*----2----*----3----*----4----*----5----*----6----*----7----*----8

    0    1


MULTI----1----*----2----*----3----*----4----*----5----*----6----*----7----*----8

    2    2    3    6

START----1----*----2----*----3----*----4----*----5----*----6----*----7----*----8

----*----1 MOP: 123456789*123456789*1234 ---*----5----*----6----*----7----*----8

PARAM----1----*----2----*----3----*----4----*----5----*----6----*----7----*----8

   3 400     40010003000000000 4 0000000                 1.8

                           -1.                        9.8060

     1.e+0

     1.E-6     1.E02                                1.000E-8              1.E+4

    2

             1.010e5              0.9E-7                20.0

SOLVR----1----*----2----*----3----*----4----*----5----*----6----*----7----*----8
```

```
5  Z1   O0    8.0e-1    1.0e-7
RPCAP----1----*----2----*----3----*----4----*----5----*----6----*----7----*----8
    6           .100      0.15      .010      3.00
    8          0.100      2.09      35.3      17.7
ELEME
A21 1              10.5000E-020.0000E+00          0.5000E-030.5000E+01-.2510E+00
A31 1              10.5000E-020.0000E+00          0.5000E-030.5000E+01-.7510E+00
A41 1              10.5000E-020.0000E+00          0.5000E-030.5000E+01-.1251E+01
A51 1              10.5000E-020.0000E+00          0.5000E-030.5000E+01-.1751E+01
A61 1              10.5000E-020.0000E+00          0.5000E-030.5000E+01-.2251E+01
A71 1              10.5000E-020.0000E+00          0.5000E-030.5000E+01-.2751E+01
A81 1              20.5000E-020.0000E+00          0.5000E-030.5000E+01-.3251E+01
A91 1              20.5000E-020.0000E+00          0.5000E-030.5000E+01-.3751E+01
AA1 1              20.5000E-020.0000E+00          0.5000E-030.5000E+01-.4251E+01
AB1 1              20.5000E-020.0000E+00          0.5000E-030.5000E+01-.4751E+01
AC1 1              20.5000E-020.0000E+00          0.5000E-030.5000E+01-.5251E+01
DUM                 0.0000E-02
A11 1              30.1000E-040.1000E-01          0.5000E-030.5000E+01-.5000E-03
AD1 1              20.5000E-020.1000E-01          0.5000E-030.5000E+01-.5751E+01

CONNE
A11 1A21 1                   30.5000E-030.2500E+000.1000E-010.1000E+01
A21 1A31 1                   30.2500E+000.2500E+000.1000E-010.1000E+01
A31 1A41 1                   30.2500E+000.2500E+000.1000E-010.1000E+01
A41 1A51 1                   30.2500E+000.2500E+000.1000E-010.1000E+01
A51 1A61 1                   30.2500E+000.2500E+000.1000E-010.1000E+01
A61 1A71 1                   30.2500E+000.2500E+000.1000E-010.1000E+01
A71 1A81 1                   30.2500E+000.2500E+000.1000E-010.1000E+01
A81 1A91 1                   30.2500E+000.2500E+000.1000E-010.1000E+01
A91 1AA1 1                   30.2500E+000.2500E+000.1000E-010.1000E+01
AA1 1AB1 1                   30.2500E+000.2500E+000.1000E-010.1000E+01
AB1 1AC1 1                   30.2500E+000.2500E+000.1000E-010.1000E+01
AC1 1AD1 1                   30.2500E+000.2500E+000.1000E-010.1000E+01

INDOM----1----*----2----*----3----*----4----*----5----*----6----*----7----*----8
ATM 3    1
           1.013E+05            0.99E+00 0.2000000000000E+02
```

```
INCON----1----*----2----*----3----*----4----*----5----*----6----*----7----*----8
AD1 1            .28400000E+00 2
         1.28214E+05             0.9E-05  .2000000000000E+02

ENDCY----1----*----2----*----3----*----4----*----5----*----6----*----7----*----8
```

Input file for side boundaries.

```
*side* ... get steady state for 2D-section of sat.-unsat. system
ROCKS----1----*----2----*----3----*----4----*----5----*----6----*----7----*----8
SAND1    3     2680.      .284   1.0e-11   1.0e-11   1.0e-11       3.1     1000.
        0.        0.      2.85       0.0
    6           .100      0.15      .010      3.00
    8          0.100      2.09      35.3      17.7
SAND2    3     2680.      .284   1.0e-11   1.0e-11   1.0e-11       3.1     1000.
        0.        0.      2.85       0.0
    6           .100      0.15      .010      3.00
    8          0.100      2.09      35.3      17.7
ATM 3    3     2680.      .999   4.0E-09   4.0E-09   1.0E-09       3.1    50000.
     0.e-8        0.      2.85       0.0
    6           .600       .01      .000        3.
    9

CHEMP----1----*----2----*----3----*----4----*----5----*----6----*----7----*----8
    0
NCGAS----1----*----2----*----3----*----4----*----5----*----6----*----7----*----8
    1
AIR
SELEC----1----*----2----*----3----*----4----*----5----*----6----*----7----*----8
    0    1

MULTI----1----*----2----*----3----*----4----*----5----*----6----*----7----*----8
    2    2    3    6
START----1----*----2----*----3----*----4----*----5----*----6----*----7----*----8
----*----1 MOP: 123456789*123456789*1234 ---*----5----*----6----*----7----*----8
PARAM----1----*----2----*----3----*----4----*----5----*----6----*----7----*----8
   39920    992010003000000000 4 0000000                 1.8
           3.1536E14       -1.                       9.8060
```

```
     1.e+0
     1.E-6     1.E02                                1.000E-8              1.E+4
    2
              1.010e5              0.9E-7                20.0
SOLVR----1----*----2----*----3----*----4----*----5----*----6----*----7----*----8
5  Z1   O0    8.0e-1    1.0e-7
RPCAP----1----*----2----*----3----*----4----*----5----*----6----*----7----*----8
    6           .100      0.15      .010      3.00
    8          0.100      2.09      35.3      17.7
INDOM----1----*----2----*----3----*----4----*----5----*----6----*----7----*----8
ATM 3    1
           1.013E+05            0.99E+00 0.2000000000000E+02


INCON----1----*----2----*----3----*----4----*----5----*----6----*----7----*----8
A11 1           0.99900000E+00 1
 0.1013000000000E+06 0.9900000000000E+00 0.2000000000000E+02
A21 1           0.28400000E+00 4
 0.1013029390561E+06 0.1000096470753E+00 0.2000000000000E+02
A31 1           0.28400000E+00 4
 0.1013087913929E+06 0.1000127812454E+00 0.2000000000000E+02
A41 1           0.28400000E+00 4
 0.1013146440709E+06 0.1000164280864E+00 0.2000000000000E+02
A51 1           0.28400000E+00 4
 0.1013204970901E+06 0.1127983015864E+00 0.2000000000000E+02
A61 1           0.28400000E+00 4
 0.1013263504504E+06 0.1821990365437E+00 0.2000000000000E+02
A71 1           0.28400000E+00 4
 0.1013322041520E+06 0.3589287863312E+00 0.2000000000000E+02
A81 1           0.28400000E+00 2
 0.1037399413075E+06 0.1243415638643E-04 0.2000000000000E+02
A91 1           0.28400000E+00 2
 0.1086347312261E+06 0.9908905031974E-05 0.2000000000000E+02
AA1 1           0.28400000E+00 2
 0.1135295320548E+06 0.6930309660344E-05 0.2000000000000E+02
AB1 1           0.28400000E+00 2
 0.1184243437933E+06 0.4346836808828E-05 0.2000000000000E+02
AC1 1           0.28400000E+00 2
```

```
 0.1233191664418E+06 0.2503829578372E-05 0.2000000000000E+02
AD1 1           0.28400000E+00 2
 0.1282140000000E+06 0.9000000000000E-05 0.2000000000000E+02
A1K 1           0.99900000E+00 1
 0.1013000000000E+06 0.9900000000000E+00 0.2000000000000E+02
A2K 1           0.28400000E+00 4
 0.1013029390561E+06 0.1000096470753E+00 0.2000000000000E+02
A3K 1           0.28400000E+00 4
 0.1013087913929E+06 0.1000127812454E+00 0.2000000000000E+02
A4K 1           0.28400000E+00 4
 0.1013146440709E+06 0.1000164280864E+00 0.2000000000000E+02
A5K 1           0.28400000E+00 4
 0.1013204970901E+06 0.1127983015864E+00 0.2000000000000E+02
A6K 1           0.28400000E+00 4
 0.1013263504504E+06 0.1821990365437E+00 0.2000000000000E+02
A7K 1           0.28400000E+00 4
 0.1013322041520E+06 0.3589287863312E+00 0.2000000000000E+02
A8K 1           0.28400000E+00 2
 0.1037399413075E+06 0.1243415638643E-04 0.2000000000000E+02
A9K 1           0.28400000E+00 2
 0.1086347312261E+06 0.9908905031974E-05 0.2000000000000E+02
AAK 1           0.28400000E+00 2
 0.1135295320548E+06 0.6930309660344E-05 0.2000000000000E+02
ABK 1           0.28400000E+00 2
 0.1184243437933E+06 0.4346836808828E-05 0.2000000000000E+02
ACK 1           0.28400000E+00 2
 0.1233191664418E+06 0.2503829578372E-05 0.2000000000000E+02
ADK 1           0.28400000E+00 2
 0.1282140000000E+06 0.9000000000000E-05 0.2000000000000E+02

ENDCY----1----*----2----*----3----*----4----*----5----*----6----*----7----*----8
```

The input file used for the steady state simulation is shown below.

```
*steady* ... get steady state for 2D-section of sat.-unsat. system
ROCKS----1----*----2----*----3----*----4----*----5----*----6----*----7----*----8
SAND1    3     2680.      .284   1.0e-11   1.0e-11   1.0e-11       3.1     1000.
        0.        0.      2.85       0.0
    6           .100      0.15      .010      3.00
    8          0.100      2.09      35.3      17.7
SAND2    3     2680.      .284   1.0e-11   1.0e-11   1.0e-11       3.1     1000.
        0.        0.      2.85       0.0
    6           .100      0.15      .010      3.00
    8          0.100      2.09      35.3      17.7
ATM 3    3     2680.      .999   4.0E-09   4.0E-09   1.0E-09       3.1    50000.
     0.e-8        0.      2.85       0.0
    6           .600       .01      .000        3.
    9


CHEMP----1----*----2----*----3----*----4----*----5----*----6----*----7----*----8
    0
NCGAS----1----*----2----*----3----*----4----*----5----*----6----*----7----*----8
    1
AIR
SELEC----1----*----2----*----3----*----4----*----5----*----6----*----7----*----8
    0    1


MULTI----1----*----2----*----3----*----4----*----5----*----6----*----7----*----8
    2    2    3    6
START----1----*----2----*----3----*----4----*----5----*----6----*----7----*----8
----*----1 MOP: 123456789*123456789*1234 ---*----5----*----6----*----7----*----8
PARAM----1----*----2----*----3----*----4----*----5----*----6----*----7----*----8
 4 39920    9920100030000000000 4 0000000                1.8
           3.1536E14       -1.                        9.8060
     1.e+1
     1.E-6     1.E02                                1.000E-8              1.E+4
    2
             1.010e5              0.9E-7                20.0
SOLVR----1----*----2----*----3----*----4----*----5----*----6----*----7----*----8
5  Z1   O0    8.0e-1    1.0e-7
```

```
RPCAP----1----*----2----*----3----*----4----*----5----*----6----*----7----*----8
    6           .100      0.15      .010      3.00
    8          0.100      2.09      35.3      17.7
INDOM----1----*----2----*----3----*----4----*----5----*----6----*----7----*----8
ATM 3    1
           1.013E+05            0.99E+00 0.2000000000000E+02

ENDCY----1----*----2----*----3----*----4----*----5----*----6----*----7----*----8
```

The input file used for the spill simulation is shown below.

```
*spill* ... multicomponent NAPL spill in unsaturated zone
ROCKS----1----*----2----*----3----*----4----*----5----*----6----*----7----*----8
SAND1    3     2680.      .284   1.0e-11   1.0e-11   1.0e-11       3.1     1000.
        0.        0.      2.85       0.0
    6           .100      0.15      .010      3.00
    8          0.100      2.09      35.3      17.7
SAND2    3     2680.      .284   1.0e-11   1.0e-11   1.0e-11       3.1     1000.
        0.        0.      2.85       0.0
    6           .100      0.15      .010      3.00
    8          0.100      2.09      35.3      17.7
ATM 3    3     2680.      .999   4.0E-09   4.0E-09   1.0E-09       3.1    50000.
     0.e-8        0.      2.85       0.0
    6           .600       .01      .000        3.
    9

CHEMP----1----*----2----*----3----*----4----*----5----*----6----*----7----*----8
    1
DIESEL
     658.4      30.0     0.202     0.310       0.0
     453.2  -7.53357   1.40968  -3.10985  -2.85992
   170.000-.1585E+020.5962E+00-.3443E-030.7528E-07
      834.    288.15 0.870E-05    293.15      1.93
-.3332E+010.1039E+04-.1768E-02 .1076E-05     369.0
 3.732E-05 0.000E+00 0.000E+00 0.000E+00
     0.557     0.000
NCGAS----1----*----2----*----3----*----4----*----5----*----6----*----7----*----8
    1
```

```
AIR
SELEC----1----*----2----*----3----*----4----*----5----*----6----*----7----*----8
    0    1


MULTI----1----*----2----*----3----*----4----*----5----*----6----*----7----*----8
    3    3    3    8    2
START----1----*----2----*----3----*----4----*----5----*----6----*----7----*----8
----*----1 MOP: 123456789*123456789*1234 ---*----5----*----6----*----7----*----8
PARAM----1----*----2----*----3----*----4----*----5----*----6----*----7----*----8
 4 39999    9999111131000020004 0000000                1.8
           9.4608e8      -1.                       9.8060
     1.e+0
     1.E-5     1.E02                               1.000E-8               1.e4
    2
            1.010e5              0.9E-7                20.0
SOLVR----1----*----2----*----3----*----4----*----5----*----6----*----7----*----8
5  Z1   O0    8.0e-1    1.0e-7
RPCAP----1----*----2----*----3----*----4----*----5----*----6----*----7----*----8
    6           .100      0.15      .010      3.00
    8          0.100      2.09      35.3      17.7
DIFFU----1----*----2----*----3----*----4----*----5----*----6----*----7----*----8
     2.e-5    6.e-10    6.e-10
     2.e-5    6.e-10    6.e-10
    8.0e-6    6.e-10    6.e-10
GENER----1----*----2----*----3----*----4----*----5----*----6----*----7----*----8
A2A14HCA01                        COM3 3.0842E-04
A2A15HCA02                        COM3 3.0842E-04
A2A16HCA03                        COM3 3.0842E-04
A2A17HCA04                        COM3 3.0842E-04

ENDCY----1----*----2----*----3----*----4----*----5----*----6----*----7----*----8
```